Trace amine-associated receptor 1 activation regulates glucose-dependent insulin secretion in pancreatic beta cells *in vitro*

by

©Arun Kumar

A thesis submitted to the School of Graduate Studies in partial fulfillment of the requirements for the degree of

Master of Science

Department of Biochemistry, Faculty of Science

Memorial University of Newfoundland

FEBRUARY 2021

St. John's, Newfoundland and Labrador

Abstract

Trace amines are a group of endogenous monoamines which exert their action through a family of G protein-coupled receptors known as trace amine-associated receptors (TAARs). TAAR1 has been reported to regulate insulin secretion from pancreatic beta cells *in vitro* and *in vivo*. This study investigates the mechanism(s) by which TAAR1 regulates insulin secretion. The insulin secreting rat INS-1E β-cell line was used for the study. Cells were pre-starved (30 minutes) and then incubated with varying concentrations of glucose (2.5 – 20 mM) or KCl (3.6 – 60 mM) for 2 hours in the absence or presence of various concentrations of the selective TAAR1 agonist RO5256390. Secreted insulin per well was quantified using ELISA and normalized to the total protein content of individual cultures. RO5256390 significantly ($P < 0.0001$) increased glucose-stimulated insulin secretion in a dose-dependent manner, with no effect on KCl-stimulated insulin secretion. Affymetrix-microarray data analysis identified genes (*Gnas*, *Gng7*, *Gngt1*, *Gria2*, *Cacna1e*, *Kcnj8*, and *Kcnj11*) whose expression was associated with changes in TAAR1 in response to changes in insulin secretion in pancreatic beta cell function. The identified potential links to TAAR1 supports the regulation of glucose-stimulated insulin secretion through K_{ATP} ion channels.

Keywords: Trace amines; TAAR1; Pancreatic beta cell; Insulin secretion; Bioinformatics

Acknowledgements

Firstly, I would like to thank my supervisor Dr. Mark D. Berry for his continuous support, valuable guidance and plethora of learning opportunities being provided through lab meetings, departmental and international conferences.

I would like to thank my committee member Dr. Sukhinder Kaur Cheema for giving me the opportunity to study at MUN and guiding me throughout my master's program.

I would also like to thank my other committee member Dr. Scott Harding and ex-committee member Dr. Ryan Mailloux for their motivation and support.

I would like to acknowledge Dr. Sherri Christian and Dr. Lourdes Peña-Castillo in providing assistance with the bioinformatics work. I am grateful to Dr. Sherri Christian for allowing me to work in her lab for most of my cell-culture studies.

I would like to thank Dr. Robert Brown for his valuable suggestions throughout my lab meetings and departmental seminars.

I would like to thank Danielle Gardiner for training and helping me with my initial cell-culture studies.

I would like to thank all my past and current lab members for their continuous support.

I would like to thank the respective funding sources QEII Diamond jubilee Scholarship program, SGS, and MUN RDC for helping me to meet my financial needs.

Finally, I would like to thank my family and friends for their constant support.

Table of Contents

Abstract....ii

Acknowledgements....iii

Table of Contents....iv

List of Figures....vii

List of Tables....ix

List of Abbreviations....x

1.0 Literature review....1

1.1 Type II diabetes....1

1.1.1 Clinical diagnosis....2

1.1.2 Complications....3

1.1.3 Current management options....4

1.2 Insulin....8

1.2.1 Insulin Physiology....9

1.2.1.1 Secretory mechanism....11

1.3 Trace amines....16

1.3.1 Endogenous TA Synthesis....17

1.3.2 TA Degradation....19

1.4 Trace amine-associated receptors....21

1.5 Trace amine-associated receptor1....26

1.5.1 Ligands....26

1.5.2 Tissue expression....27

1.5.3 Signal transduction cascades....28

1.5.4 Role in CNS.....30
1.5.5 Role in periphery.....34
1.5.5.1 Role in pancreatic beta cells.....36
1.6 INS-1E cell line.....37
1.7 Research objective and hypothesis.....38
1.7.1 Objective.....38
1.7.2 Hypothesis.....38
2.0 Materials and Methods.....39
2.1 RO5256390 formulations.....39
2.2 INS-1E cell culture.....39
2.2.1 Materials.....39
2.2.2 Cell culture.....40
2.2.3 INS-1E subculture.....41
2.2.4 Subculture into 24 and 96-well plate.....41
2.3 Insulin secretion measurements in INS1-E cells to evaluate the effect of RO5256390 on glucose and potassium chloride stimulated signaling pathway.....42
2.3.1 Insulin assay.....43
2.3.2 BCA Protein assay.....45
2.4 Membrane potential measurement using $DiBAC_4(3)$ 47
2.5 Bioinformatics.....47
2.5.1 Affymetrix microarray data analysis.....49
2.6 Data analysis.....62
3.0 Results.....63

3.1 RO5256390 effect on glucose-dependent insulin secretion.....63
3.2 RO5256390 effect on potassium-stimulated insulin secretion.....66
3.3 Glucose and potassium concentration-response effect on INS-1E membrane potential.....69
3.4 Identification of TAAR1 correlated transcripts from microarray data analysis.....74
3.4.1 Physiological conditions.....74
3.4.2 Pathological condition.....80
4.0 Discussion.....86
4.1 RO5256390 enhances glucose-dependent insulin secretion.....86
4.2 RO5256390 does not alter potassium stimulated insulin secretion.....87
4.3 No glucose or KCl concentration-response effect on membrane potential.....88
4.4 TAAR1 correlated transcripts involved in the regulation of TAAR1-mediated GSIS were identified.....88
4.4.1 TAAR1 correlated genes from the studies examining physiological processes.....89
4.4.2 TAAR1 correlated genes from the studies examining pathological processes.....94
4.5 Conclusions.....97
4.6 Future directions.....100
4.7 Limitations.....100
5.0 References.....101
6.0 Appendix.....135

List of Figures

Figure 1.1: Glucose-stimulated insulin secretion mechanism.....12

Figure 1.2: Biosynthetic pathway of trace amines.....18

Figure 1.3: Trace amines and their metabolites.....20

Figure 2.1: Sample Insulin ELISA assay standard curve for insulin (µg/L) determination.....44

Figure 2.2: Representative BSA standard linear regression line for protein (µg/10 µL) determination.....46

Figure 3.1: Glucose-dependent stimulation of insulin secretion.....64

Figure 3.2: RO5256390 selectively enhanced glucose-dependent insulin secretion at concentrations of 10 nM and above.....65

Figure 3.3: Concentration-dependent effect of KCl on insulin secretion.....67

Figure 3.4: RO5256390 does not alter potassium-stimulated insulin secretion.....68

Figure 3.5: No glucose concentration-dependent effect on membrane depolarization at a cell density of 20,000 cells/well.....70

Figure 3.6: No KCl concentration-dependent effect on membrane depolarization at a cell density of 20,000 cells/well.....71

Figure 3.7: No glucose concentration-dependent effect on membrane potential at a cell density of 50,000 cells/well.....72

Figure 3.8: No KCl concentration-dependent effect on membrane potential at a cell density of 50,000 cells/well.....73

Figure 3.9: Heat map representing hierarchical clustering of TAAR1 gene with genes positively (on left) and negatively (on right) correlated to its expression pattern across isolated rat beta cells exposed to varying glucose concentrations for 18 hours (GSE12817).....76

Figure 3.10: Heat map representing hierarchical clustering of TAAR1 gene with genes positively (on left) and negatively (on right) correlated to its expression pattern across pancreatic islet cells isolated from different aged rat (GSE47174).....77
Figure 3.11: Heat map representing hierarchical clustering of TAAR1 gene with genes positively (on left) and negatively (on right) correlated to its expression pattern across beta cells isolated from different aged C57Bl/6 mice (GSE72753).....78
Figure 3.12: TAAR1 correlated genes under physiological conditions.....79
Figure 3.13: Heat map representing hierarchical clustering of TAAR1 gene with genes positively (on top) and negatively (on bottom) correlated to its expression pattern across isolated pancreatic beta cells from cadaver pancreases of non-diabetic and type-II diabetic human subjects (GSE20966) 81
Figure 3.14: Heat map representing hierarchical clustering of TAAR1 gene with genes positively (on left) and negatively (on right) correlated to its expression pattern across isolated pancreatic islets from rats exposed to standard chow and high fat diet for ten and thirty days (GSE4407)...82
Figure 3.15: Heat map representing hierarchical clustering of TAAR1 gene with genes positively (on left) and negatively (on right) correlated to its expression pattern across two independent HDL preparations subjected to ß-TC3 cell line under different conditions (GSE17647).....83
Figure 3.16: Heat map representing hierarchical clustering of TAAR1 gene with genes positively (on left) and negatively (on right) correlated to its expression pattern across control and mice with intrinsic beta cell NIK activation fed with chow and high fat diet (GSE68317).....84
Figure 3.17: TAAR1 correlated genes under pathological conditions.....85
Figure 4.1: Proposed molecular mechanism for TAAR1 regulation of GSIS.....99

List of Tables

Table 1.1: Functional TAAR genes and pseudogenes in different vertebrate species.....22

Table 2.1: Potential target genes of TAAR1 regulation of glucose-dependent insulin secretion..50

Table 2.2: Affymetrix microarray-based studies, pertaining to pancreatic beta cells, obtained from NCBI GEO database.....58

List of Abbreviations

5-HT	Serotonin
AADC	Aromatic L-amino acid decarboxylase
ADP	Adenosine diphosphate
AKT	Protein kinase B
AMP	Adenosine monophosphate
AMPA	α-amino-3-hydroxy-5-methyl-4-isoxazolepropionic acid
AMPAR	AMPA receptors
AMPK	Adenosine monophosphate-activated protein kinase
ANOVA	Analysis of variance
AOC3	Amine oxidase, copper containing 3
ATCC	American Type Culture Collection
ATP	Adenosine triphosphate
BCA	Bicinchoninic acid
BSA	Bovine serum albumin
CAC	Citric acid cycle
CAMKII	Calcium/calmodulin-dependent protein kinase II
cAMP	Cyclic adenosine monophosphate
CM	Complete medium
CNS	Central nervous system
CoA	Coenzyme A
COMT	Catecholamine-*O*-methyltransferase
CREB	cAMP response element-binding protein

D2R	Dopamine D_2-like receptors
DAT	Dopamine transporter
DBH	Dopamine- ß-hydroxylase
$DiBAC_4(3)$	*bis*-(1,3-dibutylbarbituric acid) trimethine oxonol
DMSO	Dimethyl sulfoxide
DPP-4	Dipeptidyl peptidase-4
EAAT-2	Excitatory amino acid transporter-2
EDTA	Ethylenediaminetetraacetic acid
ELISA	Enzyme-linked immunosorbent assay
Epac	Exchange protein activated by cAMP
ERK1/2	Extracellular signal-regulated kinase 1/2
F-actin	Filamentous actin
FMO3	Flavin monooxygenase 3
GEO	Gene Expression Omnibus
GIP	Glucose-dependent insulinotropic peptide
GirK	G-protein-gated potassium ion channels
GLP-1	Glucagon-like peptide-1
GLUT	Glucose transporter
GPCR(s)	G protein-coupled receptor(s)
GSE	Gene Expression Omnibus Series
GSIS	Glucose-stimulated insulin secretion
GSK3ß	Glycogen synthase kinase-3 beta
HbA1C	Glycated haemoglobin

HDL	High-density lipoproteins
HEPES	4-(2-hydroxyethyl)-1-piperazineethanesulfonic acid
HIV	Human immunodeficiency virus
INMT	Indolethylamine *N*-methyltransferase
IP_3	Inositol 1,4,5-trisphosphate
K_{ATP}	ATP-sensitive potassium ion channel
K_m	Michaelis constant
KO	Knockout
KRBH	Krebs-Ringer bicarbonate-HEPES buffer
MAO	Monoamine oxidase
MEK1/2	Mitogen-activated protein kinase kinase 1/2
NCBI	National Center for Biotechnology Information
NFAT	Nuclear factor of activated T-cells
NIK	Nuclear factor κB-inducing kinase
NMDA	*N*-methyl-D-aspartate
NP-40	Nonidet-P40
OCT	*para*-octopamine
PAK1	p21-activated kinase
PBS	Phosphate buffered saline
PC	Prohormone convertase
PCR	Polymerase chain reaction
PCT	Proximal convoluted tubule
PDE3B	Phosphodiesterase-3B

PEA	2-phenylethylamine
PH	Phenylalanine hydroxylase
PKA	Protein kinase A
PKC	Protein kinase C
PNMT	Phenylethanolamine-*N*-methyl transferase
PPAR	Peroxisome proliferator-activated receptor
PYY	Peptide YY
Raf	Rapidly accelerated fibrosarcoma
RER	Rough endoplasmic reticulum
RFU	Relative fluorescence unit
RIM	Rab3-interacting-molecule
RMA	Robust multi-chip average
RO5166017	(S)-4-((ethyl(phenyl)amino)methyl)-4,5-dihydrooxazol-2-amine
RO5203648	(S)-4-(3,4-dichlorophenyl)-4,5-dihydrooxazol-2-amine
RO5212773	*N*-(3-ethoxyphenyl)-4-(1-pyrrolidinyl)-3-(trifluoromethyl)benzamide
RO5256390	(S)-4-((S)-2-phenylbutyl)-4,5-dihydrooxazol-2-ylamine
RO5263397	(S)-4-(3-fluoro-2-methylphenyl)-4,5-dihydrooxazol-2-amine
RP	Reserve pool
RPMI	Roswell Park Memorial Institute
RRP	Readily releasable pool
SEM	Standard error of mean
SGLT-2	Sodium-glucose cotransporter-2

SM	Sec1/Munc18-like adaptor protein
SNAP	Soluble *N*-ethylmaleimide-sensitive factor attachment protein
SNARE	Soluble *N*-ethylmaleimide-sensitive factor attachment protein receptor
SSAO	Semicarbazide-sensitive amine oxidase
SYN	*para*-synephrine
Syt	Synaptotagmin
T_1AM	3-iodothyronamine
TA(s)	Trace amine(s)
TAAR(s)	Trace amine-associated receptor(s)
TH	Tyrosine hydroxylase
TMA	Trimethylamine
TMAO	Trimethylamine-*N*-oxide
TMB	3,3',5,5'-tetramethylbenzidine
TRAF	Tumor necrosis factor receptor associated factor
TRP	Tryptamine
TYR	*para*-tyramine
VAMP2	Vesicle-associated membrane protein
VAP-1	Vascular adhesion protein-1
VTA	Ventral tegmental area

1.0 Literature review

1.1 Type II diabetes

Type II diabetes encompasses more than 90% of all cases of diabetes (Holman, Young, & Gadsby, 2015). Type II diabetes is a progressive, complex, and chronic metabolic disorder characterized by an elevated blood glucose level due to alterations in insulin secretion, insulin resistance, or both (Chatterjee, Khunti, & Davies, 2017). It is a consequence of the complex interactions between genetic, environmental, and behavioural factors such as, but not limited to, ethnicity, sex, age, epigenetics, genetic predisposition, poor dietary pattern, sedentary lifestyle, excess body weight, and heavy alcohol consumption; hence is multifactorial (Chen, Magliano, & Zimmet, 2012). The pathogenesis of type II diabetes involves the development of insulin resistance in peripheral tissues such as liver, skeletal muscle and adipose tissue, and the deterioration of pancreatic beta-cell mass together to cause impaired glucose tolerance marked by elevated blood glucose levels. The vicious cycle of insulin resistance and beta cell dysfunction over a period of time lead to the rise of diabetes symptoms and life-threatening complications (see section 1.1.2) (Leahy, 2005). The clinical symptoms of type II diabetes may vary from asymptomatic for many years during the initial phase, to symptoms like weight change, polyuria, polydipsia, tiredness, blurred vision, and numbness in the peripheral limbs (American Diabetes Association, 2009). As per the International diabetes federation's 2017 datasheet, the estimates pertaining to the risk of developing type II diabetes worldwide has increased to 352 million people. In the same report, the prevalence of diabetes of all forms is expected to rise more than 48% from 425 million in 2017 to 629 million by 2045. In 2013, 174.8 million cases of diabetes were found to be undiagnosed globally (Beagley et al., 2014), which by 2017 had increased to over 212 million (International Diabetes Federation, 2017). The global

health expenditure for managing diabetes and its complications has risen from USD 673 billion in 2015 to USD 727 billion in 2017 (International Diabetes Federation, 2017). With the increasing prevalence of type II diabetes globally and its increased burden on mortality, it is considered one of the emerging pandemics of the present century (Zheng et al., 2018).

1.1.1 Clinical diagnosis

Early diagnosis of type II diabetes is essential to achieve good glycemic control, and prevent the risk of irreversible complications (Bailey, 2015). Clinical diagnosis is based on the measurement of the plasma glucose level which could be achieved by using any of the four plasma glucose criteria (i.e. fasting plasma glucose, oral glucose tolerance test, glycated haemoglobin (HbA1c) level, and random glucose test) (Chaudhury et al., 2017). All of the plasma glucose values pertaining to diabetes diagnosis in the present thesis are taken from the 2018 Diabetes Canada clinical practice guidelines (Punthakee et al., 2018).

Following fasting of at least 8 hours, a plasma glucose level more than, or equal to, 7.0 mmol/L is diagnosed as diabetic. In an oral glucose tolerance test, a glucose load of 75 g in solution form is orally administered to the patient, followed by the measurement of the plasma glucose level after 2 hours. Glucose levels equivalent to, or more than, 11.1 mmol/L is diagnosed as diabetic. HbA1c depicts the average plasma glucose level over 2-3 months by measuring the percentage of glucose bound to haemoglobin. A glycated haemoglobin percent level more than or equal to 6.5-7.0% is considered diabetic (Chaudhury et al., 2017). In a random glucose test, the plasma glucose level is measured at any time of the day irrespective of any condition of fasting or timed interval of intake for the subject's last meal. A level equal or more than 11.1 mmol/L falls under

the diabetic range and should be further confirmed using other methods if the individual is asymptomatic. HbA1c more efficiently predicts diabetic complications compared to the other three diagnostic measures, and helps monitor the effectiveness of any glycemic management measures (Stratton, 2000). Diagnosis for individuals with type II diabetic symptoms could be confirmed using a single laboratory test, while in the absence of diabetic symptoms, a repetitive confirmatory diagnostic test is recommended (Punthakee et al., 2018).

1.1.2 Complications

If not managed, the elevated level of glucose in the blood over a period of time may result in lipotoxicity, glucotoxicity, autoimmune dysfunction, inflammation, endoplasmic reticulum stress, oxidative stress, and beta-cell apoptosis, the latter ultimately leading to the progressive loss of beta-cell functions and additional vascular complications (Cernea & Dobreanu, 2013). Traditionally, vascular complications can be broadly divided into macrovascular and microvascular. Microvascular complications are more prevalent among the two and cause damage primarily to the small blood vessels of the retina (retinopathy), nephrons in the kidney (nephropathy), and peripheral nerves (neuropathy) eventually leading to blindness, kidney failure, and sensory loss in the peripheral limbs (Stehouwer, 2018). Macrovascular complications narrow the arterial walls of the heart, brain, and peripheral blood vessels, promoting atherosclerosis, myocardial infarction, stroke, and peripheral vascular disease (Fowler, 2011). Arterial wall damage followed by chronic inflammation builds up plaques, which reduces the blood flow primarily to the heart, but also other parts of the body. This results in the aforementioned macrovascular complications and is the main pathological mechanism (Boyle, 2007). Apart from these, other possible complications can include oral health problems like

periodontal disease (Leite, Marlow, & Fernandes, 2013), birth complications, increased risk of infections like pneumonia and influenza (Deshpande, Harris-Hayes, & Schootman, 2008), mental health disorders (Strodl & Kenardy, 2006), and increased risk of cancers of the pancreas, endometrium, liver, breast, colon, and rectum (Giovannucci et al., 2010). Cardiovascular complications are the primary cause of death in individuals with type II diabetes (Zheng et al., 2018). The risk of developing cardiovascular disease in type II diabetic individuals is twice that of non-diabetic individuals, irrespective of other risk factors such as smoking status, age, body-mass index, and systolic blood pressure (Sarwar et al., 2010). Diabetic renal complications account for around 10% of the deaths caused as a result of type II diabetes (Dieren et al., 2010), and are more prevalent in Asian populations (Kong et al., 2013).

1.1.3 Current management options

To date, no complete cure for type II diabetes has been found (Olokoba, Obateru, & Olokoba, 2012). Reduction in the percent of glycated haemoglobin is a good indicator of improved glycemic control. For initiating an approach to manage hyperglycemia, there is a need to establish an HbA1c goal which is recommended to be less than or equal to 6.5-7.0% in most cases (Inzucchi et al., 2015). As per recent Canadian clinical guidelines pertaining to type II diabetes, if individuals with symptoms are diagnosed with HbA1C levels less than 1.5% above target, initial treatment options should be focused on healthy lifestyle interventions (Lipscombe et al., 2018). Lifestyle modifications involving nutrition and exercise are effective ways of improving blood glucose levels, specifically for the individuals on the borderline of type II diabetic classification (Tuomilehto et al., 2001). Benefits in the reduction of the occurrence of type II diabetes due to weight loss achieved by exercise, and dietary consumption of low free

carbohydrate, saturated and trans fats, and high complex dietary fibres has been well documented in the literature (Knowler et al., 2002; Riccardi, Capaldo, & Vaccaro, 2005; Riccardl & Wvellese, 1991). If healthy lifestyle modifications alone are not capable of achieving the HbA1c target within three months, antihyperglycemic medications should be considered. A patient with an HbA1c level of more than 1.5% above target should receive pharmacotherapy (Lipscombe et al., 2018). The choice of an antihyperglycemic agent is based on several factors including, hypoglycemic risk, the effect on body weight, side effects, cost, associated medical conditions, and patient compliance (Chaudhury et al., 2017). The first line antihyperglycemic agent recommended for type II diabetes is metformin due to its high efficacy, good safety profile, low hypoglycemic, weight gain and cardiovascular risks, and cost-effective potential (Maruthur et al., 2016). Metformin acts via both adenosine monophosphate-activated protein kinase (EC 2.7.11.31; AMPK)-dependent and independent mechanisms to exert its glucose-lowering effect (Foretz et al., 2014). It exhibits its action by suppressing the gluconeogenesis pathway, causing a reduction in hepatic glucose production, and enhancing the insulin sensitivity of peripheral tissues, such as skeletal and adipose tissue (Natali & Ferrannini, 2006). The safety profile of metformin is better than other developed biguanides, but it is still associated with rare risks of lactic acidosis, diarrhoea, abdominal cramps, and vitamin B12 deficiency (Inzucchi et al., 2015), and is contraindicated in patients with chronic kidney disease, dehydration, acidosis, or hypoxia (Inzucchi et al., 2015). If HbA1c targets are not met after metformin monotherapy, combination with other antihyperglycemic agents is recommended (Lipscombe et al., 2018) which has been shown to lower the HbA1c levels more than metformin alone (Phung et al., 2014). The second line antihyperglycemic agents for type II diabetes which can be used in combination with metformin include glucagon-like peptide-1 (GLP-1) receptor agonists, dipeptidyl peptidase-4

(EC 3.4.14.5; DPP-4) inhibitors, insulin secretagogues, thiazolidinediones targeting the nuclear transcription factor peroxisome proliferator-activated receptor gamma (PPAR-γ), sodium-glucose cotransporter-2 (SGLT-2) inhibitors, and insulin (Lipscombe et al., 2018).

GLP-1 receptor agonists are injectable, and stimulate insulin secretion in a glucose-dependent manner, inhibit glucagon secretion, delay gastric emptying to promote satiety, and aid in weight loss to effectively improve glucose homeostasis (Lipscombe et al., 2018). They are efficacious compared to other agents with no risk of hypoglycemia or weight gain, but are associated with side effects like diarrhoea, nausea, vomiting, pancreatitis, and C-cell hyperplasia of the thyroid (Inzucchi et al., 2015).

DPP-4 is a serine protease widely distributed in the body which rapidly metabolizes the incretins GLP-1 and glucose-dependent insulinotropic peptide (GIP) (Ahrén & Schmitz, 2004). DPP-4 inhibitors inhibit DPP-4, thereby raising the level of active incretins (Pratley & Salsali, 2007). Adverse reactions associated with the use of DPP-4 inhibitors include headache, upper respiratory tract infection, urticaria, dermatological effects, nasopharyngitis, and in some cases, acute pancreatitis (Chaudhury et al., 2017).

Insulin secretagogues, like sulfonylureas and meglitinide, increase insulin secretion by binding to sulfonylurea receptors in pancreatic beta cells, and blocking adenosine triphosphate (ATP)-sensitive potassium channels (K_{ATP}) (Proks et al., 2002). They are known to have high risks of hypoglycemia, with other side effects like weight gain, dizziness, nausea, headache, and hypersensitivity reactions (Chaudhury et al., 2017).

Thiazolidinedione compounds act as agonists at PPAR-γ (Thangavel et al., 2017). PPAR-γ activation lowers plasma free fatty acid levels and circulating triglycerides by primarily increasing the synthesis of acyl-CoA synthase (EC 2.3.1.86), lipoprotein lipase (EC 3.1.1.34) and phosphoenolpyruvate carboxykinase (EC 4.1.1.32) (Bermudez et al., 2010). Activation of PPAR-γ has also been shown to elevate the expression of insulin receptor substrates 1 and 2, glucokinase (EC 2.7.1.2) and glucose transporter 4 (GLUT4) (Kim & Ahn, 2004). Taken together, PPAR-γ activation by thiazolidinediones enhances glucose metabolism and insulin sensitivity and reduces triglyceride concentrations in the blood (Kahn, Chen, & Cohen, 2000). Thiazolidinediones are associated with oedema, heart failure, hepatotoxicity, weight gain, increased susceptibility to fractures, diarrhoea, and increased incidence of bladder cancer (Davidson et al., 2018).

SGLT-2 is a transport protein primarily expressed in the proximal convoluted tubule (PCT) of the kidney, which facilitates the active transport of glucose across the PCT by the sodium gradient that is generated by the sodium-potassium ATPase pump (Taylor & Harris, 2013). SGLT-2 inhibitors are glucosuric agents which prevent the reabsorption of glucose and facilitate its excretion through micturition (Inzucchi et al., 2015). Although they possess low risks of hypoglycemia and weight gain, they still come with pronounced side effects such as increased urinary tract infections, genital mycotic infections, acute kidney injury, bone fractures, and skin reactions (Filippas-Ntekouan, Filippatos, & Elisaf, 2018).

If type II diabetic individuals are not able to meet their HbA1c targets despite the use of intensive drug therapy involving the use of two or more antihyperglycemic agents, insulin

analogues should be considered as an addition to the treatment (Inzucchi et al., 2015). Combination therapy with insulin and other antihyperglycemic agents has been shown to give better glycemic control compared to when either is used alone (Lipscombe et al., 2018). Insulin therapy however, shows low patient compliance and is associated with the risk of developing hypoglycemia and significant weight gain (Lipscombe et al., 2018).

1.2 Insulin

Insulin is an endocrine hormone secreted by the beta cells of the pancreatic islets of Langerhans. Biologically active, secreted insulin consists of two peptide chains, A and B, containing 21 and 30 amino acids, which are linked together by two disulfide bonds (Fargion et al., 2005). The *INS* gene on chromosome 11 is initially transcribed to preproinsulin mRNA and then translated to the peptide preproinsulin. Preproinsulin is processed to proinsulin in the rough endoplasmic reticulum (RER) by cleavage of the signal sequence of preproinsulin by signal peptidase (EC 3.4.21.89) (Patzelt et al., 1978). This removal aids proinsulin to stabilize and acquire its 3D structure by linking the A and B chains with the C chain through three disulfide bonds. From here, proinsulin transits through the Golgi apparatus where it is packed in immature storage vesicles. Proinsulin is further processed by the prohormone convertases (PC1; EC 3.4.21.93 and PC2; EC 3.4.21.94), resulting in the cleavage of the C-peptide chain (Steiner et al., 1992). Once immature storage vesicles transcend out of the Golgi apparatus, they are transformed to mature secretory vesicles now containing biologically active insulin, by the enzyme carboxypeptidase E (EC 3.4.17.10) (Hutton, 1994). Within the matured secretory vesicles insulin exists in a hexameric crystalline form coupled with a zinc cation. Along with the insulin in the secretory vesicles, an equimolar concentration of C-peptide is present, which can be utilized to indirectly

measure the endogenous insulin secretion. This process of insulin biosynthesis is both very efficient (with only approximately 1-2% of proinsulin left in the matured secretory vesicles) and rapid (taking less than 2 hours to complete) (Tokarz, MacDonald, & Klip, 2018).

1.2.1 Insulin Physiology

Insulin secretory granules, through a series of tightly regulated mechanisms as described in the section 1.2.1.1, dock with the plasma membrane to release the insulin outside the beta cells into the interstitial space of the pancreas in response to glucose or other secretagogues. From here insulin enters the portal circulation where it can undergo hepatic clearance to ensure desired blood concentrations are maintained (Tokarz, MacDonald, & Klip, 2018).

One of the major functions of insulin is to increase glucose uptake in the liver by increasing the activity of glucokinase and thus phosphorylation of glucose, and in skeletal muscle and adipose tissue by stimulating the translocation of glucose transporter (GLUT) 4 to the plasma membrane. In liver and skeletal muscle, insulin also promotes glycogenesis, defined as the biochemical process for the synthesis of glycogen from glucose. In the same tissues, insulin inhibits glycogenolysis, the biochemical process of breakdown of glycogen to glucose, by reducing the phosphorylation of glycogen phosphorylase (EC 2.4.1.1) and glycogen synthase (EC 2.4.1.11). Insulin also inhibits gluconeogenesis, the biochemical process for the synthesis of glucose from the non-carbohydrate precursors such as glycerol, lactate, and amino acids, to promote glucose storage. Apart from storing energy, insulin promotes glycolysis with subsequent generation of ATP for utilization by the cells (Han et al., 2016).

Other than glucose, insulin also promotes the uptake of fatty acids from the bloodstream into adipose tissues. Insulin stimulates lipogenesis, defined as the biochemical process of synthesis of fatty acid from the carbon precursors of acetyl-CoA, predominantly in the liver and adipose tissues. It does so by stimulating the activity of pyruvate dehydrogenase phosphatase (EC 3.1.3.43), and the rate-limiting enzyme acetyl-CoA carboxylase (EC 6.4.1.2). Insulin in concert with β-adrenergic stimulation favours the storage of fatty acids and inhibits the rate of lipolysis by regulating cyclic adenosine monophosphate (cAMP) levels (Jönsson et al., 2019). It does so by inhibiting protein kinase B (EC 2.7.11.11; AKT) phosphorylation at both Ser^{473} and Thr^{308}, with subsequent activation of phosphodiesterase-3B (EC 3.1.4.17; PDE3B) which hydrolyzes cAMP to AMP (Jönsson et al., 2019). Activation of β-adrenergic receptors stimulate adenylate cyclase (EC 4.6.1.1)-dependent production of cAMP, with subsequent activation of protein kinase A (EC 2.7.11.11; PKA). PKA phosphorylates hormone-sensitive lipase (EC 3.1.1.79) and perilipin-1, which along with monoacylglycerol lipase (EC 3.1.1.23), hydrolyzes triacylglycerol to glycerol and fatty acid in adipose tissues (Nilsson et al., 1980). Hence, insulin-driven hydrolysis of cAMP via PDE3B inhibits the lipolytic activity of adipose tissue. Insulin also reduces the rate of fatty acid oxidation in liver and skeletal muscle, which along with the insulin-induced decreased lipolysis in adipose tissue, aids in regulating glucose utilization by these tissues (Dimitriadis et al., 2011). In skeletal muscle, insulin promotes the uptake of amino acids from the circulation and enhances muscle protein synthesis while inhibiting protein breakdown (Wolfe, 2000).

Although the concentration of insulin reaching the central nervous system (CNS) is one-third of that in the bloodstream, it evokes several centrally regulated functions by activating insulin

receptors present in the CNS. This includes the regulation of appetite by lowering neuropeptide Y expression, the regulation of body temperature, and the suppression of gluconeogenesis regulated in part by insulin receptors expressed specifically in the agouti-related protein expressing neurons (Kleinridders et al., 2014). The regulation of gluconeogenesis by insulin in the CNS occurs via ATP-dependent potassium channels and phosphoinositide 3-kinase (EC 2.7.1.137) mediated pathways (Obici et al., 2002). A recent study has also shown insulin modulates memory, cognition, and mood (Lee et al., 2016). The molecular mechanisms for these responses are not known and need further study.

1.2.1.1 Secretory mechanism

Glucose is the primary metabolic stimulus for insulin secretion, although other hormones, macronutrients, and inputs from the CNS may alter this response. The molecular mechanism involving the relay of the biochemical signal to the electrical signal contributing to insulin exocytosis in response to glucose is depicted in Figure 1.1. Briefly, glucose enters the pancreatic beta cells through glucose transporter GLUT1 in humans, and GLUT2 in rodents (McCulloch et al., 2011). Once inside the cell, it undergoes phosphorylation catalyzed by the glucokinase enzyme to form glucose-6-phosphate. Glucose-6-phosphate through the glycolysis cascade generates the downstream metabolite pyruvate. Pyruvate feeds the mitochondrial citric acid cycle (CAC) ultimately generating ATP through oxidative phosphorylation. Both glucokinase and the GLUT2 transporter together act as the glucose-sensors because their K_m values are in the range (7 mmol/L – 17 mmol/L) of normal changes in the physiological glucose concentrations

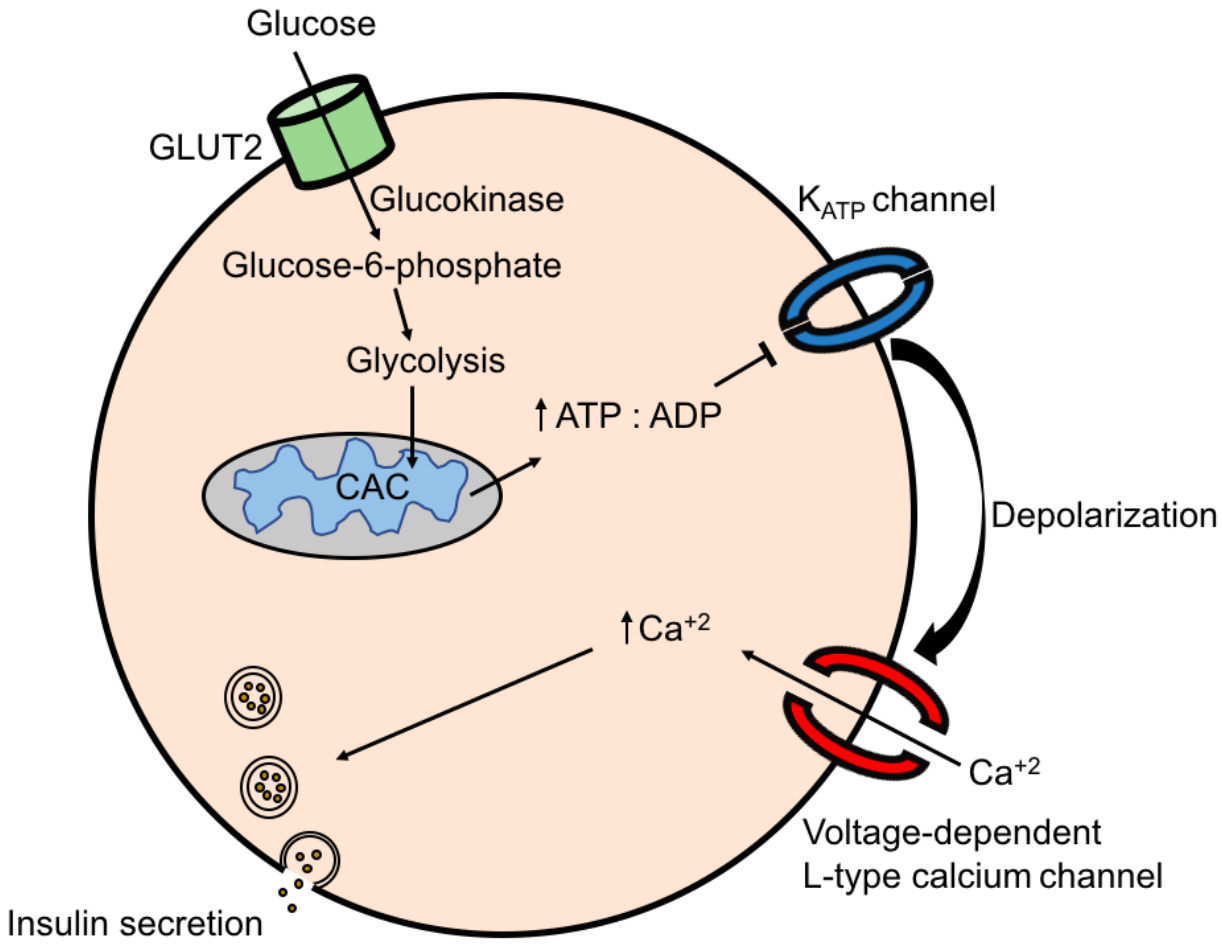

Figure 1.1: Glucose-stimulated insulin secretion mechanism

Glucose enters the beta cell via GLUT2 receptor and initiates the signaling cascade via glycolysis, and CAC to generate ATP, resulting in an increased cytosolic ATP/ADP ratio. This leads to the closure of the K_{ATP} ion channels which subsequently depolarize the plasma membrane resulting in the opening of the voltage-dependent L-type calcium ion channels. The increased influx of Ca^{+2} triggers the fusion of the insulin granules with the plasma membrane causing insulin secretion.

contributing to glucose homeostasis (Efrat, Tal, & Lodish, 1994). The resulting increase in the cytosolic ATP/ADP ratio results in the closure of K_{ATP} ion channels. This depolarizes the plasma membrane of the beta-cell. This step marks the transition of the biochemical signal to the electrical signal. If the membrane adequately depolarizes to a threshold potential of approximately -55 mV to -50 mV, voltage-dependent L-type calcium ion channels are activated allowing the influx of calcium into the cell (Rorsman, Braun, & Zhang, 2012). The increased influx of calcium ions then couples with the synaptotagmins (Syts) family of proteins, particularly Syt7 in pancreatic beta cells (Gustavsson et al., 2008). Subsequent interaction with soluble *N*-ethylmaleimide-sensitive factor attachment protein (SNAP) receptor (SNARE) core complex formed between the *target (t-)* SNARE proteins syntaxin 1 and SNAP 25 located on the plasma membrane, and *vesicle (v-)* SNARE protein synaptobrevin 2, also known as vesicle-associated membrane protein 2 (VAMP2), incorporated into the insulin vesicle membrane has been shown to modulate insulin exocytosis (Brewer et al., 2015; Choi et al., 2010).

Synaptotagmins are characterized by the presence of two C-terminal subdomains, C2A and C2B, in their structure. Both of them contain calcium-binding motifs allowing binding with calcium ions (Sutton et al., 1995). The SNARE complex has been shown to be regulated by Sec1/Munc18-like (SM) adaptor protein (Zhu et al., 2015). Munc18 binds to syntaxin 1 (Misura, Scheller, & Weis, 2000), followed by the recruitment of SNAP-25 at the plasma membrane (Gandasi & Barg, 2014). Rab3A, a small guanine nucleotide triphosphatase (GTPase) from the Rab family that is associated with the insulin granule, binds with Rab3-interacting-molecule (RIM)2α to then initiate vesicle docking (Yasuda et al., 2010). Rab3A binding with munc18 has also been reported and implicated in vesicle docking (Tsuboi & Fukuda, 2006). Another member

of the SM protein family, munc13, has been shown to bind with the syntaxin-munc18 complex priming the granule for exocytosis (Ma et al., 2011). Binding of Rab3A and RIM2α with munc13 has also been shown to facilitate the munc13 priming function (Dulubova et al., 2005). The increase in the influx of calcium ions therefore triggers the binding of Syt7 with the SNARE core complex resulting in the fusion of insulin granules with the plasma membrane eliciting insulin release from the beta cells (Röder et al., 2016).

Glucose-stimulated insulin secretion (GSIS) is bi-phasic in humans, where the first phase is marked by the rapid release of the insulin granules from the readily releasable pool (RRP), consisting of less than 5% of total insulin granules, that have already docked at the plasma membrane. This phase lasts up to 10 minutes (Wang & Thurmond, 2009). The second phase of insulin secretion involves insulin granules from the reserve pool (RP), containing 75% - 95% of insulin granules, mobilizing to the cell membrane, following actin cytoskeleton remodelling regulated by glucose-stimulated Rho family protein members, particularly Rho, Cdc42, and Rac, and subsequent docking to the cell membrane (Wilson, Ludowyke, & Biden, 2001). Glucose-stimulated activation of a small GTPase, Cdc42, triggers phosphorylation of p21-activated kinase (EC 2.7.11.1; PAK1) with subsequent activation of Rac1 (Kalwat & Thurmond, 2013). Rac1 in its GTP-bound form has been shown (Azuma et al., 1998) to signal through calcium-dependent filamentous actin (F-actin) binding protein gelsolin to promote reorganization of the F-actin cytoskeletal network. Gelsolin has been shown to interact with the t-SNARE protein syntaxin 4 at the plasma membrane to stimulate insulin exocytosis (Kalwat et al., 2012). Taken together, the second phase of insulin secretion represents the recruitment of the RP insulin granules to the plasma membrane through actin reorganization in response to glucose or other stimuli (see

below). Overall, insulin secretion encompassing both the phases corresponds to the total dose of glucose being administered (Tokarz, MacDonald, & Klip, 2018). Loss of the first phase of insulin secretion, and reduced second phase insulin secretion is a characteristic feature of impaired glucose tolerance and type II diabetes (Davis et al., 1993).

Apart from glucose, insulin secretion is also modulated by other nutrients, hormones, and autonomic inputs which can modify the insulin secretory response by either altering the electrical/calcium responses or controlling the efficacy of the exocytotic machinery of beta cells. For instance, incretin hormones secreted from the intestinal endocrine cells act on G protein-coupled receptors (GPCRs), to potentiate insulin secretion in a glucose-dependent manner via the G_s protein signalling cascade (Tengholm, 2012), enhancing the cytosolic cAMP levels which further downstream phosphorylates the exocytotic machinery of beta cells in PKA-dependent manner, and stimulates calcium release in an exchange protein activated by cAMP (Epac)-dependent fashion (Kolic & Macdonald, 2015).

Considering the data from the international diabetes federation, side effects associated with the current management therapies of type II diabetes, and the complications associated with type II diabetes, there is a need to develop safe and alternative therapies. Recent studies have focused on novel GPCRs and their role in modulating glucose homeostasis. One such GPCR, termed trace amine-associated receptor (TAAR)1 is activated by a class of compounds called trace amines. Multiple groups (Cripps et al., 2020; Michael et al., 2019; Raab et al., 2016) have recently reported TAAR1 as a potential novel target for the treatment of type II diabetes.

1.3 Trace amines

Trace amines (TAs) are a group of endogenous amines which are present in vertebrate tissues at very low concentrations, usually below 500 ng/g tissue (Gainetdinov, Hoener, & Berry, 2018) or in the range 0.1-100 nM, representing less than 1% of the total biogenic amines (Durden & Davis, 1993; Durden & Philips, 1980). TAs include 2-phenylethylamine (PEA), *para*-tyramine (TYR), tryptamine (TRP), *para*-octopamine (OCT), and *para*-synephrine (SYN). They are structurally analogous to the classical biogenic amines like epinephrine, norepinephrine, dopamine, and serotonin (5-HT).

TAs are not thought to be neurotransmitters because they are not released in response to potassium-induced depolarization (Dyck, 1989), suggesting they are not stored in synaptic vesicles (Juorio, Greenshaw, & Wishart, 1988), readily diffuse across lipid bilayers (Berry, 2004) and exert no effect alone on neuronal excitability at their physiological concentrations (Berry et al., 1994; Jones, 1981). They have a rapid turnover rate compared to classical biogenic amines, and a half-life of less than 15 seconds (Durden & Philips, 1980), consistent with not being stored in synaptic vesicles (Berry et al., 2013). Despite this, TAs in the CNS interact with various neurotransmitter systems, and are suggested to modulate neurotransmitter responses to maintain the basal tone of neurons (Henwood, Boulton, & Phillis, 1979; Lundberg, Oreland, & Engberg, 1985; Paterson, 1993). Deregulation of trace amine concentrations has been linked to several neurological disorders including schizophrenia, depression, mood change, and substance abuse disorders (Berry, 2007).

Exogenously TA are found in commonly consumed foods like chocolate, red wine, soy products, fermented meats, aged cheese (Berry et al., 2017), and foods produced upon anaerobic fermentation (Gardini et al., 2016; Toro-Funes et al., 2015). They can also be produced by the intestinal microbiota, through decarboxylation of dietary amino acids (Yang et al., 2016).

1.3.1 Endogenous TA Synthesis

TAs, specifically PEA, TYR, and TRP, are synthesized by the decarboxylation of the aromatic amino acid precursors L-phenylalanine, L-tyrosine, and L-tryptophan by aromatic L-amino acid decarboxylase (EC 4.1.1.28; AADC) (Boulton, 1982) (Figure 1.2). Subsequently, *p*-octopamine and *p*-synephrine can be synthesized upon action by the enzymes dopamine-ß-hydroxylase (EC 1.14.17.1; DßH) and phenylethanolamine-*N*-methyl transferase (EC 2.1.1.28; PNMT) (Boulton & Wu, 1972) (Figure 1.2). The latter enzyme further aids in the synthesis of *N*-methylated secondary amines such as *N*-methylphenylethylamine from PEA, and *N*-methyltyramine from TYR. Similar to this, indolethylamine *N*-methyltransferase (EC 2.1.1.49; INMT) yields *N*-methyltryptamine upon its action on TRP (Lindemann & Hoener, 2005). For TA synthesis, since AADC is the only enzyme involved, it is considered as a rate-limiting factor (Berry et al., 1996). Not only is the structure of TAs similar to classical monoamine neurotransmitters but also the pathway by which they are synthesized is analogous (Figure 1.2).

D-neurons of the CNS have been shown to specifically express AADC, but not the other enzymes involved in the synthesis of catecholamines or 5HT, suggesting D-neurons may be a dedicated neuronal system for TAs (Berry et al., 2017). AADC has also been found to be expressed in non-neuronal cells outside the CNS such as kidney, liver, pancreas, lungs, and

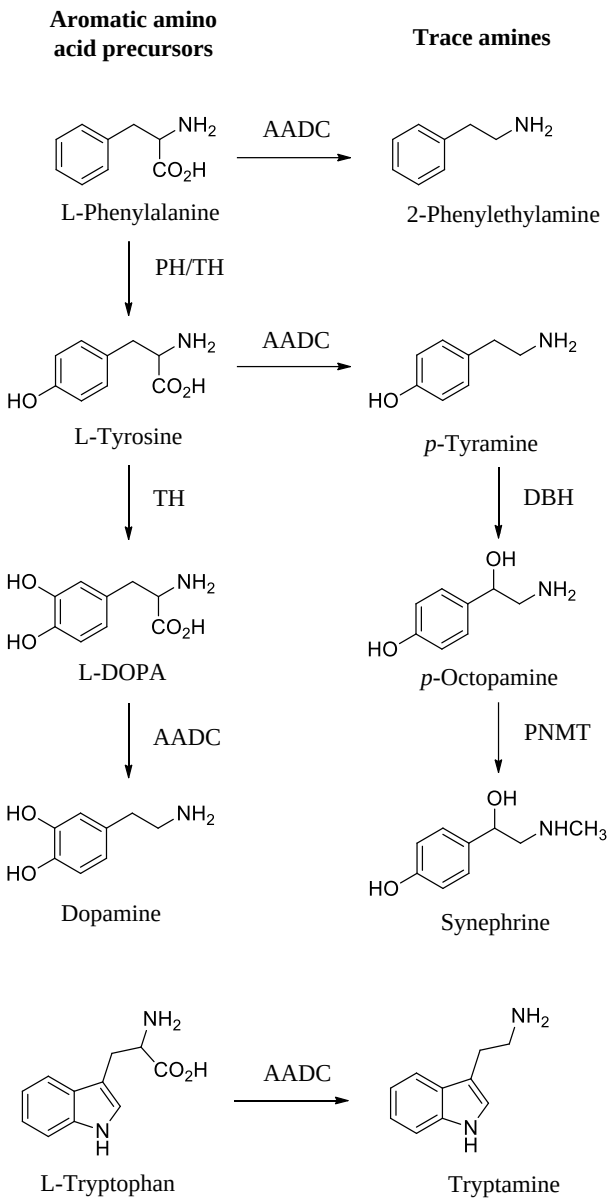

Figure 1.2: Biosynthetic pathway of trace amines

AADC: Aromatic L-amino acid decarboxylase; DBH: Dopamine ß-hydroxylase; PH: Phenylalanine hydroxylase; PNMT: Phenylethanolamine *N*-methyl transferase; TH: Tyrosine hydroxylase

gastrointestinal tract (Berry et al., 1996) where it can synthesize TAs from the aromatic amino acid precursors to elicit TA action peripherally. AADC has been shown to be regulated both at the gene expression and enzyme activity level. AADC is regulated in a biphasic manner with the initial short-term changes due to altered phosphorylation status of the enzyme, followed by delayed long lasting changes in its expression (Berry et al., 1996). AADC activity is decreased in response to dopaminergic and adrenergic receptor agonists, with subsequent decreases in TA levels (Hadjiconstantinou et al., 1993; Rossetti et al., 1990; Zhu et al., 1993), while activity is increased in response to antagonists at these receptors, leading to elevated TA levels (Neff et al., 2006; Zhu et al., 1992). This suggests that the regulation of AADC activity modulates the TA levels in response to monoaminergic neurotransmitter signalling.

1.3.2 TA Degradation

TAs are primarily metabolized by the oxidation of the aliphatic amino group by the enzyme monoamine oxidase (EC 1.4.3.4; MAO) (Philips & Boulton, 1979) (Figure 1.3). MAO has two isoforms, MAO-A and MAO-B (Shih & Chen, 2004). Apart from PEA which is a highly selective substrate for MAO-B (Yang & Neff, 1973), all other TAs are metabolized by both MAO-A and MAO-B (Durden & Philips, 1980; Philips & Boulton, 1979). Apart from MAO, TAs have also been reported to be catabolized by the enzyme semicarbazide-sensitive amine oxidase (SSAO; EC 1.4.3.21), also known as amine oxidase, copper containing 3 (AOC3) or vascular adhesion protein-1 (VAP-1) (Elliott, Callingham, & Sharman, 1989). Tyramine has also been shown to be metabolized by cytochrome P_{450} isozymes and flavin monooxygenase 3 (FMO3; EC 1.14.13.8) in isolated human livers (Niwa et al., 2011).

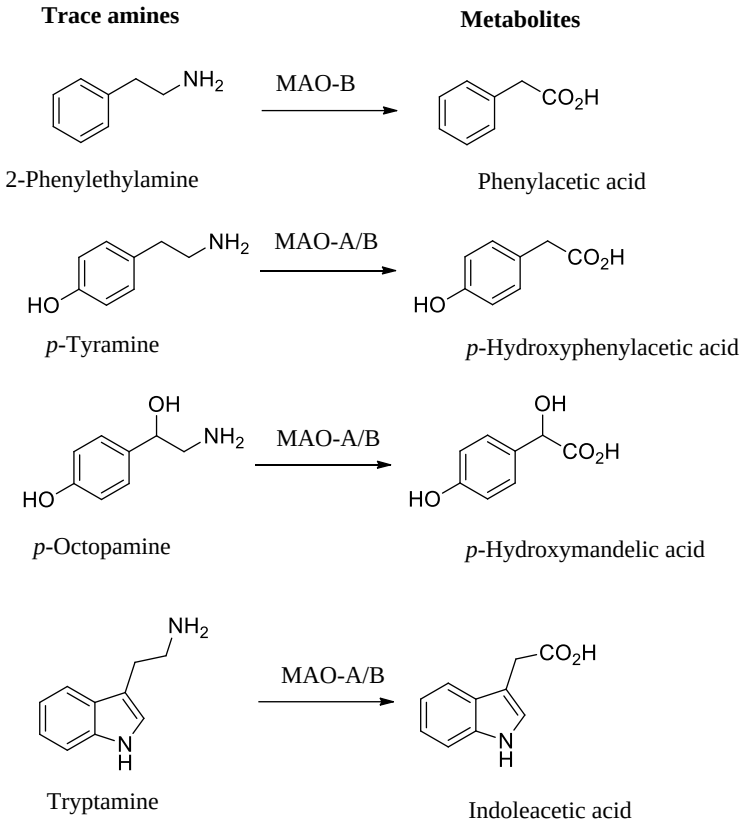

Figure 1.3: Trace amines and their metabolites

MAO-A: Monoamine oxidase A; MAO-B: Monoamine oxidase B

1.4 Trace amine-associated receptors

TAs have been known for 150 years, but not many studies were carried out on this unique class of compounds because of the lack of knowledge regarding their receptor targets. This trend changed in 2001 when two independent groups of researchers identified a new class of GPCRs which are highly selective for TAs, specifically PEA and TYR (Borowsky et al., 2001; Bunzow et al., 2001). Later these GPCRs under a standardized system of nomenclature became named as trace amine-associated receptors (TAARs) (Lindemann et al., 2005).

The receptors for detecting TAs are evolutionarily distinct in vertebrates and invertebrates (Lindemann et al., 2005). This makes TAARs specific to vertebrates, and they have been shown to be present in all vertebrate species examined so far (Gainetdinov et al., 2018) except bottlenose dolphin (Eyun et al., 2016). Twenty-eight sub-families of vertebrate TAARs have been identified (Hussain et al., 2009). Out of these, TAAR1-9 are expressed in terrestrial mammals while TAAR10-28 are only found in aquatic vertebrates. Individual TAARs can also have multiple isoforms, many of which appear to be species-specific (Eyun et al., 2016; Hussain et al., 2009; Vallender et al., 2010). All TAARs are single exon genes with the exception of TAAR2 (Lindemann et al., 2005) and are clustered in a single chromosomal location in non-aquatic vertebrates (Eyun et al., 2016; Lindemann et al., 2005). In humans, TAAR genes are localized to chromosomal 6q23.1 (Lindemann et al., 2005).

The existence of different functional TAAR genes and pseudogenes between vertebrate species indicates huge species variation (Table 1.1). This difference in the TAAR expression profile

Table 1.1: Functional TAAR genes and pseudogenes in different vertebrate species

Species	Functional TAAR genes	TAAR Pseudogenes	References
Human	6	3	(Lindemann et al., 2005)
Chimpanzee	3	6	(Lindemann et al., 2005)
Orangutan	3	5	(Vallender et al., 2010)
Mouse	15	1	(Hashiguchi & Nishida, 2007; Lindemann et al., 2005)
Rat	17	2	(Eyun et al., 2016; Lindemann et al., 2005)

between species is evolutionarily dictated by environmental adaptive responses (Churcher et al., 2015). Out of TAAR1-9, humans express a single functional variant of TAAR1, TAAR2, TAAR5, TAAR6, TAAR8, and TAAR9 with three pseudogenes also present, TAAR 3, TAAR4, and TAAR7 (Lindemann et al., 2005).

TAARs are expressed throughout the body but due to their low expression levels, and lack of selective reagents, knowledge of their roles in any species is sparse except for TAAR1 (Berry et al., 2017). TAAR1 tissue distribution and associated role in the body is described in detail in later sections (1.5.1, 1.5.4 and 1.5.5). Except TAAR1, all other TAARs are present in the olfactory epithelium and serve chemosensory functions in identifying social and ecologically relevant cues (Horowitz et al., 2014; Liberles, 2015; Liberles & Buck, 2006; Santos et al., 2016). In the olfactory epithelium, they are co-expressed with G_{olf} to induce cAMP accumulation (Liberles & Buck, 2006).

In addition to the olfactory epithelium (Liberles & Buck, 2006), TAAR2 is found in human and mouse leukocytes (Babusyte et al., 2013), and in rat heart and testis (Chiellini et al., 2012). Although no ligand for TAAR2 has been identified, TAAR2 is required to initiate leukocyte migration in response to PEA (Babusyte et al., 2013). This may suggest that TAAR2 is required to elicit TAAR1 mediated chemotactic responses through heterodimerization with TAAR1 (Babusyte et al., 2013). In a study with small sample size, a single nucleotide polymorphism in TAAR2 was reported to be linked to schizophrenia (Bly, 2005).

TAAR5 is expressed primarily in the olfactory epithelium (Li et al., 2013; Wallrabenstein et al., 2013), although low levels have also been shown in leukocytes (Babusyte et al., 2013), and different brain regions of the mouse (Dinter et al., 2015; Espinoza et al., 2020). A recent study (Aleksandrov et al., 2018) using a novel, synthetic and selective TAAR5 agonist, 2-(α-naphthoyl)ethyltrimethylammonium iodide has suggested a role for TAAR5 in sensory gating in rats, possibly indicating a role for TAAR5 in schizophrenia, which is marked by sensory gating deficits. Trimethylamine (TMA), a tertiary amine, has been found to be a highly selective agonist at human TAAR5 (Liberles & Buck, 2006; Wallrabenstein et al., 2013). Degradation of TMA in hepatic tissue via FMO3 generates trimethylamine-*N*-oxide (TMAO) (Fennema, Phillips, & Shephard, 2016), a metabolite positively correlated with an increased risk of developing cardiovascular and metabolic disease (Zhang & Davies, 2016). A direct correlation of TMA levels with atherosclerosis in HIV patients has also been observed (Srinivasa et al., 2015). Raised TMA levels have also been reported to be a biomarker for renal cell carcinoma (Gao et al., 2008). Elevated levels of TMA in urine, sweat or blood, a pathological condition termed as trimethylaminuria, is an indicator of potential kidney damage (Chhibber-Goel et al., 2016). A genetic deficiency in FMO3 would also result in trimethylaminuria (Humbert et al., 1970). A recent report of loss of function mutation in TAAR5 in some Icelandic populations affecting odor perception has been demonstrated (Gisladottir et al., 2020). This suggests human TAAR5 as a functional chemosensory receptor. Another tertiary amine *N*,*N*-dimethylethylamine has been shown to exert a less potent partial agonistic response at human TAAR5 (Zhang et al., 2013). The TAAR1 agonist and thyroid hormone metabolite 3-iodothyronamine (T_1AM) has been reported to be an inverse agonist at human TAAR5 (Dinter et al., 2015).

TAAR6 expression beyond the olfactory epithelium has been reported in mouse duodenal cells (Ito et al., 2009), rat testis and spinal cord (Chiellini et al., 2012), and in humans is present in several brain regions such as basal ganglia, frontal cortex, substantia nigra (Duan et al., 2004), hippocampus and amygdala (Borowsky et al., 2001; Duan et al., 2004), kidney (Borowsky et al., 2001), and leukocytes (Babusyte et al., 2013). No ligand for TAAR6 has been identified. Different studies have identified TAAR6 genetic variants (Pae et al., 2010) and single nucleotide polymorphisms (Chang et al., 2015) in individuals diagnosed with schizophrenia (Pae et al., 2008) and mood disorders (Pae et al., 2010). This suggests a potential link between TAAR6 polymorphisms and schizophrenia (Duan et al., 2004; Pae et al., 2008). TAAR6 polymorphisms have also been shown to influence the therapeutic responses to aripiprazole (Serretti et al., 2009), an atypical anti-psychotic drug, and responsiveness to corticosterone in asthma patients (Chang et al., 2015).

Ligands for human TAAR8 and TAAR9 are also unknown. However, isoforms of rat TAAR8 and TAAR9 have been shown to be activated by the tertiary amines *N*-methylpiperidine and *N*,*N*,-dimethylcyclohexylamine (Ferrero et al., 2012; Liberles & Buck, 2006). One study (Li et al., 2015) has also shown the presence of a diamine binding pocket in TAAR8. TAAR8 transcripts have been reported in the human amygdala (Borowsky et al., 2001) and leukocytes (Babusyte et al., 2013). Different isoforms of TAAR8 have been shown to be present in rat cerebellum and cortex (Chiellini et al., 2012), spinal cord (Gozal et al., 2014), various mouse brain regions (Mühlhaus et al., 2014), kidney, intestines, heart, lung, spleen, stomach and testis (Chiellini et al., 2012).

Human TAAR9 mRNA has been reported in leukocytes (Babusyte et al., 2013), skeletal muscle, and pituitary gland (Vanti et al., 2003). TAAR9 mRNA has also been found in rat spinal cord (Gozal et al., 2014), mouse spleen (Regard et al., 2007) and duodenal mucosal cells (Ito et al., 2009).

1.5 Trace amine-associated receptor1

1.5.1 Ligands

Among TAARs, TAAR1 is the most studied member because of its well-established endogenous ligands (Gainetdinov et al., 2018). TAAR1 is activated by primary amines and considered as a major target for PEA and TYR (Berry et al., 2017). Along with PEA and TYR other endogenous compounds such as TRP, *p*-octopamine (Bunzow et al., 2001; Lindemann et al., 2005), T_1AM (Scanlan et al., 2004), and the dopamine metabolite 3-methoxytyramine (Sotnikova et al., 2010) are also high-affinity ligands which exert full agonistic responses at TAAR1. Dopamine and 5-HT also activate TAAR1 as partial agonists (Lindemann et al., 2005). In addition, drugs of abuse such as amphetamine, methamphetamine, and 3,4-methylenedioxymethamphetamine potently activate TAAR1 (Simmler et al., 2016). Recently a novel series of synthetic TAAR1 ligands, based on a 2-aminooxazoline scaffold, which are highly potent, and selective at human TAAR1 were generated at Hoffmann-La Roche (Galley et al., 2016). Four ligands from this series (RO5166017, RO5203648, RO5263397 and RO5256390) were chosen to further characterize TAAR1 mediated functions, RO5166017 and RO5256390 are highly selective full agonists, while the remaining two are partial agonists (Galley et al., 2016). Apart from the above ligands Hoffmann-La Roche also developed the first TAAR1 antagonist RO5212773 (EPPTB) (Bradaia

et al., 2009), which is highly potent at mouse TAAR1, but has limited activity at the rat and human receptors (Berry et al., 2017).

1.5.2 TAAR1 Tissue expression

Due to the low expression profile of TAAR1, and specifically a lack of commercially available selective antibodies for the individual TAARs, it is challenging to demonstrate TAAR1 protein expression (Berry et al., 2017), although this is better characterized than other members of the TAAR family (Berry et al., 2017). Hoffmann-La Roche has recently developed two highly selective TAAR1 antibodies directed against human (Raab et al., 2016) and rat (Harmeier et al., 2015) receptors that are functional in immunohistochemistry protocols (human) and western blot analysis (rat). TAAR1 protein has been confirmed to be present throughout the body except the olfactory epithelium (Liberles & Buck, 2006), in both the central nervous system (Borowsky et al., 2001; Lindemann et al., 2008) as well as in peripheral tissues (Adriaenssens et al., 2015; Babusyte et al., 2013; Ito et al., 2009; Pitts et al., 2019; Raab et al., 2016).

In the CNS of both rodents and primates TAAR1 mRNA and protein has been found to be heterogeneously expressed in dopaminergic, serotonergic, and glutamatergic neurons and their projection areas (Berry et al., 2017). Specific areas in the brain where TAAR1 expression has been demonstrated in the dopaminergic system are the ventral tegmental area (VTA) and substantia nigra pars compacta; in the serotonergic system the dorsal raphe and VTA; and in the glutamatergic system in the amygdala, hippocampus and subiculum. Not only is TAAR1 expressed at the origin of these monoaminergic neurons but it is also distributed across their neuronal projection areas such as the prefrontal cortex, basal ganglia, and limbic regions

(Borowsky et al., 2001; Lindemann et al., 2008). TAAR1 expression has also been demonstrated in rat spinal cord (Gozal et al., 2014).

In the periphery, TAAR1 is expressed in the somatostatin producing stomach D-cells (Adriaenssens et al., 2015), insulin-secreting pancreatic beta cells (Regard et al., 2007; Raab et al., 2016), and intestinal endocrine cells involved in nutrient-induced hormone secretion (Ito et al., 2009; Raab et al., 2016). Expression of TAAR1 mRNA and protein has also been reported in various leukocyte populations (Babusyte et al., 2013; Nelson et al., 2007) and breast cancer cell lines (Pitts et al., 2019). Compared to breast cancer cell lines, a higher TAAR1 mRNA expression has been reported in normal breast tissue (Pitts et al., 2019).

Unlike most GPCRs, TAAR1 protein has been consistently reported to be intracellular (Bunzow et al., 2001; Lindemann & Hoener, 2005; Pitts et al., 2019; Raab et al., 2016) due to lack of *N*-glycosylation sites (Barak et al., 2008). However, heterodimerization with other GPCRs may promote the translocation of TAAR1 to the plasma membrane (Espinoza et al., 2011; Harmeier et al., 2015).

1.5.3 Signal transduction cascades

TAAR1 is coupled to the G_s protein promoting the activation of adenylyl cyclase with subsequent cAMP production (Borowsky et al., 2001; Bunzow et al., 2001). In both dopaminergic and serotonergic neuronal projection areas, TAAR1 has been shown to also couple with G-protein-gated potassium ion channels (GirK) (Bradaia et al., 2009). TAAR1-mediated GirK activation in these neurons induces opening of the inwardly rectifying potassium channels,

resulting in membrane hyperpolarization and a reduction in the neuronal firing frequency (Revel et al., 2011).

TAAR1 has also been shown to heterodimerize with dopamine D_2-like receptors (D2R) both *in-vitro* and *in-vivo*. This interaction results in TAAR1 regulation of both pre- and post-synaptic D2R, and vice versa (Espinoza et al., 2011; Harmeier et al., 2015). D2R can signal through the G-protein independent ß-arrestin 2 cascade leading to AKT dephosphorylation, and subsequent glycogen synthase kinase-3 beta (EC 2.7.11.26; GSK3ß) activation (Beaulieu, Gainetdinov, & Caron, 2009). Heterodimerization of TAAR1 with D2R has been reported to increase TAAR1 interactions with ß-arrestin 2 (Harmeier et al., 2015). This TAAR1-mediated ß-arrestin 2 recruitment phosphorylates AKT with subsequent inactivation of GSK3ß signalling (Espinoza et al., 2015; Harmeier et al., 2015). The AKT/GSK3ß signalling pathway has been suggested to have aetiologic relevance in the pathology of neuropsychiatric disorders (Beaulieu, Gainetdinov, & Caron, 2009). Considering this TAAR1-D2R mediated negative modulation of GSK3ß signaling might have future clinical implications.

In a study based on TAAR1 signalling in rhesus monkey lymphocytes two downstream targets of TAAR1 activation, nuclear factor of activated T-cells (NFAT) and cAMP response element-binding protein (CREB) were identified, and associated with immune activation (Panas et al., 2012). In the same study, TAAR1 activation by methamphetamine was reported to phosphorylate PKA and protein kinase C (EC 2.7.11.13; PKC). Very recently an *in-vitro* study on TAAR1 signalling, in pancreatic beta-cell lines, has identified several downstream TAAR1 targets, including adenylyl cyclase, cAMP, PKA, Epac, the inositol trisphosphate (IP_3) receptor,

calcium/calmodulin-dependent protein kinase II (EC 2.7.11.17; CaMKII), rapidly accelerated fibrosarcoma (Raf), mitogen-activated protein kinase kinase 1/2 (EC 2.7.12.2; MEK1/2), extracellular signal-regulated kinase 1/2 (EC 2.7.11.24; ERK1/2), and CREB, all of which are involved in enhanced insulin secretion and beta-cell proliferation upon TAAR1 activation (Michael et al., 2019).

1.5.4 Role in CNS

Several studies in mouse, rat, rhesus monkey, and human CNS have demonstrated the expression of TAAR1 in the primary dopaminergic areas such as the VTA and substantia nigra where it modulates dopaminergic neurotransmission (Berry et al., 2017; Borowsky et al., 2001; Lindemann & Hoener, 2005; Xie et al., 2007). In a study (Bradaia et al., 2009) using TAAR1-KO mice, the firing frequency of dopaminergic neurons of the VTA, determined through electrophysiological measurements, was shown to be significantly enhanced. In the same study using wild type mice, the firing rate of these neurons was potently increased by using the TAAR1 antagonist RO5212773 and decreased upon using different TAAR1 agonists. Overall TAAR1 activation in the dopaminergic system acts to prevent hyperactivity of the neurons (Revel et al., 2011). This also suggests the potential role of TAAR1 in modulating dopaminergic neurotransmission involved in eliciting locomotor, behavioral and emotional responses (Lindemann et al., 2008). This TAAR1 modulation of dopaminergic neurotransmission can occur at both pre-synaptic (Xie & Miller, 2008, 2009) and post-synaptic sites (Espinoza et al., 2015) by interacting with pre- and post-synaptic D2R (Berry et al., 2017). TAAR1 has also been suggested to regulate dopamine transporter (DAT) function (Xie, Westmoreland, & Miller, 2008). G_{13} coupled-TAAR1 activation of small GTPase RhoA inside the brain has been shown to

stimulate DAT internalization (Underhill et al., 2019). The same study has also shown that Gs coupled-TAAR1 signaling through PKA with subsequent RhoA phosphorylation inhibits DAT endocytosis. Interestingly, TAAR1 retains its functions even in the absence of DAT (Leo et al., 2018) supporting the presence of a mechanism of entry of TAAR1 ligands into the cells. It could be diffusion across the lipid bilayers (Berry et al., 2013) or probably membrane transporter OCT2 as reported earlier (Berry et al., 2016).

The expression of TAAR1 in the serotonergic system suggests its role in the modulation of serotonergic neurotransmission. TAAR1 activation in the dorsal raphe neurons of the serotonergic system has been shown to reduce the firing rate of these neurons (Revel et al., 2011). Consistent with this, in the same study, TAAR1-KO mice demonstrated an increased firing rate of the serotonergic neurons, with no effect of TAAR1 agonist. In another study, TAAR1 partial agonism in the dorsal raphe neurons also augmented the firing rate of the serotonergic neurons (Revel et al., 2012). TAs in the serotonergic system have been suggested to also modulate serotonin transporter functions through $5HT_{1A}$ autoreceptors and TAAR1 (Xie et al., 2008).

In the glutamatergic system TAAR1 has been shown to regulate transmission by regulating *N*-methyl-D-aspartate (NMDA) receptor subunit GluN1, resulting in enhanced excitatory post-synaptic potentials (Espinoza et al., 2015). TAAR1 agonists in the same system also reverse the hyperlocomotion induced by NMDA receptor antagonists, suggesting an additional antipsychotic potential of TAAR1 (Revel et al., 2011). Studies (Espinoza et al., 2015) in the prefrontal cortex of TAAR1-KO mice have shown a decrease in the total levels of GluN1 and GluN2B NMDA

receptor subunits, and an exacerbated phosphorylation of the post-synaptic GluA1 AMPA receptor (AMPAR) subunit (Alvarsson et al., 2015). This results in an overall decrease in the NMDA/AMPA receptor ratio that was associated with increased preservative and impulsive behavioral responses that are associated with cognitive symptoms of schizophrenia (Espinoza et al., 2015). TAAR1 agonists have been shown to reduce these behaviors in wild-type mice suggesting a potential role in preventing the cognitive deficits associated with decreased NMDA receptor function (Revel et al., 2013; Revel et al., 2011). Mapping of TAAR1 to layer V cortical neurons (Espinoza et al., 2015), many of which project to the striatum, and alterations in both total and phosphorylated levels of GluN1 in the striatum of TAAR1-KO mice, suggests a further role for TAAR1 in modulating corticostriatal glutamatergic neurotransmission (Sukhanov et al., 2016). Methamphetamine-mediated TAAR1 activation in human astrocytes has been shown to reduce glutamate clearance by down regulating excitatory amino acid transporter-2 (EAAT-2) (Cisneros & Ghorpade, 2014; Ding et al., 2017). Overall TAAR1-mediated selective regulation of both glutamate receptors and transporters can prevent hypoactivity of the glutamatergic system (Gainetdinov et al., 2018; Revel et al., 2011).

Together, the above studies suggest TAAR1 ligands may be useful in the treatment of neuropsychiatric disorders such as schizophrenia, depression, bipolar disorder, drug abuse and addiction as well as in neurodegenerative disorders such as Parkinson's disease (Berry, 2007; Berry et al., 2017). That the localization of human TAAR genes overlaps with the schizophrenia susceptibility locus SCZD5 particularly suggests a potential role of TAARs in this disorder (Duan et al., 2004). The unique ability of TAAR1 agonists to simultaneously prevent the hyperactivity of dopaminergic and hypoactivity of glutamatergic neural circuits make them a

particularly relevant and unique pharmacotherapeutic agent for treating schizophrenia (Berry et al., 2017) and beneficial effects in disease-relevant animal model systems have been observed (Revel et al., 2013). Indeed, clinical trials of SEP-363856, a TAAR1-directed agent for schizophrenia are in progress and has been reported to have a good safety and efficacy profile in schizophrenia patients (Dedic et al., 2019).

Reduced levels of TAs in the CNS were previously correlated with depression-like symptoms (Davis & Boulton, 1994; Sandler et al., 1980). In the forced swim stress test, a validated paradigm for the assessment of antidepressant-like activity, TAAR1 partial agonists have been shown to reduce the time spent immobile in a dose-dependent manner, suggesting an anti-depressant effect of TAAR1 (Revel et al., 2013; Revel et al., 2012). Along with its anti-psychotic potential, the above study indicates a putative role of TAAR1 in the management of bipolar disorder (Revel et al., 2013). TAAR1 agonism in the dopaminergic system has also been shown to prevent pleasure or reward-seeking effects that are mediated by the dopaminergic system indicating a possible role of TAAR1 in the pharmacotherapy of drug abuse and addiction disorders (Gainetdinov et al., 2018). Indeed, the ability of TAAR1 to heterodimerize with D2R with subsequent recruitment of ß-arrestin 2 cascade has been shown to be the basis of TAAR1 regulation of cocaine-mediated effects (Asif-Malik et al., 2017). TAAR1 has been shown to be beneficial in reducing the addictive/abuse potential of amphetamines (Cotter et al., 2015), cocaine (Pei et al., 2014; Thorn et al., 2014a), nicotine (Liu et al., 2018), ethanol (Lynch et al., 2013), and binge eating of palatable food (Ferragud et al., 2017).

Parkinson's disease is a progressive neurodegenerative disorder resulting in the deficiency of dopamine (Beitz, 2014). Therefore, the dopamine precursor levodopa is used to treat Parkinson's symptoms (Katzenschlager & Lees, 2002). However, levodopa is associated with dyskinesia (Cenci, Ohlin, & Rylander, 2009), and alternate periods of exacerbated movements and immobility (Menza et al., 1990) which make its long term use difficult. The TAAR1 agonists RO5166017 (Alvarsson et al., 2015) and 3-methoxytyramine (Sotnikova et al., 2010) have been shown to prevent such levodopa-induced dyskinesias. Along with TAAR1 agonists, TAAR1 antagonists are also suggested to be effective in preventing levodopa-induced dyskinesias (Sotnikova et al., 2008). Inhibitors of MAO and catecholamine-*O*-methyltransferase (COMT; EC 2.1.1.6), key enzymes involved in the degradation of TAs, have also been clinically used in the treatment of Parkinson's disease (Espinoza et al., 2012).

Taken together, there is convincing evidence that TAAR1 in the CNS regulates reward, cognitive, limbic, and mood-related neurocircuitry by modulating dopaminergic, serotonergic, and glutamatergic responses (Berry et al., 2017).

1.5.5 Role in the periphery

Most of the studies of TAAR1 have focused on its CNS effects with much less known about its role in the periphery. TAAR1 expression in the periphery has now been ascertained in stomach D cells (Adriaenssens et al., 2015), pancreatic beta cells, and intestinal neuroendocrine cells (Raab et al., 2016). Somatostatin release from the stomach D cells following TAAR1 activation has been demonstrated, which suggests a role of TAAR1 in the control of post-feeding hormone secretion and nutrient absorption (Adriaenssens et al., 2015). Immunohistochemical staining

using a specific anti-human TAAR1 antibody, identified a co-expression of TAAR1 with GLP-1 and the gut hormone peptide YY (PYY) in human duodenal sections (Raab et al., 2016). The same group has also shown that TAAR1 activation in the intestinal tissues of C57BL/6 mice significantly elevates GLP-1 and PYY levels 30 minutes after an oral glucose load. These two hormones are involved in improving glucose homeostasis (Baggio & Drucker, 2007), and promoting satiety (Manning & Batterham, 2014). TAAR1 activation has also been reported to lower food intake, and body weight in C57BL/6 mice resulting in improved insulin sensitivity (Raab et al., 2016).

TAAR1 expression has also been identified in different leukocytes populations, including T cells, B cells, granulocytes, and natural killer cells (Babusyte et al., 2013; Nelson et al., 2007). TAAR1 in leukocytes has been shown to be involved in the regulation of secretion of cytokines and immunoglobulins, and in mediating chemotactic responses (Babusyte et al., 2013).

Unlike its low expression profile elsewhere, TAAR1 mRNA in mouse pancreatic islets (Regard et al., 2007; Revel et al., 2012) and the rat pancreatic beta cell line INS-1E (Raab et al., 2016) have been shown to be among the most enriched and highly expressed. TAAR1 mRNA abundance in isolated human islets preparations was also confirmed by independent studies (Raab et al., 2016; Regard et al., 2007). This indicates TAAR1 might be involved in the regulation of hormones secreted from pancreatic beta cells.

1.5.5.1 Role in pancreatic beta cells

Consistent with the TAAR1 mRNA expression in pancreatic beta cells, immunohistochemical staining using a high quality and selective anti-human TAAR1 antibody revealed a co-localization of TAAR1 protein with insulin, but not with glucagon, in isolated human islets (Raab et al., 2016). TAAR1 activation by the physiological ligands TYR, PEA and T_1AM in different studies using the rat INS-1 cells, MIN6 and INS-1E cell lines has been shown to potentiate GSIS (Cripps et al., 2020; Michael et al., 2019; Regard et al., 2007). Similarly, TAAR1 activation by a selective TAAR1 agonist RO5166017 in both INS-1E cells and human islets has been shown to augment GSIS (Raab et al., 2016). Consistent with this, a recent study (Cripps et al., 2020) using the selective TAAR1 antagonist RO5212773 in INS-1 cells has shown a TAAR1 antagonism induced reduction in GSIS.

The increase in GSIS following TAAR1 activation has been reported to be observed only at elevated, but not at basal, glucose concentrations (Michael et al., 2019; Raab et al., 2016) suggesting TAAR1 mediated insulin secretion is glucose-dependent and would have a lower risk of inducing hypoglycemia in vivo. An *in-vivo* study in C57BL/6 mice has also shown an enhanced GSIS following TAAR1 activation (Raab et al., 2016) along with a significant reduction in the glucose area under the curve following an oral glucose challenge. Such effects were not seen in TAAR1 KO littermates, suggesting that the improved oral glucose tolerance effects are specifically TAAR1-mediated (Raab et al., 2016). This cAMP-mediated GSIS is similar to GLP-1 receptor signalling, suggesting that TAAR1 induces similar effects to the endogenous incretin GLP-1 (Michael et al., 2019; Raab et al., 2016).

Taken together, the TAAR1 role in potentiating GSIS both *in-vitro* and *in-vivo* at higher, but not at basal, glucose concentrations suggests that TAAR1 could be a potential therapeutic target for type II diabetes treatment (Raab et al., 2016). However, the downstream signalling cascade of TAAR1 involved in the regulation of GSIS is not entirely understood and warrants further study. Very recently these downstream events have begun to be elucidated. TAAR1-mediated GSIS utilizes the G_s-coupled adenylyl cyclase-cAMP dependent signaling pathway (Cripps et al., 2020; Michael et al., 2019). Epac and PKA, downstream targets of cAMP, together have been shown to be sufficient to elicit maximal GSIS response upon TAAR1 activation (Michael et al., 2019). TAAR1 activation has also been shown to stimulate calcium flux from internal stores via the IP_3 receptor followed by further cytosolic calcium influx from external sources (Michael et al., 2019). However, whether this enhanced calcium flux following TAAR1 activation could potentiate GSIS has not been shown. Together, there is a need to validate these results to further determine the molecular mechanism of TAAR1 regulation of GSIS.

1.6 INS-1E cell line

INS-1E cells represent a functional beta cell model which were isolated from the parental INS-1 cells (Janjic et al., 1999). INS-1 cells were initially isolated from an x-ray-induced rat insulinoma (Asfari et al., 1992). To overcome the issue of low stability of INS-1 cells over passages, and its non-clonal nature, INS-1E cells with better characteristics were isolated from the parental INS-1 cells. INS-1E cells are usually stable over a wide range of passages but are recommended to be used within the passage range of 40-100 to ensure insulin responsivity to varying glucose concentrations (2.5 – 20 mM) (Merglen et al., 2004). A comprehensive study (Merglen et al., 2004) on INS-1E characterization has shown that INS-1E cells exhibit glucose- and

secretagogue-stimulated insulin secretory responses, strong cell to cell communication properties and glucose-stimulated electrophysiological properties that mimic native pancreatic beta-cell functions, making them a useful tool for studying insulin secretory mechanisms. INS-1E cells have also been shown to express abundant TAAR1 mRNA as revealed by quantitative real-time PCR analysis and protein (Raab et al., 2016). Overall, these characteristics make INS-1E cell lines a favourable *in-vitro* beta-cell model for my study.

1.7 Research objective and hypothesis

1.7.1 Objective

The primary objective of this thesis is to determine the molecular mechanism(s) of TAAR1 regulation of glucose-dependent insulin secretion.

1.7.2 Hypothesis

TAAR1 regulates the activity of K_{ATP} ion channel component of the glucose-stimulated insulin secretion pathway.

2.0 Materials and Methods

2.1 RO5256390 formulations

RO5256390 ((S)-4-((S)-2-phenylbutyl)-4,5-dihydrooxazol-2-ylamine), chemically a 2-aminooxazoline, a highly selective ligand of TAAR1 exhibiting full agonistic response (Galley et al., 2016), was a generous gift by F. Hoffmann-La Roche Ltd., Basel, Switzerland. RO5256390 concentrations of 100 nM, 10 nM and 1 nM were used for all the *in-vitro* experiments in the present study. Stock solutions of RO5256390 (10 mM) were prepared in 100% dimethyl sulfoxide (DMSO). These were then diluted 100 times using de-ionized water to give 100 µM RO5256390 in 1% DMSO. Further working dilutions were prepared using 1% DMSO for *in-vitro* cell culture studies. Working dilutions were freshly prepared on the day of the experiment; 10 mM stock solutions were stored at -20 °C for up to two months.

2.2 INS-1E cell culture

2.2.1 Materials

Gibco™ RPMI 1640 powdered medium, Gibco™ fetal bovine serum, Gibco™ sodium pyruvate (100mM), Gibco™ HEPES (1 M), Gibco™ penicillin-streptomycin (10,000 U/mL), Gibco™ 2-mercaptoethanol, Gibco™ trypan blue solution (0.4%), Corning™ T-25 and T-75 culture flasks, Falcon™ 24-well polystyrene microplates, and Thermo Scientific™ Nunc™ microwell™ 96-well optical-bottom plates with coverglass base were obtained from Fisher Scientific (Ottawa, Ontario); trypsin-EDTA solution (0.25%), poly-L-ornithine solution (0.01%), and phosphate buffered saline tablets were obtained from Sigma-Aldrich, (Oakville, Ontario); the INS-1E cell line was obtained from ATCC having an initial passage number of 30.

2.2.2 Cell culture

INS-1E cells were cultured using a protocol previously described (Sebokova et al., 2010). RPMI 1640 medium was prepared by mixing RPMI 1640 powder with deionized water, followed by the addition of analytical grade sodium bicarbonate (2 g/L) and adjusting the pH to 7.20. Complete INS-1E growth medium was prepared by adding 10% fetal bovine serum, 1 mM sodium pyruvate, 10 mM HEPES, 100 U/mL penicillin-streptomycin and 50 µM 2-mercaptoethanol to filter sterilized RPMI 1640 medium under aseptic conditions in a level 2 biosafety cabinet.

All culture flasks and plates were coated with poly-L-ornithine. For coating, 0.01% poly-L-ornithine (T-75 flask – 5 mL, T-25 flask – 2.5 mL, 24-well plate – 0.5 mL/well, and 96-well plate – 50 µL/well) was added to the cell culture vessel and placed into a CO_2 incubator at 37°C for 24 hours. The poly-L-ornithine solution was then aspirated, and the culture vessel was rinsed three times with pyrogen free water. The coated culture vessels were allowed to dry at room temperature in the biosafety cabinet and then stored in the cooler at 2-8°C for further experiments.

Prior to handling INS-1E frozen cells, a T-25 culture flask coated with poly-L-ornithine was filled with 5 mL complete INS-1E medium and placed into the incubator at 37 °C for at least 15 minutes. A frozen vial containing INS-1E cells was thawed quickly in a 37 °C water bath and cells were transferred to a centrifuge tube containing 5 mL complete INS-1E medium. The tube was then centrifuged at 400 x g for 5 minutes and the cell pellet resuspended into fresh 10 mL of complete INS-1E medium. INS-1E cells were plated into T-25 culture flasks at a density of 1 x

10^5 viable cells determined by trypan blue exclusion using a hemocytometer. To determine the number of cells per mL, the average cell count was multiplied by 10 (dilution factor) x 10,000 (hemocytometer factor). Cells were grown at 37 °C in a 5% CO_2 atmosphere until > 80% confluency was attained. The medium was changed every 2 days and upon reaching > 80% confluency, the cells were sub-cultured as per the protocol described below.

2.2.3 INS-1E sub-culture

After the cells reached > 80% confluency, the medium was removed from the T-25 flask and cells were rinsed once with 5 mL phosphate buffered saline (PBS) solution, which contained 0.01 M phosphate buffer, 0.0027 M KCl, and 0.137 M NaCl, pH 7.4 at 25°C. After rinsing, 2 mL of trypsin-EDTA (0.25%) solution was added to the cells, and incubated at 37 °C for 5 minutes. The flask was tapped 2-3 times to detach INS-1E cells from the surface of the flask. The cell suspension in the flask was then transferred to a centrifuge tube containing 5 mL of complete INS-1E medium and centrifuged at 400 x g for 5 minutes. After discarding the supernatant, the pellet was resuspended in fresh 10 mL of complete INS-1E medium by trituration. To a poly-L-ornithine coated T-75 flask filled with 20 mL of complete INS-1E medium, 1mL of the prepared cell suspension was added and placed in the incubator. The medium for the cells in T-75 flasks was changed every 2 days. Once cells reached > 80% confluency, they were harvested for seeding into culture plates, as per the protocol described below.

2.2.4 Sub-culture into 24 and 96-well plates

INS-1E cells for all the experiments in the current study were used within passages 33 - 67. Once cells grown in T-75 flasks reached > 80% confluency they were harvested as previously

described (Merglen et al., 2004). The total number of viable cells was determined by trypan blue exclusion using a hemocytometer. For all the experiments, each well of a 24-well plate was filled with 1 mL of cell suspension containing 2 x 10^5 INS-1E cells, whereas for 96-well plates, 100 µL of a cell suspension, prepared using complete INS-1E growth medium, containing either 2 x 10^4 or 5 x 10^4 INS-1E cells was used per well (Merglen et al., 2004). Seeded plates were incubated at 37 °C and 5% CO_2 for 72 hours to achieve > 80% confluency of INS-1E cells prior to use.

2.3 Insulin secretion measurements in INS1-E cells

This study was conducted in 24-well plates. INS-1E cells, seeded at 2 x 10^5 cells per well, were allowed to reach more than 80% confluency as described above. All subsequent steps were performed in Krebs-Ringer-bicarbonate-HEPES (KRBH) buffer (pH 7.4) containing 140 mM NaCl, 3.6 mM KCl, 0.5 mM of NaH_2PO_4, 0.5 mM $MgSO_4$, 2 mM $NaHCO_3$, 10 mM of HEPES, 1.5 mM $CaCl_2$ and 0.1% bovine serum albumin (BSA). Growth medium from the cells was aspirated and cells were rinsed three times with the KRBH buffer. Cells were starved by incubating in 1 mL of KRBH buffer for 30 minutes at 37 °C and 5% CO_2. The buffer was aspirated, and cells were rinsed once with KRBH buffer. Cells were then incubated with KRBH supplemented to give varying concentrations of glucose (2.5 , 5 , 10 , 15 and 20 mM) or KCl (3.6 , 15, 30 and 60 mM) in the absence or presence of various concentrations of RO5256390 (1, 10 and 100 nM) at 37 °C and 5% CO_2 for 2 hours. Following incubation, the KRBH buffer was collected for secreted insulin quantification, and cells were collected in Nonidet-P40 (NP-40) cell lysis buffer for the determination of total protein per well as per the protocol described below.

2.3.1 Insulin assay

Secreted insulin was determined using a Mercodia High Range Rat Insulin ELISA kit (Mercodia, Uppsala, Sweden). The insulin concentration was determined by reference to a calibration curve generated with the standard calibrators of the kit having rat insulin in the concentration range 3 – 150 µg/L (Fig. 2.1). For insulin quantification, 10 µL each of calibrator or cell samples was pipetted to the supplied 96-well microplate pre-coated with mouse monoclonal anti-insulin antibodies. To each well 50 µL of the enzyme conjugate 1X solution, containing peroxidase-conjugated mouse monoclonal anti-insulin antibodies was added and the plate was incubated on a plate shaker at 400 rpm for two hours at room temperature. Each well of the plate was washed with 350 µL of 1X wash buffer to remove unbound antibodies. Following washing, 200 µL of 3,3',5,5'-tetramethylbenzidine (TMB), a substrate for the peroxidase-conjugated antibody, was added to each well and the plate was incubated for 15 minutes at room temperature. The reaction was stopped by adding 50 µL of stop solution containing 0.5 M H_2SO_4. The absorbance of each well was measured at 450 nm using a Biotek Powerwave XS UV/Vis microplate spectrophotometer (Winooski, VT, USA) within 30 minutes of the reaction being stopped. A standard curve was plotted using GraphPad Prism 6.0e software (La Jolla California, USA) by cubic spline fit of absorbance values at each insulin concentration (µg/L) of the standard calibrators (Figure 2.1). Absorbance values of the experimental samples were interpolated from the standard curve for the determination of insulin concentration (µg/L). Secreted insulin was then normalized to the total cellular protein of each well as described below.

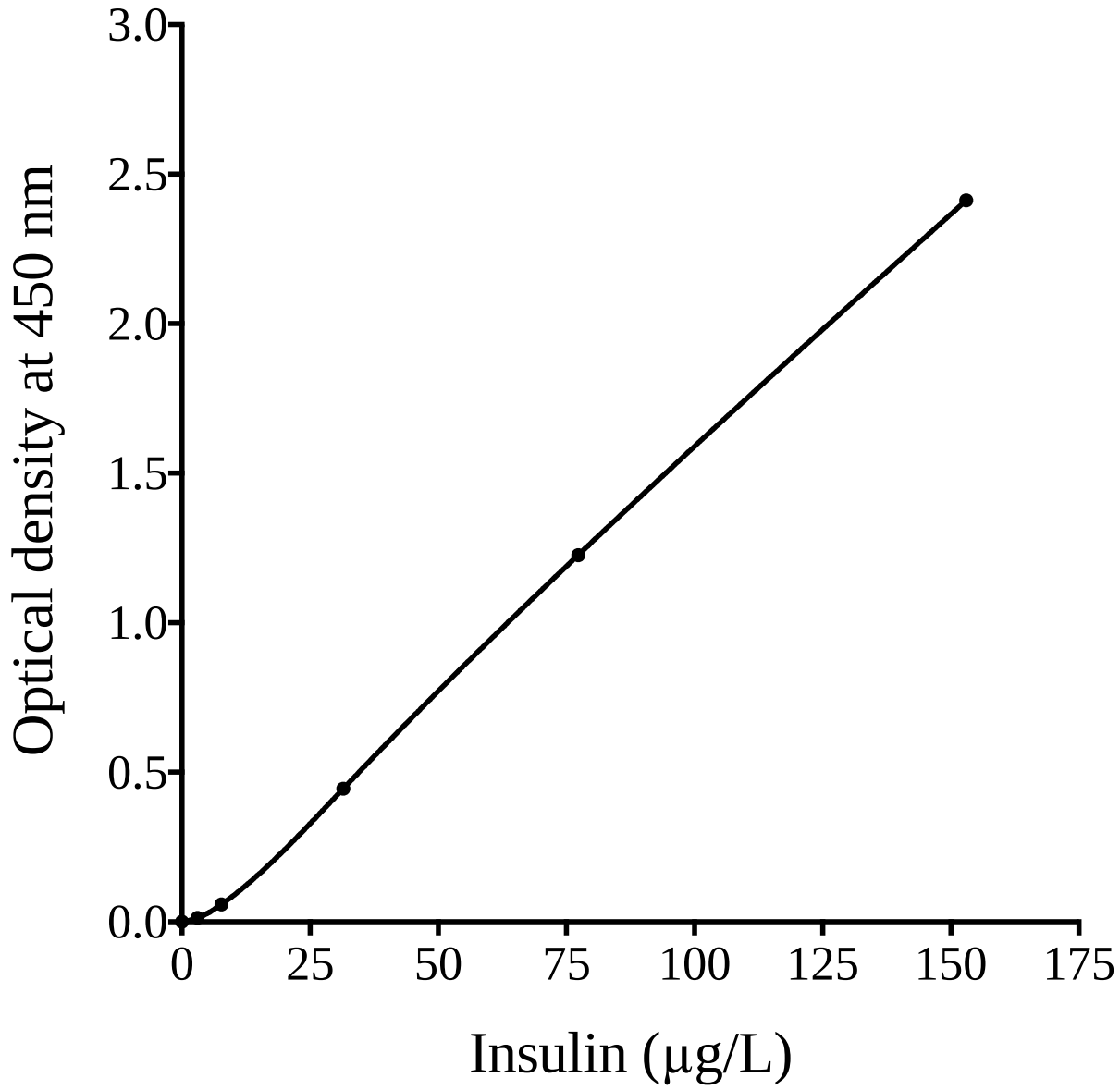

Figure 2.1: Sample Insulin ELISA assay standard curve for insulin (µg/L) determination

Baseline absorbance was corrected using a blank. The unknown insulin concentration was determined by interpolation of the absorbance values measured at 450 nm into the standard cubic spline regression curve determined using GraphPad Prism 6.0e.

2.3.2 BCA Protein assay

INS-1E cells in each well of the 24-well plate were collected by incubation with 50 µL NP-40 cell lysis buffer (20 mM Tris, 137 mM NaCl, 2 mM EDTA, 10% (v/v) glycerol, and 1% (v/v) NP-40), pH 8 at 37 °C and 5% CO_2 for 1 hour. Protein content per well was measured using a Thermo Scientific™ Pierce™ BCA Protein Assay Kit. Protein concentration (µg/10 µL) was determined by using a standard curve generated with BSA solutions in the concentration range 0 – 20 µg/10 µL (Figure 2.2). For protein quantification 10 µL each of BSA standard, or lysed cell samples were pipetted to Corning™ Clear Polystyrene 96-well microplates in duplicate. To each well of the plate, 200 µL of BCA working reagent was added and thoroughly mixed on a plate shaker at 400 rpm for 30 seconds. The plate was then incubated at 37 °C for 30 minutes. The absorbance of each well was measured at 562 nm using a Biotek Powerwave XS UV/Vis microplate spectrophotometer (Winooski, VT, USA). The protein concentration (µg/10 µL) was determined by computerized interpolation of absorbance values from a BSA standard linear regression curve (Figure 2.2) plotted using GraphPad Prism 6.0e software and corrected from µg/10 µL to total protein per well.

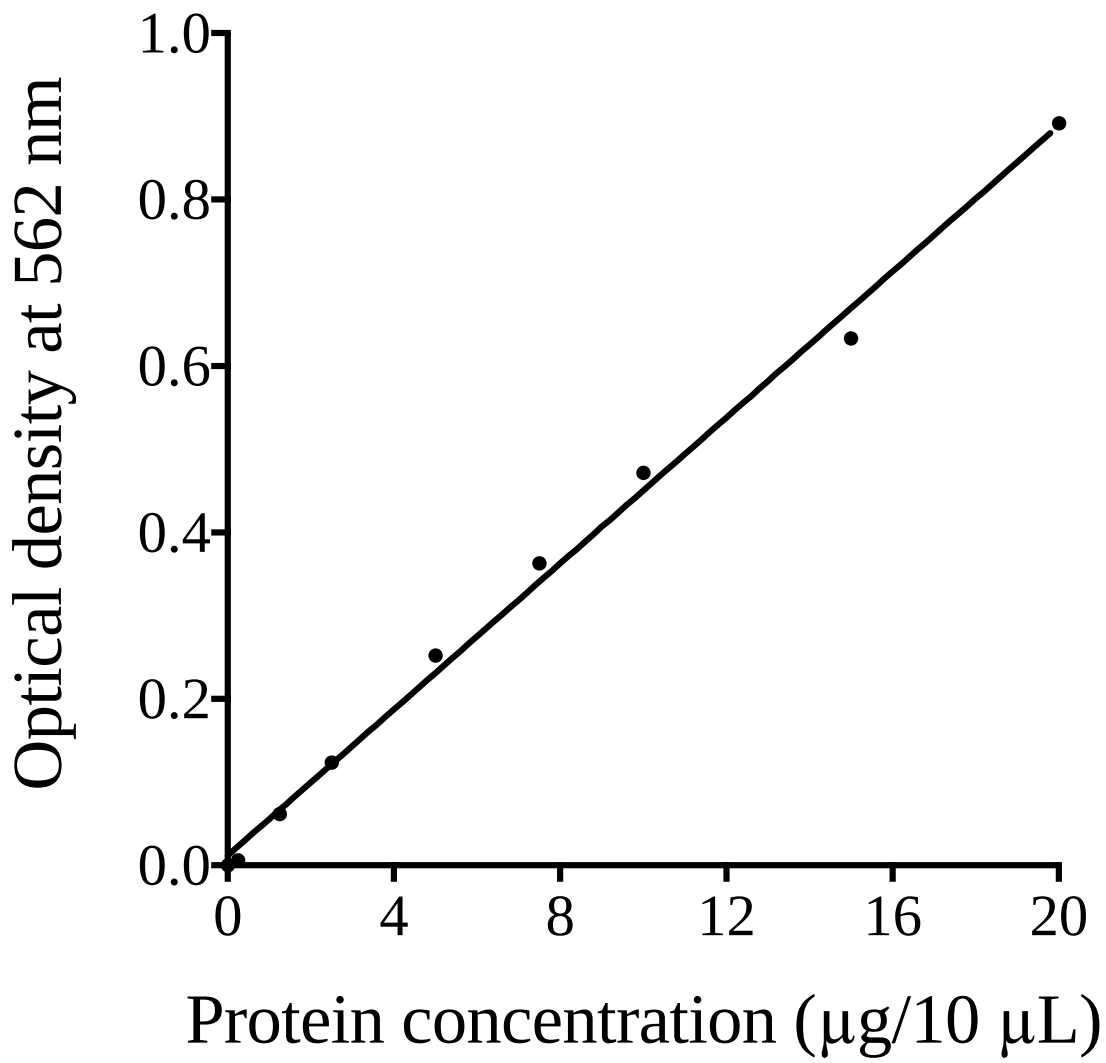

Figure 2.2: Representative BSA standard linear regression line for protein (µg/10 µL) determination

The absorbance measured at 562 nm versus increasing BSA standard concentrations yielded a linear regression line, from which the sample protein concentrations were determined.

2.4 Membrane potential measurement using $DiBAC_4(3)$

Invitrogen™ (bis-(1,3-dibutylbarbituric acid)trimethine oxonol) $DiBAC_4(3)$, obtained from Thermo Fisher Scientific (Ottawa, Ontario), is a slow-responsive voltage sensitive anionic dye that measures depolarization-induced change in plasma membrane potential by exhibiting fluorescence. The study was conducted in Thermo Scientific™ Nunc™ Microwell™ black walled, clear bottom 96-well plates at 20,000 and 50,000 cells/well. From the preliminary studies, $DiBAC_4(3)$ concentration (in KRBH buffer) that exhibits maximum fluorescence with > 80% confluent INS-1E cell culture was found to be 25 µM and was used for all subsequent experiments. Medium from the confluent cells in the 96-well plate was aspirated, and cells were rinsed three times with KRBH buffer. Cells were starved for 30 minutes using KRBH buffer containing $DiBAC_4(3)$ at 37 °C for 30 minutes in a SpectraMax M5e plate reader (Molecular devices, San Jose, California, USA). Baseline fluorescence was measured every 10 seconds of the last 5 minutes of the starvation period, at excitation and emission wavelengths of 490 nm and 516 nm respectively. Immediately following starvation, cells were incubated with KRBH buffer containing $DiBAC_4(3)$ and varying concentrations of glucose (2.5 , 5, 10, and 15 mM) or KCl (3.6, 15, 30 and 60 mM). Fluorescence was then measured at every 2 minutes over a period of two hours.

2.5 Bioinformatics

Bioinformatics is a multidisciplinary field of science that helps to analyze, and understand biological data by the application of computational tools (Luscombe, Greenbaum, & Gerstein, 2001). One of its main goals is to understand different biological pathways and processes through transcriptomics, which is the study of the whole set of RNA transcripts in a particular

cell under a specific condition (Raghavachari & Garcia-Reyero, 2018). Affymetrix DNA microarray-based gene chips, available commercially, contain different DNA sequences which upon hybridization with cDNA obtained from reverse-transcribed RNA isolated from a specific cell under defined conditions reveals differentially expressed genes (Bumgarner, 2013). A huge volume of such unique gene expression data has been submitted by the research community to several publicly available databases. One such database is GenBank at the National Center for Biotechnology Information (NCBI) which is the most accessed public database (Diniz & Canduri, 2017). Within different NCBI databases, the Gene Expression Omnibus (GEO) database provides microarray-based gene expression data pertaining to specific cells or experiments. GEO records provide a focal point to studies of a similar kind, linked altogether, and stored as GEO series (GSE), each identified with a unique accession number (Edgar, 2002). By applying clustering algorithms to the gene expression data from different GEO series pertaining to similar experiments, related gene expression profiles can be determined (Oyelade et al., 2016). One of the commonly used gene clustering algorithms is agglomerative average linkage hierarchical clustering, in which genes with similar expression patterns form clusters based on the minimal average distance between all pairs of cases within a cluster, such that genes with similar or opposite expression patterns would cluster together (Yim & Ramdeen, 2015). This expression pattern can be displayed by colour image plots termed heat maps (Sturn & Quackenbush, 2002). To assess the correlation between the expression pattern of genes, the distance between the clusters can be analyzed based on the type of data, e.g. Pearson correlation for a linear relationships, and Spearman correlation for monotonic relationships within the data (Jaskowiak, Campello, & Costa, 2014). Spearman rank correlation provides a rank-based similarity to the desired gene expression pattern and is more robust in its handling of outliers

compared to other distance measures (Timofeeva, 2019). Here I have used such techniques to identify genes whose expression correlates to that of TAAR1 across different microarray-based studies on insulin-secreting pancreatic beta cells in order to gain insight into the potential downstream networks of TAAR1 in pancreatic beta cells.

2.5.1 Affymetrix microarray data analysis

To gain insights into the potential regulatory networks of TAAR1 relevant to modulation of glucose-dependent insulin secretion, TAAR1 correlated transcripts in pancreatic beta-cells were identified using bioinformatic screening of publically available DNA microarray analysis datasets. Prior to analysis, based on the previous literature (see Introduction), a list of 149 genes with known relevance to either TAAR1 (marked with 'A') or glucose-stimulated insulin secretion (marked with 'B') or which were already known to be implicated in both (marked with 'C') was developed (Table 2.1). A total of seven Affymetrix microarray-based gene expression studies from humans, rats and mice, having at least three biological replicates, and specific to pancreatic beta cells were identified and downloaded from the publicly available genomic database NCBI GEO (Edgar, 2002). Based on the conditions the beta cells were exposed to, these studies were divided into two groups: beta cells under physiological conditions (three studies); and beta cells under pathological conditions (four studies) (Table 2.2). Affymetrix microarray data composed of CEL files was imported from the GEO database to R (version 3.5.1). The microarray expression data was then corrected for the background noise and normalized to all the genes in the Affymetrix gene chip using the Bioconductor (version 3.7) package "oligo" in R. The same package generated robust multi-chip average (RMA) normalized data.

Table 2.1: Potential target genes of TAAR1 regulation of glucose-dependent insulin secretion

Gene symbol	Gene name	Relevance to TAAR1 (A) or GSIS (B) or both the pathways (C)
Taar1	trace amine associated receptor 1	C
Gnas	GNAS complex locus	A
Gnb1	G protein subunit beta 1	A
Gnb2	G protein subunit beta 2	A
Gnb3	G protein subunit beta 3	A
Gnb4	G protein subunit beta 4	A
Gnb5	G protein subunit beta 5	A
Gngt1	G protein subunit gamma transducin 1	A
Gngt2	G protein subunit gamma transducin 2	A
Gng2	G protein subunit gamma 2	A
Gng3	G protein subunit gamma 3	A
Gng4	G protein subunit gamma 4	A
Gng5	G protein subunit gamma 5	A
Gng7	G protein subunit gamma 7	A
Gng8	G protein subunit gamma 8	A
Gng10	G protein subunit gamma 10	A

Gng11	G protein subunit gamma 11	A
Gng12	G protein subunit gamma 12	A
Gng13	G protein subunit gamma 13	A
Gng14	G protein subunit gamma 14	A
Adcy1	adenylate cyclase 1	A
Adcy2	adenylate cyclase 2	A
Adcy3	adenylate cyclase 3	A
Adcy4	adenylate cyclase 4	A
Adcy5	adenylate cyclase 5	A
Adcy6	adenylate cyclase 6	A
Adcy7	adenylate cyclase 7	A
Adcy8	adenylate cyclase 8	A
Adcy9	adenylate cyclase 9	A
Adcy10	adenylate cyclase 10	A
Prkaca	protein kinase cAMP-activated catalytic subunit alpha	A
Prkacb	protein kinase cAMP-activated catalytic subunit beta	A
Prkacg	protein kinase cAMP-activated catalytic subunit gamma	A
Prkar1A	protein kinase cAMP-dependent type I regulatory subunit alpha	A
Prkar1B	protein kinase cAMP-dependent type I regulatory subunit beta	A
Prkar2A	protein kinase cAMP-dependent type II regulatory subunit alpha	A

Prkar2B	protein kinase cAMP-dependent type II regulatory subunit beta	A
Prkca	protein kinase C, alpha	A
Prkcb	protein kinase C, beta	A
Prkcg	protein kinase C, gamma	A
Creb1	cAMP responsive element binding protein 1	C
Kcnj3	potassium inwardly-rectifying channel, subfamily J, member 3	A
Kcnj6	potassium inwardly-rectifying channel, subfamily J, member 6	A
Kcnj9	potassium inwardly-rectifying channel, subfamily J, member 9	A
Arrb2	arrestin, beta 2	A
Gsk3B	glycogen synthase kinase 3 beta	A
Ctnnb1	catenin beta 1	A
Drd2	dopamine receptor D2	A
Htr1A	5-hydroxytryptamine receptor 1A	A
Rhoa	ras homolog family member A	A
Akt2	AKT serine/threonine kinase 2	A
Grin1	glutamate ionotropic receptor NMDA type subunit 1	A
Grin2A	glutamate ionotropic receptor NMDA type subunit 2A	A
Grin2B	glutamate ionotropic receptor NMDA type subunit 2B	A
Grin2C	glutamate ionotropic receptor NMDA type subunit 2C	A

Grin2D	glutamate ionotropic receptor NMDA type subunit 2D	A
Nfatc1	nuclear factor of activated T-cells 1	A
Nfatc2	nuclear factor of activated T-cells 2	A
Nfkb1	nuclear factor kappa B subunit 1	A
Nfkb2	nuclear factor kappa B subunit 2	A
Gria1	glutamate ionotropic receptor AMPA type subunit 1	A
Gria2	glutamate ionotropic receptor AMPA type subunit 2	A
Gria3	glutamate ionotropic receptor AMPA type subunit 3	A
Gria4	glutamate ionotropic receptor AMPA type subunit 4	A
Slc1A2	solute carrier family 1 member 2	A
Erbb2	erb-b2 receptor tyrosine kinase 2	A
Ppp1R1B	protein phosphatase 1, regulatory inhibitor subunit 1B	A
Adra2A	adrenoceptor alpha 2A	A
Mapk1	mitogen-activated protein kinase 1	A
Mapk3	mitogen-activated protein kinase 3	A
Sstr3	somatostatin receptor 3	A
Gcg	glucagon	A
Pyy	peptide YY	A
Cftr	CF transmembrane conductance regulator	A
Ins2	insulin 2	B
Slc2A2	solute carrier family 2 member 2	B
Gck	glucokinase	B

Kcnj8	potassium inwardly-rectifying channel, subfamily J, member 8	B
Kcnj11	potassium inwardly-rectifying channel, subfamily J, member 11	B
Abcc8	ATP binding cassette subfamily C member 8	B
Abcc9	ATP binding cassette subfamily C member 9	B
Cacna1s	calcium voltage-gated channel subunit alpha1 S	B
Cacna1c	calcium voltage-gated channel subunit alpha1 C	B
Cacna1d	calcium voltage-gated channel subunit alpha1 D	B
Cacna1f	calcium voltage-gated channel subunit alpha1 F	B
Cacna1e	calcium voltage-gated channel subunit alpha1 E	B
Adora1	adenosine A1 receptor	B
Adora2A	adenosine A2a receptor	B
Adora2B	adenosine A2b receptor	B
Adora3	adenosine A3 receptor	B
Adra1A	adrenoceptor alpha 1A	B
Adra1B	adrenoceptor alpha 1B	B
Pde3B	phosphodiesterase 3B	B
Pde4A	phosphodiesterase 4A	B
Pde4B	phosphodiesterase 4B	B
Pde4C	phosphodiesterase 4C	B
Pde4D	phosphodiesterase 4D	B
Stc2	stanniocalcin 2	B

Dlk-1	delta like non-canonical Notch ligand 1	B
Ryr2	ryanodine receptor 2	B
Fam105a	family with sequence similarity 105, member A	B
Plcxd3	phosphatidylinositol specific phospholipase C, X domain containing 3	B
Eno2	enolase 2	B
Pdx1	pancreatic and duodenal homeobox 1	B
Prkaa1	protein kinase AMP-activated catalytic subunit alpha 1	B
Prkaa2	protein kinase AMP-activated catalytic subunit alpha 2	B
Prkab1	protein kinase AMP-activated non-catalytic subunit beta 1	B
Prkab2	protein kinase AMP-activated non-catalytic subunit beta 2	B
Prkag1	protein kinase AMP-activated non-catalytic subunit gamma 1	B
Prkag2	protein kinase AMP-activated non-catalytic subunit gamma 2	B
Prkag3	protein kinase AMP-activated non-catalytic subunit gamma 3	B
Syt7	synaptotagmin 7	B
Syt11	synaptotagmin 11	B
Syt13	synaptotagmin 13	B
Unc13A	unc-13 homolog A	B
Rab3A	RAB3A, member RAS oncogene family	B
Rab3B	RAB3B, member RAS oncogene family	B

Rab3C	RAB3C, member RAS oncogene family	B
Stx1A	syntaxin 1A	B
Rims2	regulating synaptic membrane exocytosis 2	B
Pclo	piccolo (presynaptic cytomatrix protein)	B
Bsn	bassoon (presynaptic cytomatrix protein)	B
Ptbp1	polypyrimidine tract binding protein 1	B
Mafa	MAF bZIP transcription factor A	B
Nnat	neuronatin	B
Wfs1	wolframin ER transmembrane glycoprotein	B
Pax6	paired box 6	B
Xbp1	X-box binding protein 1	B
Rapgef4	Rap guanine nucleotide exchange factor 4	C
Ip6K1	inositol hexakisphosphate kinase 1	B
Eif2A	eukaryotic translation initiation factor 2A	B
Eif2Ak3	eukaryotic translation initiation factor 2 alpha kinase 3	B
Glp1R	glucagon-like peptide 1 receptor	C
Gipr	gastric inhibitory polypeptide receptor	B
Ffar1	free fatty acid receptor 1	B
Crtc2	CREB regulated transcription coactivator 2	B
Mark2	microtubule affinity regulating kinase 2	B
Gpr119	G protein-coupled receptor 119	B
Gpr142	G protein-coupled receptor 142	B
Gpr39	G protein-coupled receptor 39	B

Cebpb	CCAAT/enhancer binding protein beta	B
Ffar3	free fatty acid receptor 3	B
Il6	interleukin 6	B
Camk2A	calcium/calmodulin-dependent protein kinase II alpha	C
Camk2B	calcium/calmodulin-dependent protein kinase II beta	C
Camk2D	calcium/calmodulin-dependent protein kinase II delta	C
Camk2G	calcium/calmodulin-dependent protein kinase II gamma	C
Chrm3	cholinergic receptor, muscarinic 3	B
Mlxip	MLX interacting protein	B

Table 2.2: Affymetrix microarray-based studies, pertaining to pancreatic beta cells, obtained from NCBI GEO database

Physiological condition				
Study	**Organism**	**Samples**	**Replicates**	**GEO Series Accession number**
Glucose dose-response effect on gene expression levels of pancreatic islets cultured *in vitro* in varying glucose concentrations for 18hours (Bensellam et al., 2009).	Rattus norvegicus	• 2 mM glucose • 5 mM glucose • 10 mM glucose • 30 mM glucose	4 4 4 4	GSE12817
Effect of postnatal maturation (neonates to adult) on the transcriptome of isolated rat pancreatic beta cells (Martens et al., 2013).	Rattus norvegicus	• Beta cells of 2-3 days old neonates • Non-endocrine islet cells of 2-3 days old neonates • Beta cells of 10 weeks old adults	3 3 5	GSE47174
Gene expression profile of pancreatic beta cells isolated from different aged	Mus musculus	• Beta cells of 3.5-9 weeks old mice • Beta cells of 1-year old mice • Beta cells of 2-year old mice	3 4 4	GSE72753

C57Bl/6 mice (Aguayo-Mazzucato et al., 2017).				
Pathological condition				
Gene expression profile of beta cells acquired from non-diabetic and type II-diabetic cadaver pancreases (Marselli et al., 2010).	Homo sapiens	• Beta cells of non-diabetic subjects • Beta cells of type II-diabetic subjects	10 10	GSE20966
Effect of obesity on the gene expression profile of isolated rat pancreatic islets (Rebuffat et al., 2013).	Rattus norvegicus	• Standard chow diet fed for 10 days • High fat diet fed for 10 days • Standard chow diet fed for 30days • High fat diet fed for 30 days	5 5 4 5	GSE44047
Effect of two different preparations of high-density lipoproteins (HDL) i.e. GSK3 and GSK4 on the transcriptome of pancreatic beta cells using insulin-	Mus musculus	• Complete medium (CM) + vehicle_GSK3 • CM + HDL_GSK3 • Starved medium (SM) + vehicle_GSK3	3 3 3	GSE17647

secreting mouse beta-cell line ß-TC3 (Pétremand et al., 2009).		• SM + HDL_GSK3 • CM + vehicle_GSK4 • CM + HDL_GSK4 • SM + vehicle_GSK4 • SM + HDL_GSK4	3 3 3 3 3	
Transcriptomic analysis to determine the genes regulated by nuclear factor κB-inducing kinase (NIK) activation in mice pancreatic beta cells in the context of its link to beta cell failure in obesity (Malle et al., 2015). NIK activation was achieved by generating beta cell specific TRAF2 and TRAF3 knockout mice.	Mus musculus	• Chow fed TRAF2 KO mice • High fat fed TRAF2 KO mice • Chow fed TRAF3 KO mice • High fat fed TRAF3 KO mice • Chow fed floxed littermates • High fat fed floxed littermates	3 3 3 3 3 3	GSE68317

The Limma package of R was then used to calculate the expression values of all the genes across all the samples of a dataset. All target genes with their expression values were annotated in Microsoft® Excel (version 16.16.1) and averaged across all the replicates. This data was exported to Genesis software (Oracle Corporation)(version 1.8.1) for the generation of heat maps. Averaged gene expression data was again normalized to all the target genes in Genesis software and then analyzed by Spearman rank correlation, as a measure of clustering distance, and average linkage hierarchical clustering algorithm. The number of genes qualified to be a part of a cluster was manually determined based on the minimum (7) and maximum (51) genes that could possibly form a cluster in the Genesis software across all the studies. The analysis yielded clusters of genes (7-51) in a rank-wise manner based on similarity with the TAAR1 gene expression pattern. The target genes expression values, across the study groups within a study, were represented by the heat map corresponding to the expression values within the range -3 (least expression) to +3 (maximal expression). Genes within a cluster with similar TAAR1 gene expression pattern, as represented by the color plot in the heat map, were designated as positively correlated to TAAR1 gene expression pattern. However, genes in a cluster having exactly opposite expression pattern or color plot in the heat map, were designated as negatively correlated to TAAR1 gene expression pattern. Each of the seven studies yielded a positively and a negatively correlated cluster to the TAAR1 gene expression pattern based on the clustering distance measure; Spearman rank correlation; and average linkage hierarchical clustering agglomeration algorithm applied to all the target gene expression values. TAAR1 correlated genes, consistent across all the studies under a given condition, were identified using Venn diagrams through a web-based tool InteractiVenn as described (Heberle et al., 2015).

2.6 Data analysis

All data are expressed as mean +/- standard error of mean (SEM) and were statistically analyzed using one-way or two-way analysis of variance (ANOVA) with Dunnett's multiple comparisons *post-hoc* test as appropriate. For membrane potential studies area under curve which includes positive and negative peaks are compared across varying concentrations of glucose and KCl. Bioinformatic data was analyzed as described above. GraphPad Prism 6.0e software was used for all data analysis with the exception of bioinformatics analyses. Statistical significance was taken at $P < 0.05$; *$*P<0.05$, $**P<0.01$, $***P<0.001$*.

3.0 Results

3.1 RO5256390 effect on glucose-dependent insulin secretion

Glucose-dependent stimulation of insulin secretion was first confirmed with INS-1E cells. A significant (*P=0.0018)* effect of glucose on secreted insulin at varying glucose concentrations (2.5 mM – 20 mM) was observed (Figure 3.1). Dunnett's multiple comparisons *post-hoc* test showed significant differences between the secreted insulin at individual glucose concentrations (5, 10, 15 and 20 mM) and the basal glucose concentration 2.5 mM (Figure 3.1). With RO5256390 treatment, significant effects of glucose concentrations (*P<0.0001*) and R05256390 concentrations (*P<0.0001*), with no significant interaction (*P=0.4984*) between the two, were observed (Figure 3.2). *Post-hoc* test revealed that at concentrations of 10 nM and above, RO5256390 selectively enhanced glucose-dependent insulin secretion (Figure 3.2).

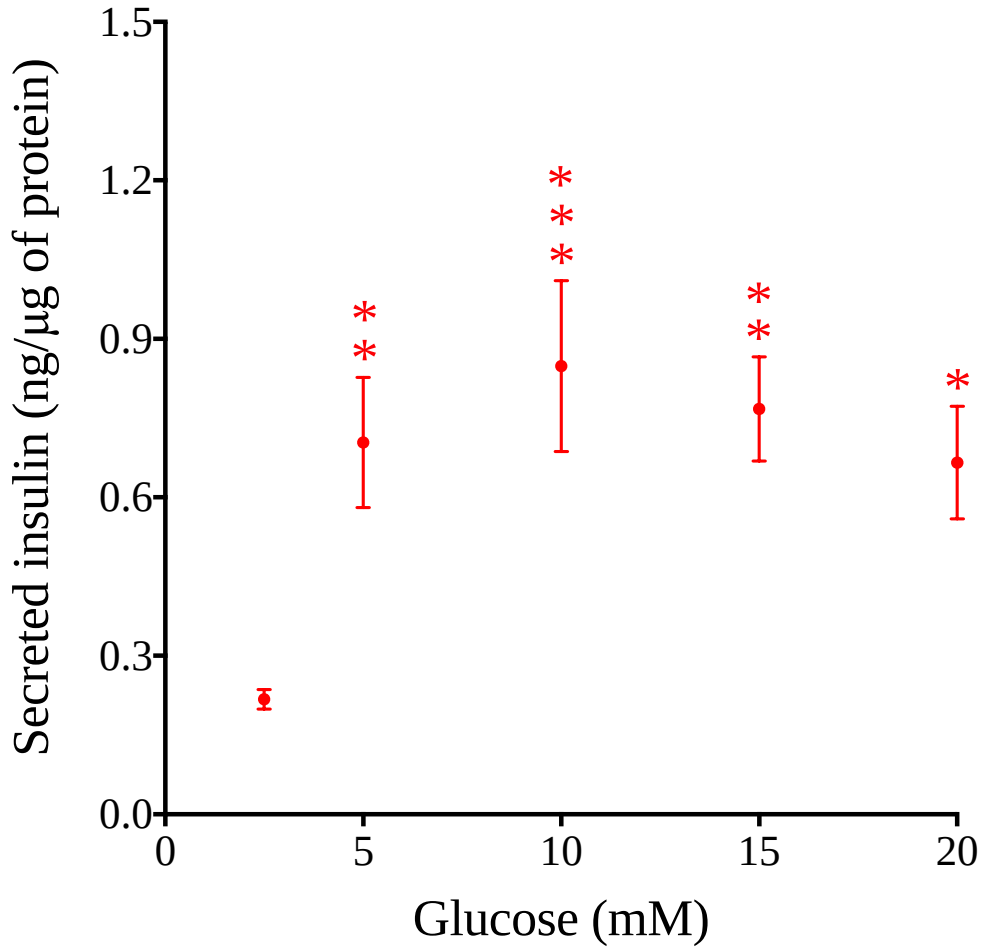

Figure 3.1: Glucose-dependent stimulation of insulin secretion

Secreted insulin (ng/µg of protein) in response to varying glucose concentrations (2.5 mM – 20 mM) was measured. Data are mean ± SEM, n=14, one-way ANOVA with Dunnett's multiple comparisons *post-hoc* test , **P <0.05, **P <0.01, ***P<0.001* with respect to 2.5 mM glucose.

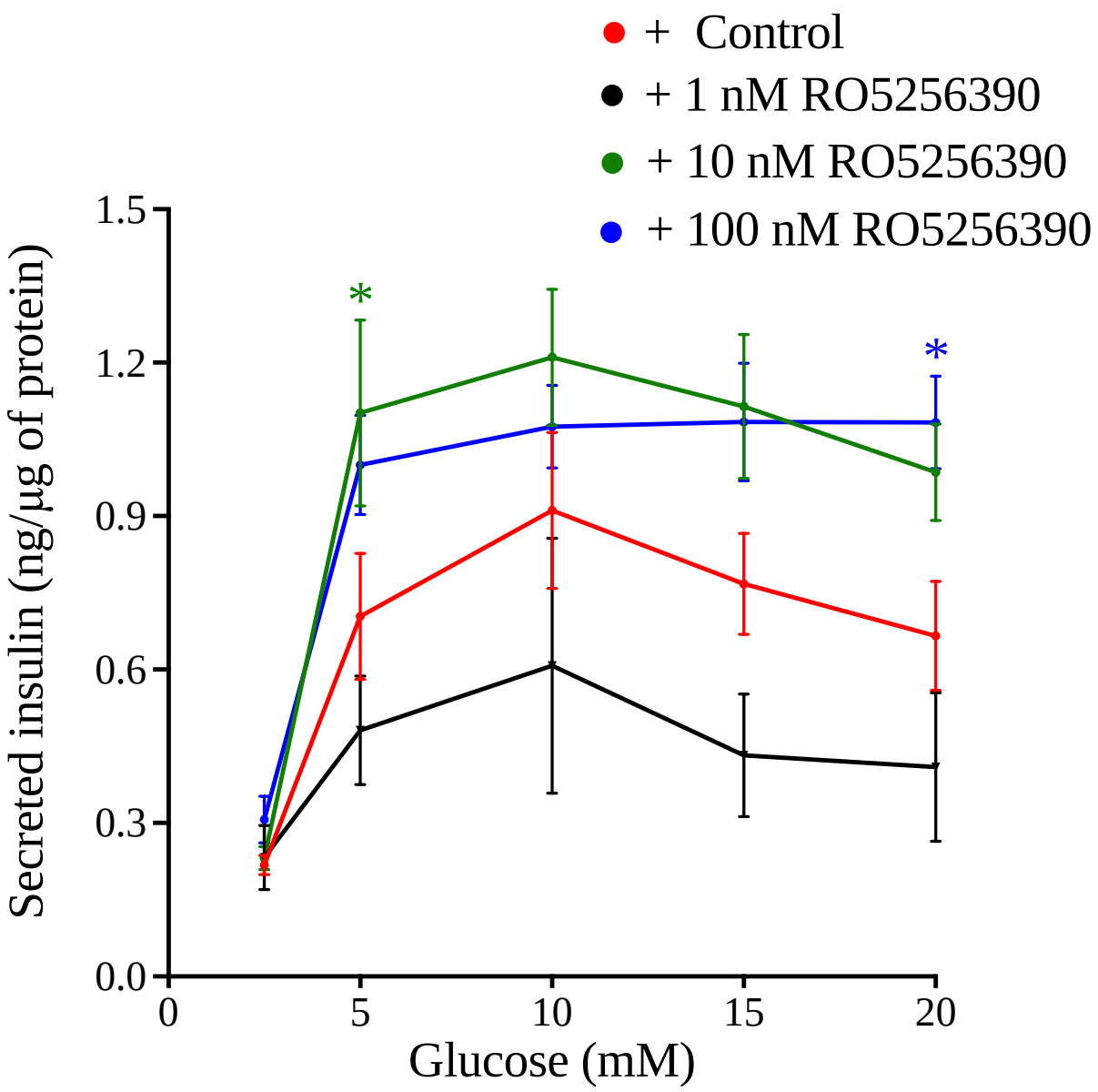

Figure 3.2: RO5256390 selectively enhanced glucose-dependent insulin secretion at concentrations of 10 nM and above

Secreted insulin (ng/µg of protein) in response to varying RO5256390 (1 nM – 100 nM) concentrations, induced by glucose (2.5 mM – 20 mM), was measured. Data are mean ± SEM, n=7-14, two-way ANOVA with Dunnett's multiple comparisons *post-hoc* test , *$P < 0.05$ with respect to control at the same glucose concentration.

3.2 RO5256390 effect on potassium-stimulated insulin secretion

INS-1E plasma membranes were then depolarized using varying KCl concentrations to stimulate insulin secretion and see if RO5256390 concentrations would have similar effect as with glucose-stimulated insulin secretion. KCl significantly (*P = 0.0006)* enhanced insulin secretion in a concentration-dependent manner (Figure 3.3). A significant effect of KCl concentrations (*P<0.0001*) was still observed; however, RO5256390 concentrations had no further effect (*P = 0.3358*) on KCl-stimulated insulin secretion. No significant interaction (*P=0.9866*) was found between the two factors; KCl and RO5256390 concentrations (Figure 3.4).

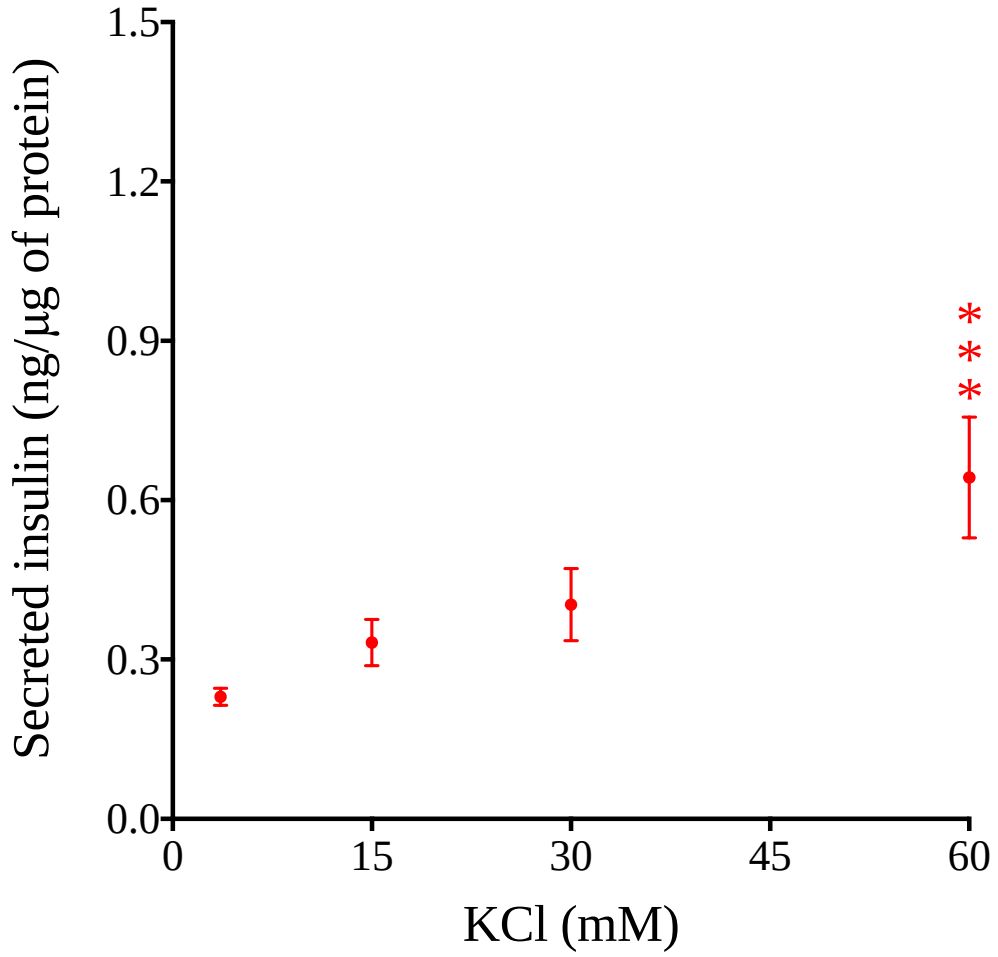

Figure 3.3: Concentration-dependent effect of KCl on insulin secretion

Secreted insulin (ng/µg of protein) in response to varying KCl concentrations (3.6 mM – 60 mM) was measured. Data are mean ± SEM, n=14, one-way ANOVA with Dunnett's multiple comparisons *post-hoc* test , ****P<0.001* with respect to secreted insulin response at 3.6 mM KCl.

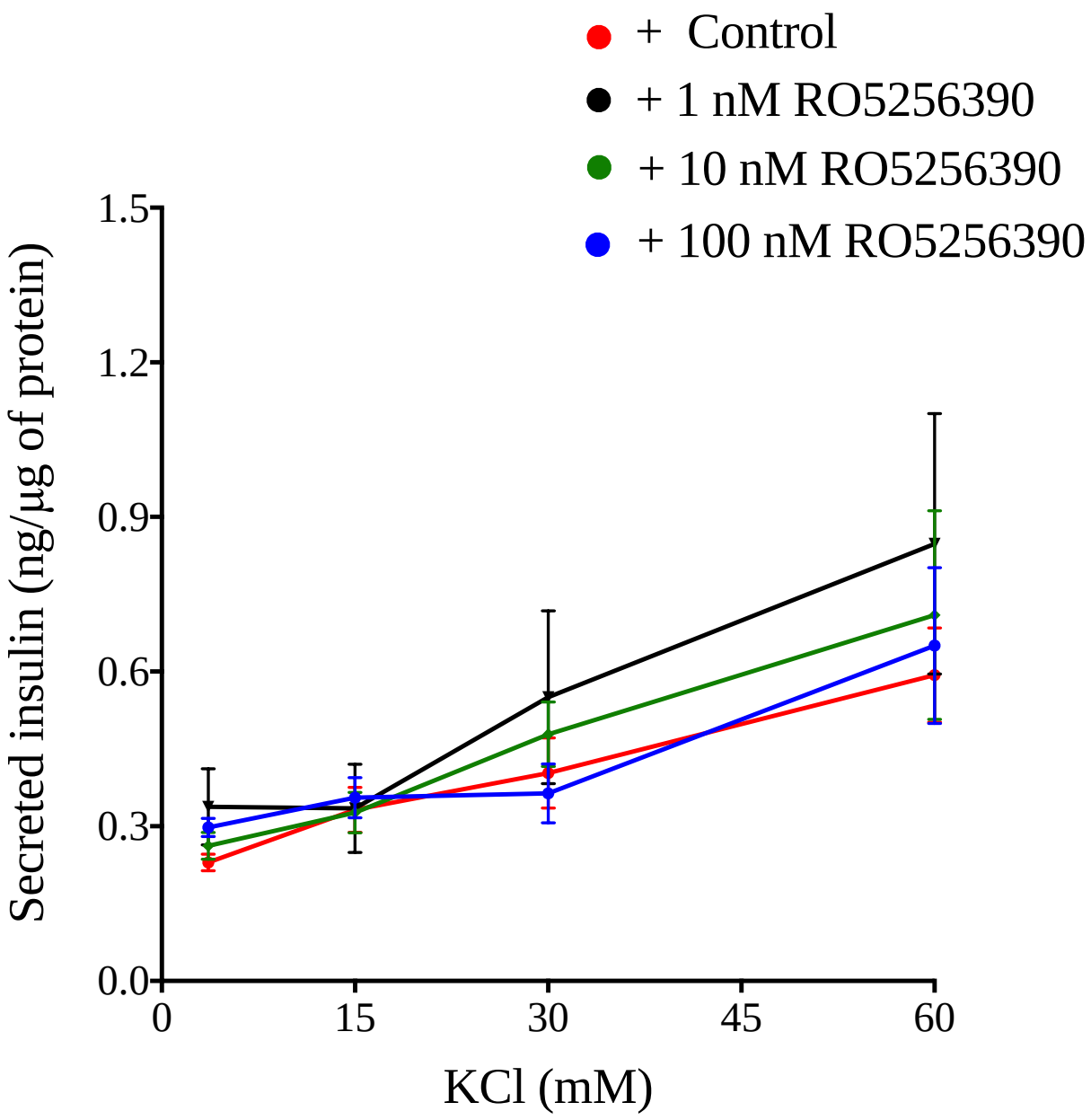

Figure 3.4: RO5256390 does not alter potassium-stimulated insulin secretion

Secreted insulin (ng/µg of protein) in response to varying RO5256390 (1 nM – 100 nM) concentrations, induced by KCl (3.6 mM – 60 mM), was measured. Data are mean ± SEM, n=7-14, two-way ANOVA with Dunnett's multiple comparisons *post-hoc* test.

3.3 Glucose and potassium concentration-response effect on INS-1E membrane potential

The effect of varying concentrations of glucose (2.5 mM – 15 mM) and KCl (3.6 mM – 60 mM) on INS-1E plasma membrane potential were measured by using DiBAC4(3). At 20,000 cells/well, a small initial increment in fluorescence was observed upon addition of glucose (Figure 3.5) or KCl (Figure 3.6), however there was no clear concentration-dependent effect of either treatment. When the cell density was increased to 50,000 cells/well, although there was a more pronounced increase in the fluorescence immediately after addition of either glucose or KCl, there was still no clear concentration-dependent effect (Figure 3.7 and 3.8).

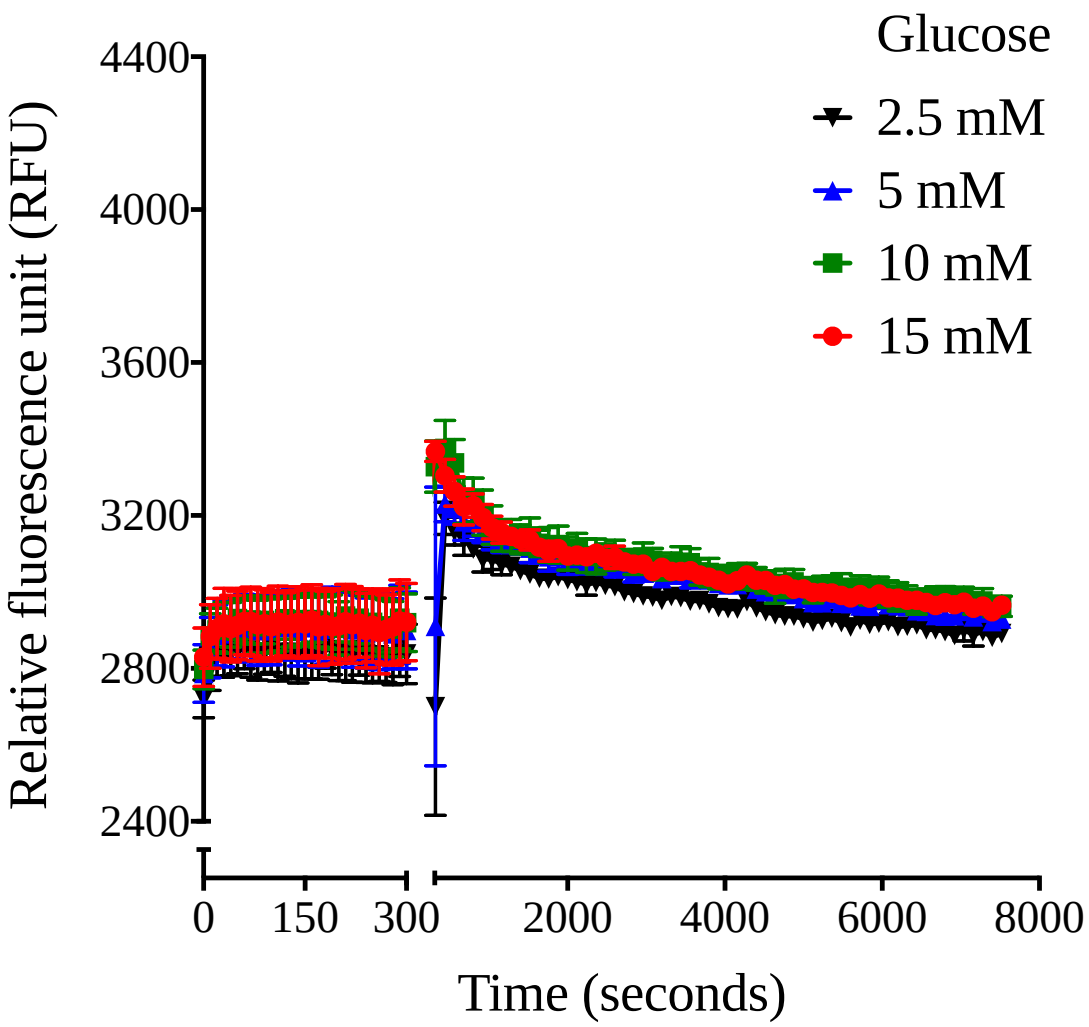

Figure 3.5: No glucose concentration-dependent effect on membrane depolarization at a cell density of 20,000 cells/well

Changes in the fluorescence, representing membrane depolarization, in response to varying concentrations of glucose (2.5 mM – 15 mM) was tracked in INS-1E cells seeded at 20,000 cells/well using excitation and emission wavelengths of 490 nm and 516 nm (n=4).

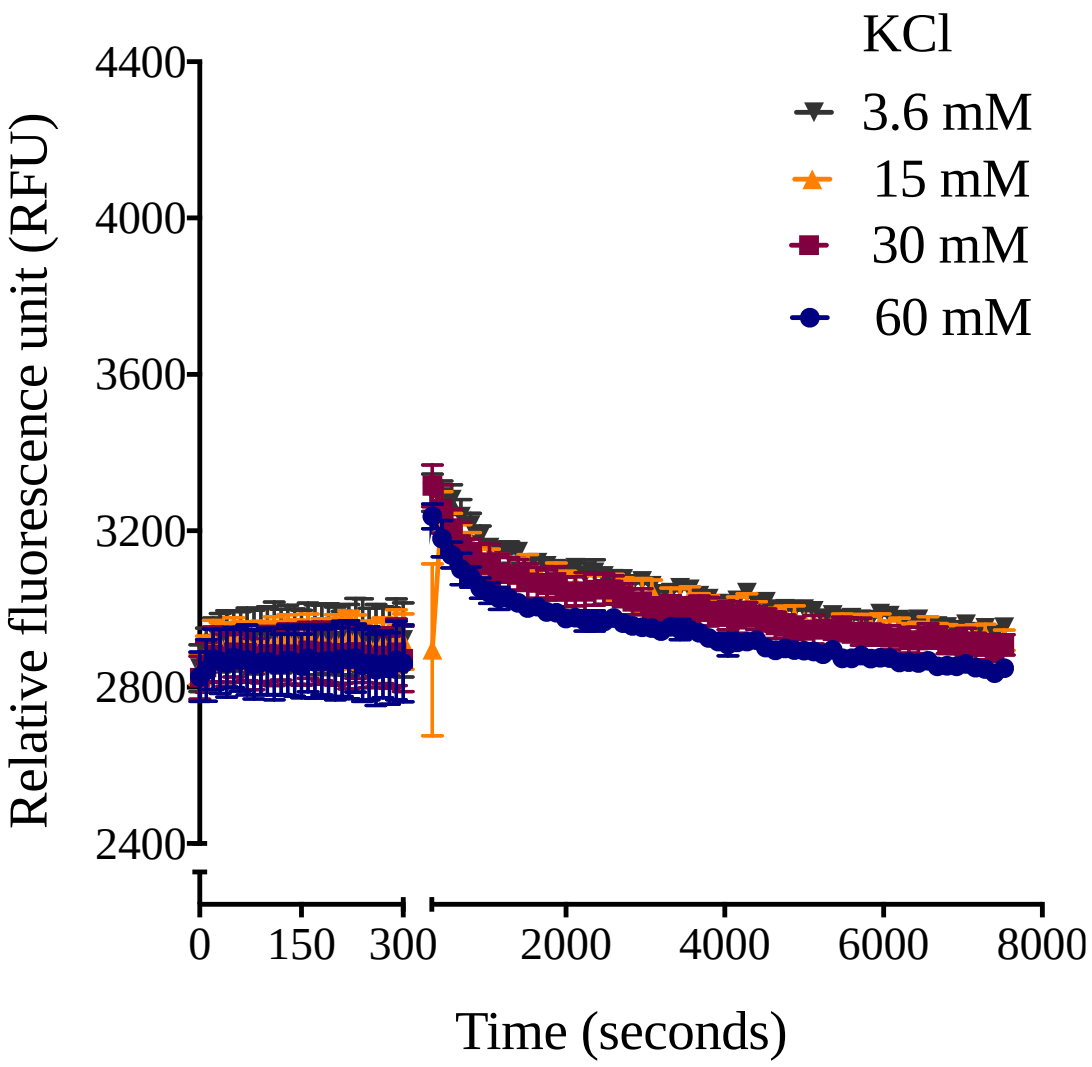

Figure 3.6: No KCl concentration-dependent effect on membrane depolarization at a cell density of 20,000 cells/well

Changes in the fluorescence, representing membrane depolarization, in response to varying concentrations of KCl (3.6 mM – 60 mM) was tracked in INS-1E cells seeded at 20,000 cells/well using excitation and emission wavelengths of 490 nm and 516 nm (n=4).

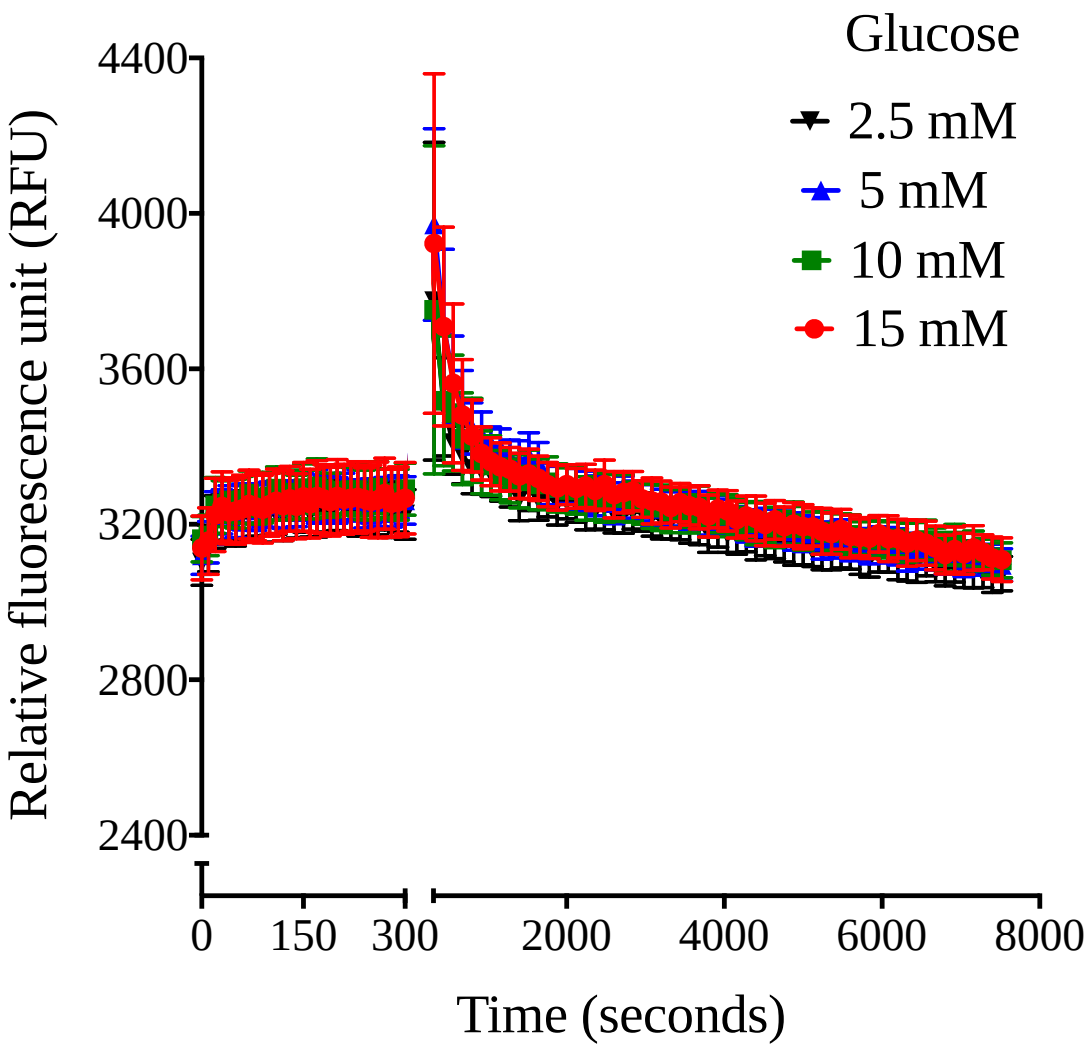

Figure 3.7: No glucose concentration-dependent effect on membrane potential at a cell density of 50,000 cells/well

Changes in the fluorescence, representing membrane depolarization, in response to varying concentrations of glucose (2.5 mM – 15 mM) was tracked in INS-1E cells seeded at 50,000 cells/well using excitation and emission wavelengths of 490 nm and 516 nm (n=5).

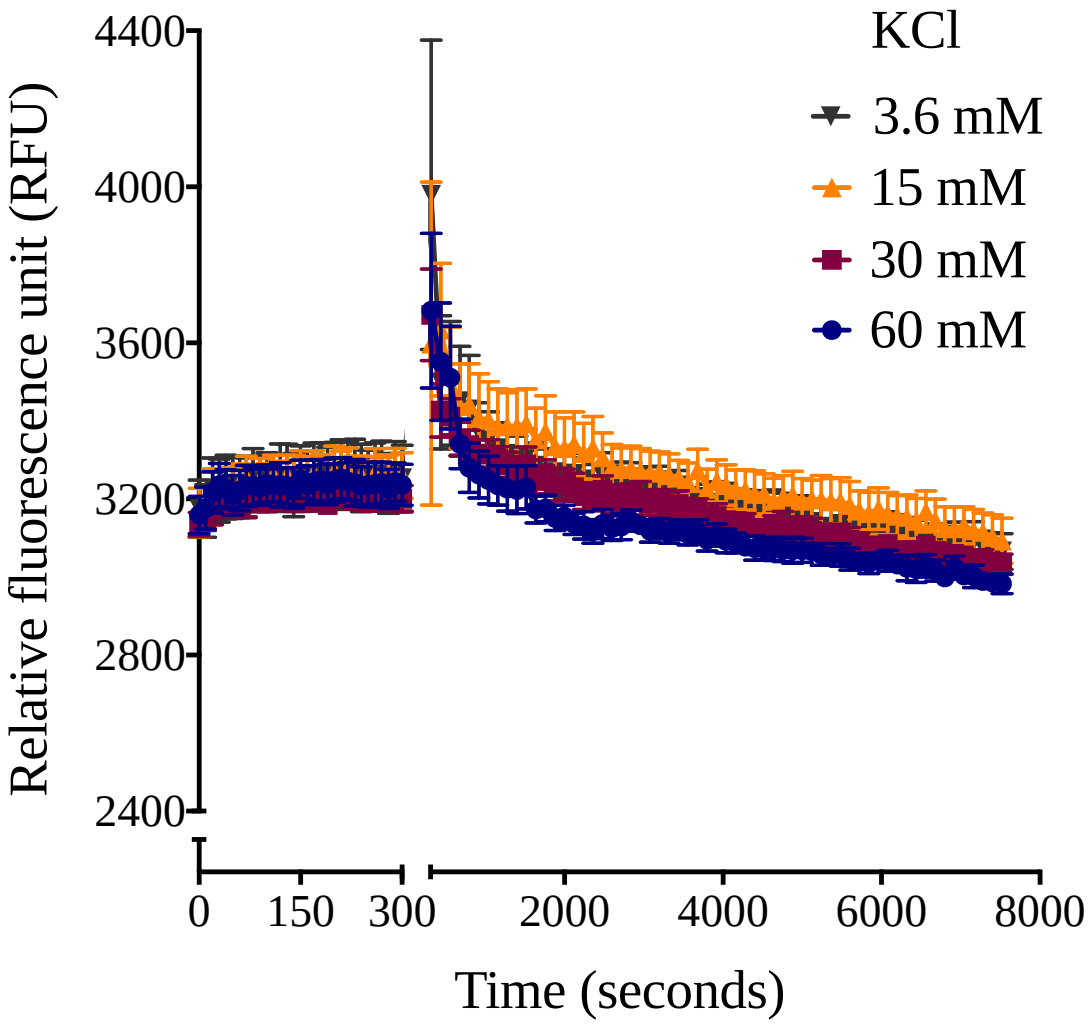

Figure 3.8: No KCl concentration-dependent effect on membrane potential at a cell density of 50,000 cells/well

Changes in the fluorescence, representing membrane depolarization, in response to varying concentrations of KCl (3.6 mM – 60 mM) was tracked in INS-1E cells seeded at 50,000 cells/well using excitation and emission wavelengths of 490 nm and 516 nm (n=5).

3.4 Identification of TAAR1 correlated transcripts from microarray data analysis

A total of seven Affymetrix microarray-based gene expression studies on humans, rats and mice, having at least three biological replicates, and specific to pancreatic beta cells were identified and subdivided into those examining physiological processes, and those studying pathological processes. Each study upon analysis (see section 2.5.1) yielded a positively and a negatively correlated cluster (7-51 gene products) to the TAAR1 gene expression pattern and the genes that consistently changed with the TAAR1 gene expression pattern were identified using Venn diagrams.

3.4.1 Physiological conditions

Three studies examining the physiological processes associated with pancreatic beta cells were identified and analyzed. Heat maps of the TAAR1 gene expression pattern from each of them were generated (Figure 3.9 – 3.11).

Venn diagrams identified three genes (*Cacna1e, Gng7, and Gria2*) that were consistently positively correlated to TAAR1 expression levels across these three studies (Figure 3.12 (A)). Apart from these, genes encoding different GirK protein subtypes GirK1 (*Kcnj3*), GirK2 (*Kcnj6*), GirK3 (*Kcnj9*) and pore forming subunits Kir6.1 (*Kcnj8*) and Kir6.2 (*Kcnj11*) of inward rectifier K_{ATP} channel protein, were found to be positively correlated with TAAR1 across the three studies, although none of the individual subunits were identified in all three studies.

Similarly, three genes (*Fam105a, Gnb2, and Nfatc1*) that were most negatively correlated to TAAR1 expression levels were identified (Figure 3.12 (B)). Apart from these, genes encoding

different subunits of AMP-activated protein kinase such as α1 (*Prkaa1*), α2 (*Prkaa2*), ß1 (*Prkab1*), ß2 (*Prkab2*), γ1 (*Prkag1*), γ2 (*Prkag2*), and γ3 (*Prkag3*) were found to be negatively correlated with TAAR1 in all three studies, although none of the individual subunits were identified in all three studies.

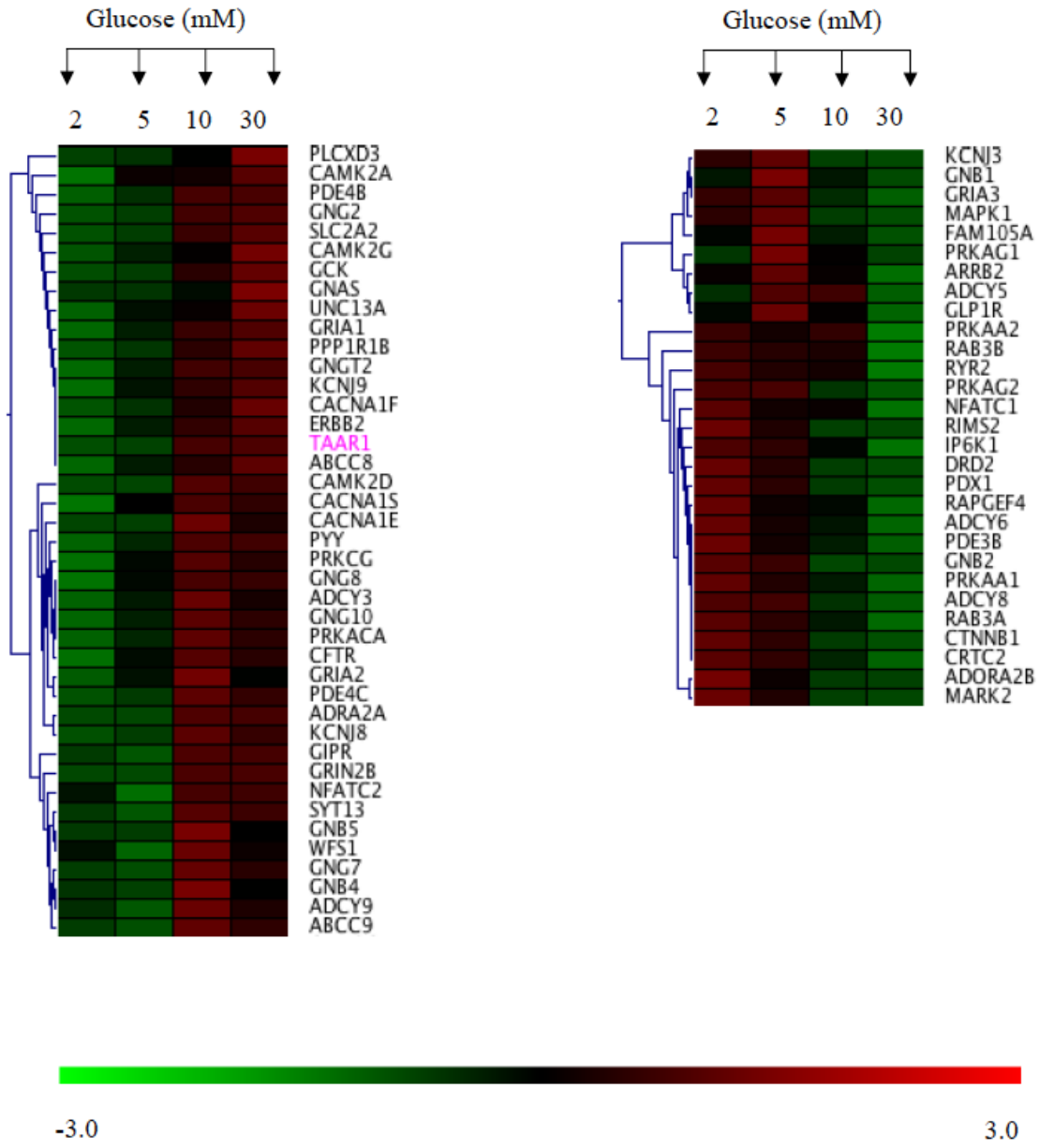

Figure 3.9: Heat map representing hierarchical clustering of TAAR1 gene with genes positively (on left) and negatively (on right) correlated to its expression pattern across isolated rat beta cells exposed to varying glucose concentrations for 18 hours (GSE12817)

Rat beta cells were subjected to different glucose concentrations (2 mM – 30 mM) as indicated at the top of the heat map while genes correlated with TAAR1 expression pattern are towards right hand side of the heat map. TAAR1 is highlighted in pink. Color bar at the bottom indicates the intensity of expression; Green denotes lower expression while red denotes higher expression.

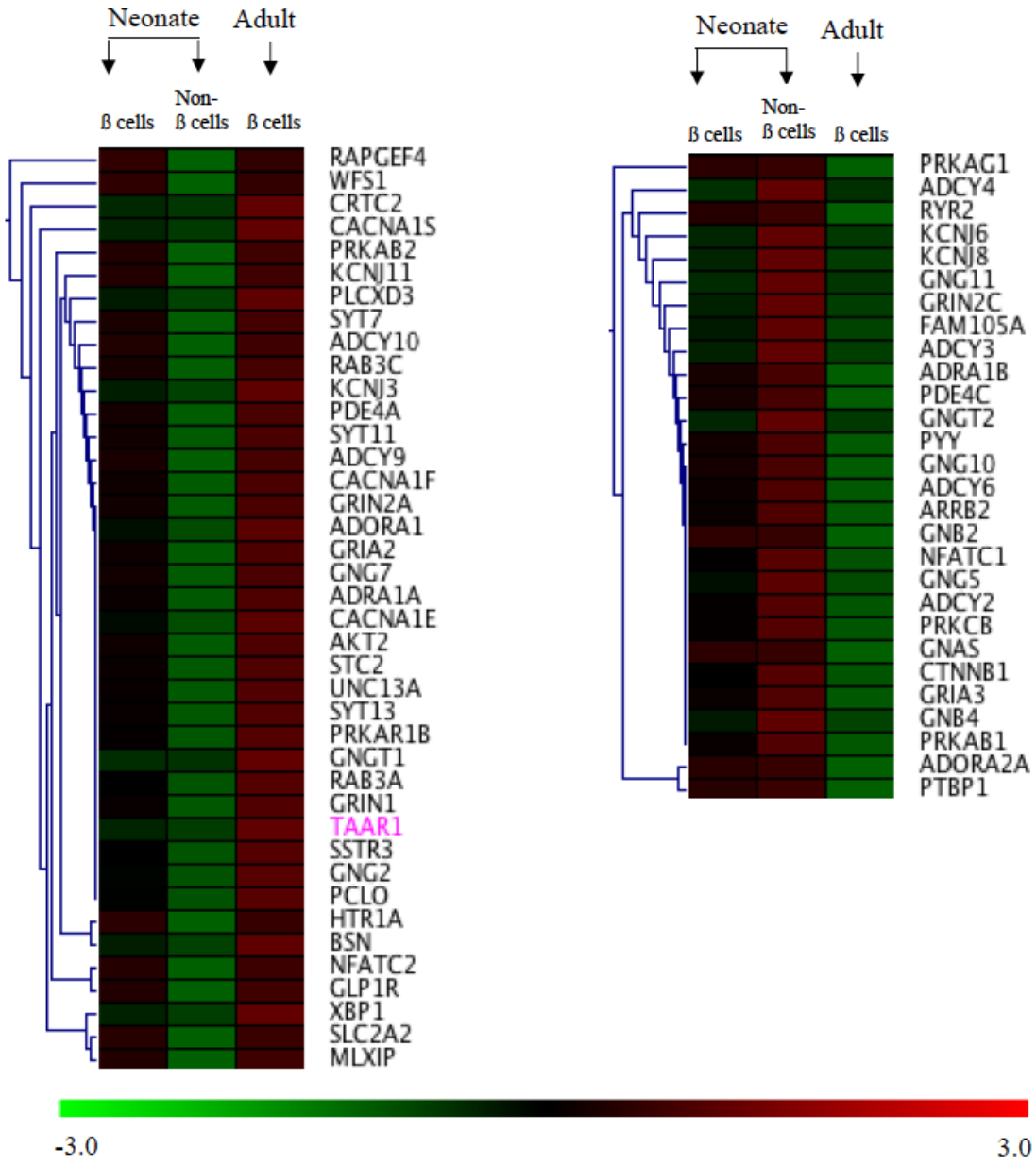

Figure 3.10: Heat map representing hierarchical clustering of TAAR1 gene with genes positively (on left) and negatively (on right) correlated to its expression pattern across pancreatic islet cells isolated from different aged rat (GSE47174)

Pancreatic islet cells isolated from neonate and adult rats are indicated at the top of the heat map while genes correlated with TAAR1 expression pattern are towards right hand side of the heat map. TAAR1 is highlighted in pink. Color bar at the bottom indicates the intensity of expression; Green denotes lower expression while red denotes higher expression.

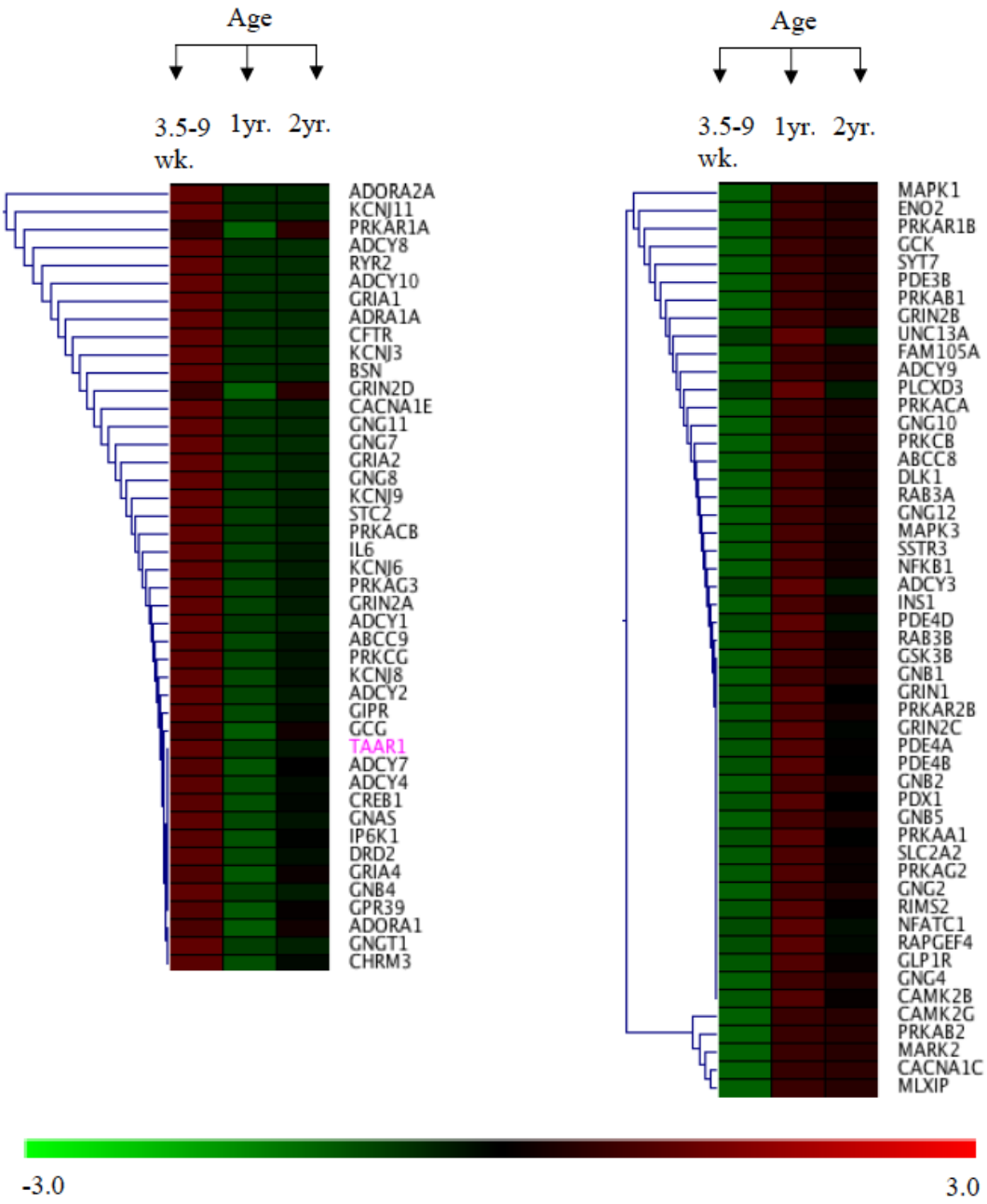

Figure 3.11: Heat map representing hierarchical clustering of TAAR1 gene with genes positively (on left) and negatively (on right) correlated to its expression pattern across beta cells isolated from different aged C57Bl/6 mice (GSE72753)

Pancreatic beta cells isolated from different aged mice are indicated at the top of the heat map while genes correlated with TAAR1 expression pattern are towards right hand side of the heat map. TAAR1 is highlighted in pink. Color bar at the bottom indicates the intensity of expression; Green denotes lower expression while red denotes higher expression.

A. **B**

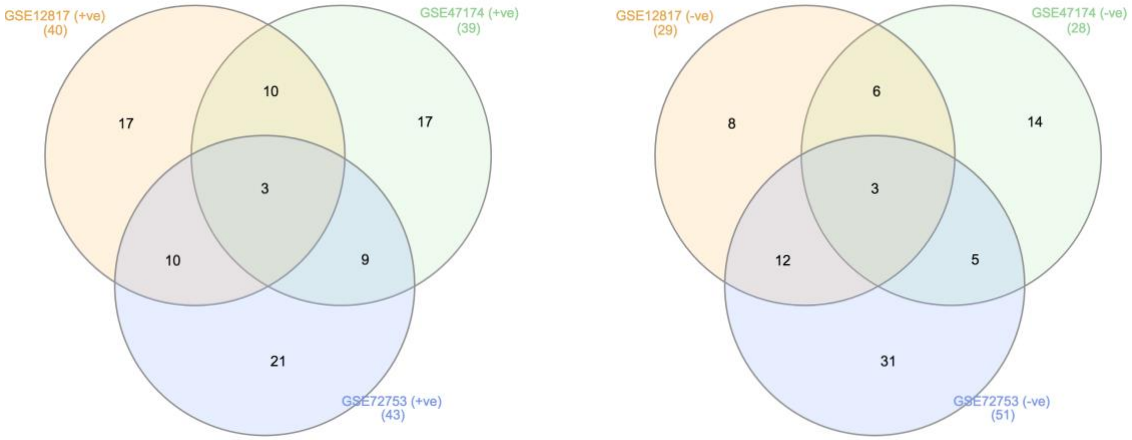

Figure 3.12: TAAR1 correlated genes under physiological conditions

Hierarchical clustering analysis followed by Venn diagram identified the following genes that were consistently changed with TAAR1 gene expression pattern across all the three studies:
A) *Cacna1e*, *Ggng7*, and *Gria2* were consistently positively correlated to TAAR1 gene expression pattern.
B) *Fam105a*, *Gnb2*, and *Nfatc1* were consistently negatively correlated to TAAR1 gene expression pattern.

3.4.2 Pathological condition

Four studies examining pathological processes associated with pancreatic beta cells were identified and analyzed. Heat maps of the TAAR1 gene expression pattern from each of them were generated (Figure 3.13 – 3.16).

Venn diagrams were generated, and no common gene was identified to be consistently changed with TAAR1 expression levels across all four studies (Figure 3.17). However, in three out of four studies *Adora1*, *Gnas* and *Gngt1* were found to be consistently positively correlated to TAAR1 expression levels (Figure 3.17 (A)). Apart from these, genes encoding different subunits of the glutamate ionotropic AMPAR receptor; GluA1 (*Gria1*), GluA2 (*Gria2*), GluA3 (*Gria3*) and GluA4 (*Gria4*) were found to be positively correlated to TAAR1 across the four studies, although none of the individual subunits were identified in all four studies.

Similarly, in three out of four studies *Gng5* and *Mapk1* were found to be most negatively correlated to TAAR1 expression levels (Figure 3.17 (B)). Apart from these, genes encoding different isoforms of Ca^{+2}/calmodulin-activated protein kinase II; α (*Camk2a*), γ (*Camk2g*), and δ (*Camk2d*) were found to be negatively correlated to TAAR1 across the four studies, although none of the individual subunits were identified in all four studies.

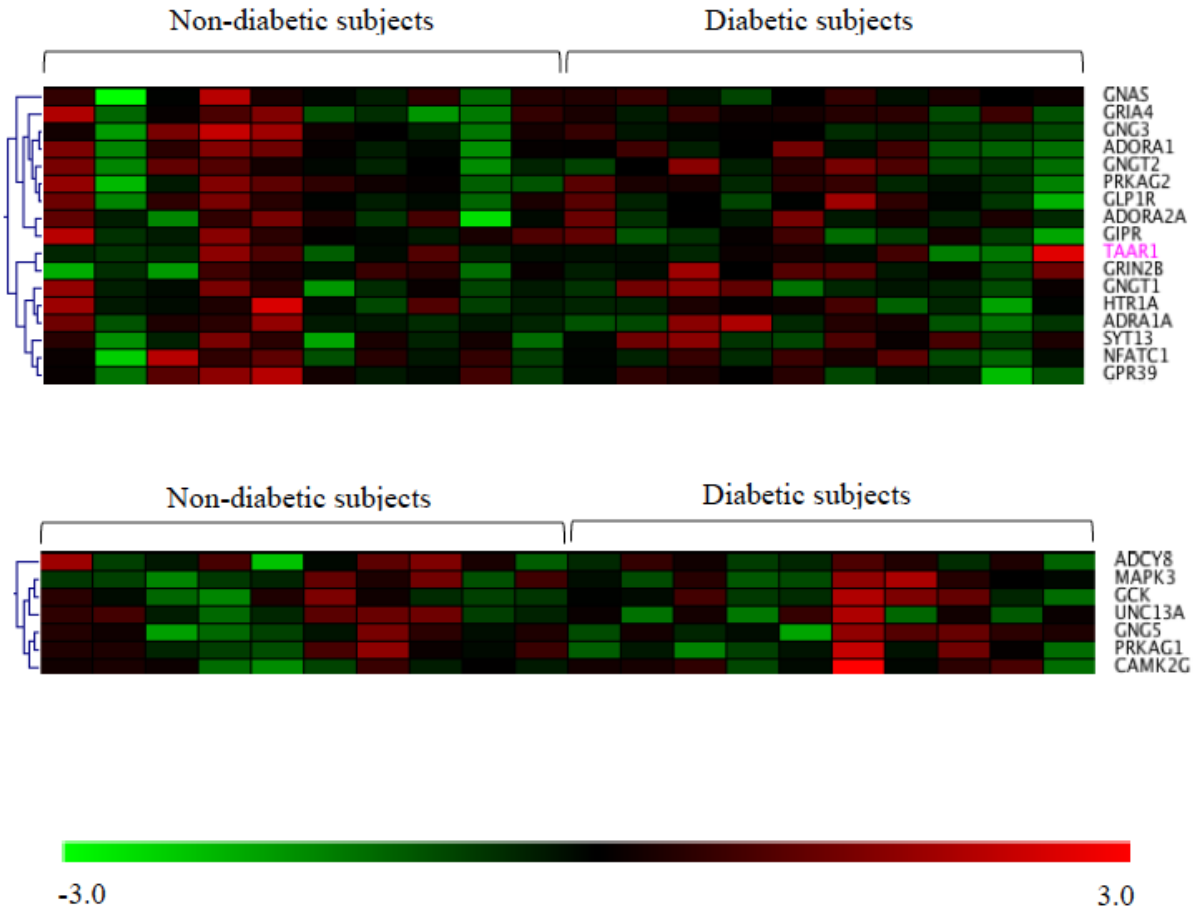

Figure 3.13: Heat map representing hierarchical clustering of TAAR1 gene with genes positively (on top) and negatively (on bottom) correlated to its expression pattern across isolated pancreatic beta cells from cadaver pancreases of non-diabetic and type-II diabetic human subjects (GSE20966)

Pancreatic beta cells isolated from non-diabetic and type-II diabetic cadaver pancreases are indicated at the top of the heat map while genes correlated with TAAR1 expression pattern are towards right hand side of the heat map. TAAR1 is highlighted in pink. Color bar at the bottom indicates the intensity of expression; Green denotes lower expression while red denotes higher expression.

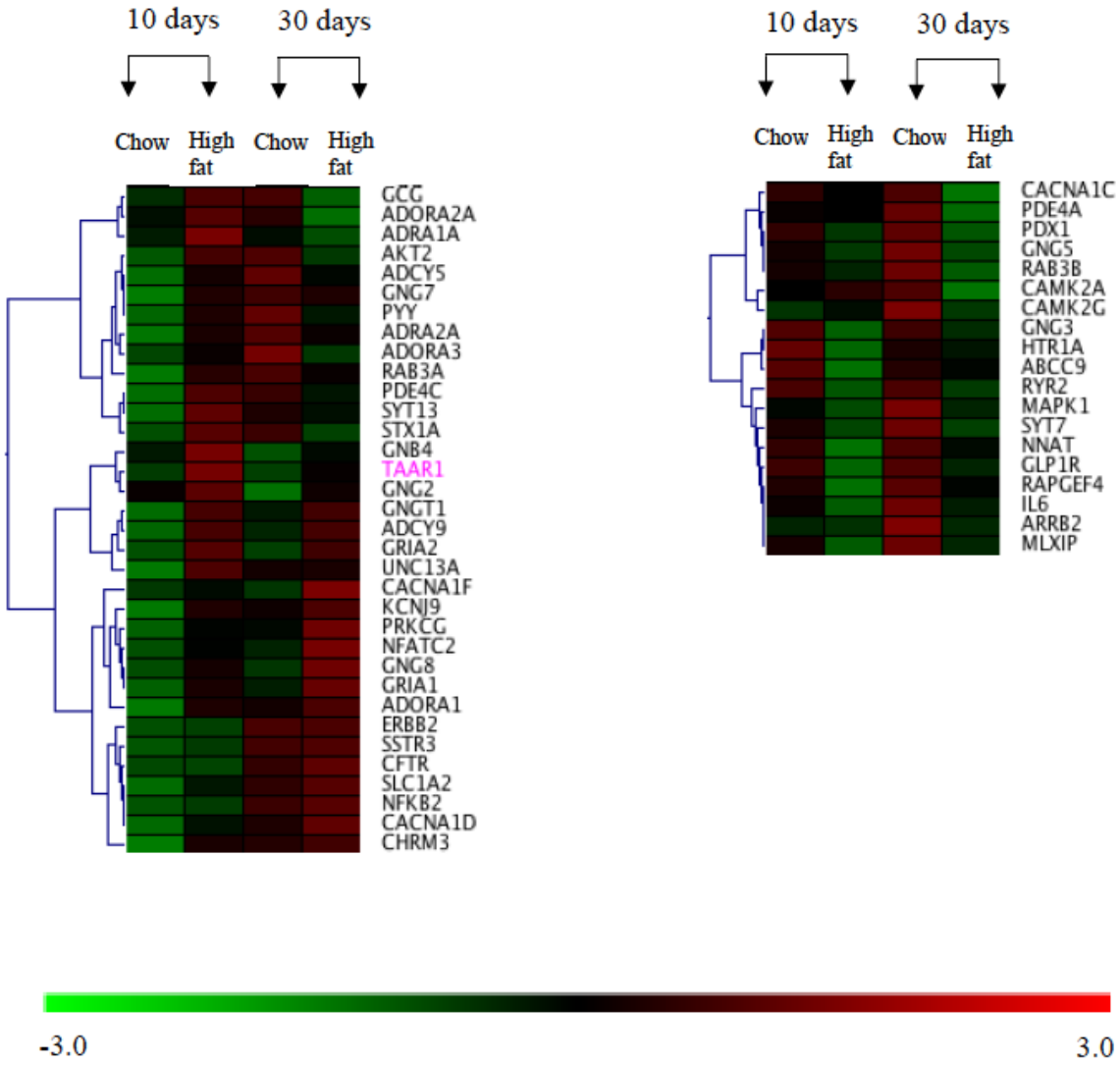

Figure 3.14: Heat map representing hierarchical clustering of TAAR1 gene with genes positively (on left) and negatively (on right) correlated to its expression pattern across isolated pancreatic islets from rats exposed to standard chow and high fat diet for ten and thirty days (GSE4407)

Pancreatic islets isolated from rats exposed to high fat diet for ten and thirty days compared to chow diet are indicated at the top of the heat map while genes correlated with TAAR1 expression pattern are towards right hand side of the heat map. TAAR1 is highlighted in pink. Color bar at the bottom indicates the intensity of expression; Green denotes lower expression while red denotes higher expression.

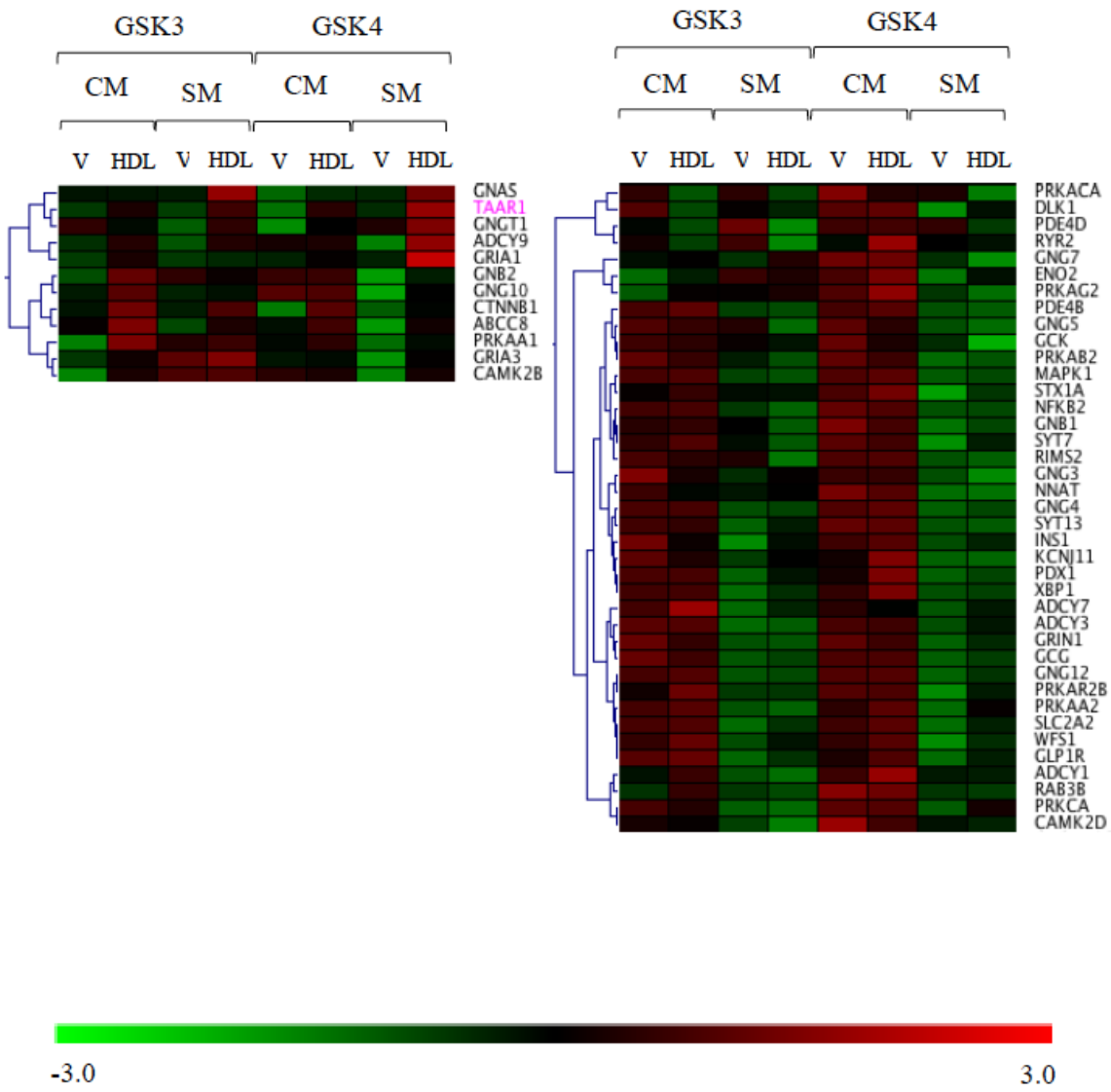

Figure 3.15: Heat map representing hierarchical clustering of TAAR1 gene with genes positively (on left) and negatively (on right) correlated to its expression pattern across two independent HDL preparations subjected to ß-TC3 cell line under different conditions (GSE17647)

Two independent HDL preparations (GSK3 and GSK4) subjected to mouse beta-TC3 cells for six hours in the presence of complete and starved media with controls are indicated at the top of the heat map while genes correlated with TAAR1 expression pattern are towards right hand side of the heat map. TAAR1 is highlighted in pink. Color bar at the bottom indicates the intensity of expression; Green denotes lower expression while red denotes higher expression.

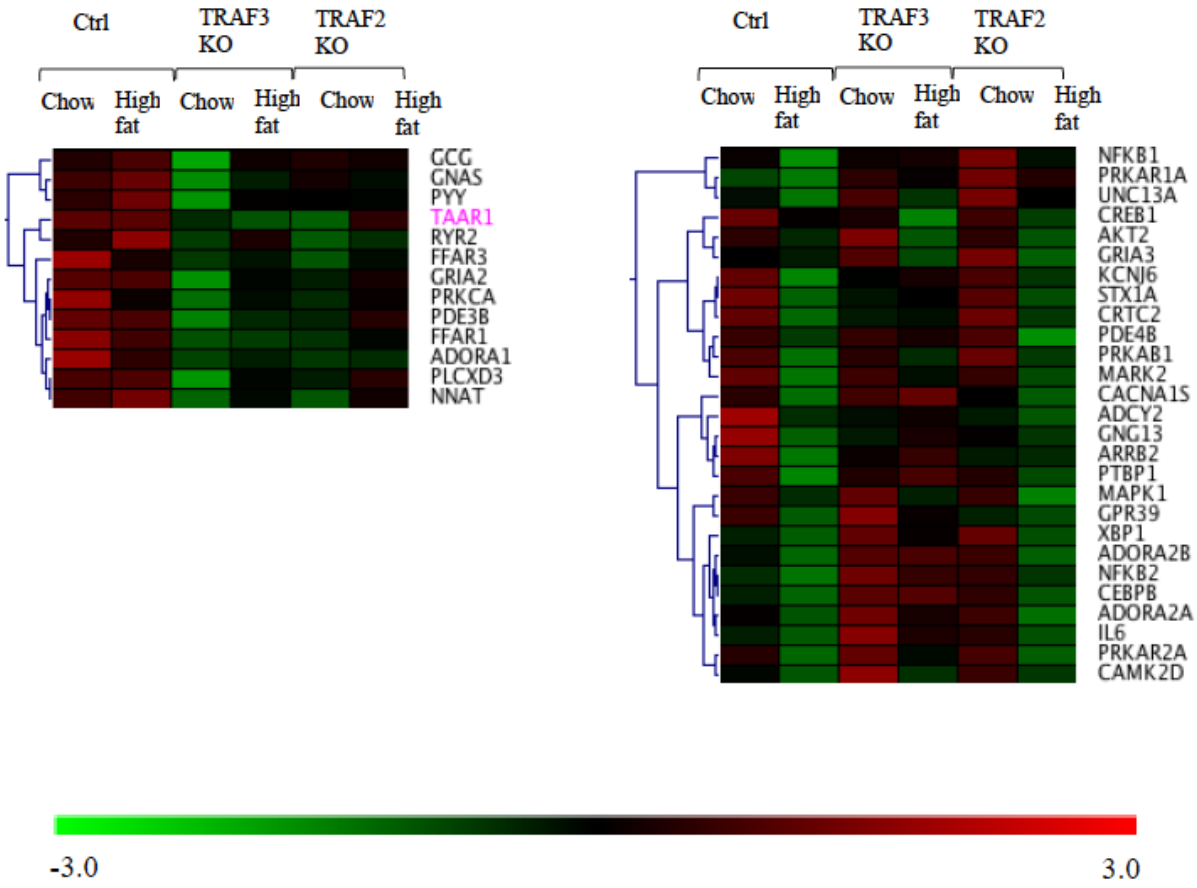

Figure 3.16: Heat map representing hierarchical clustering of TAAR1 gene with genes positively (on left) and negatively (on right) correlated to its expression pattern across control and mice with intrinsic beta cell NIK activation fed with chow and high fat diet (GSE68317)

TRAF3 and TRAF2 KO mice fed with chow and high fat diet compared to controls are indicated at the top of the heat map while genes correlated with TAAR1 expression pattern are towards right hand side of the heat map. TAAR1 is highlighted in pink. Color bar at the bottom indicates the intensity of expression; Green denotes lower expression while red denotes higher expression.

A. **B**

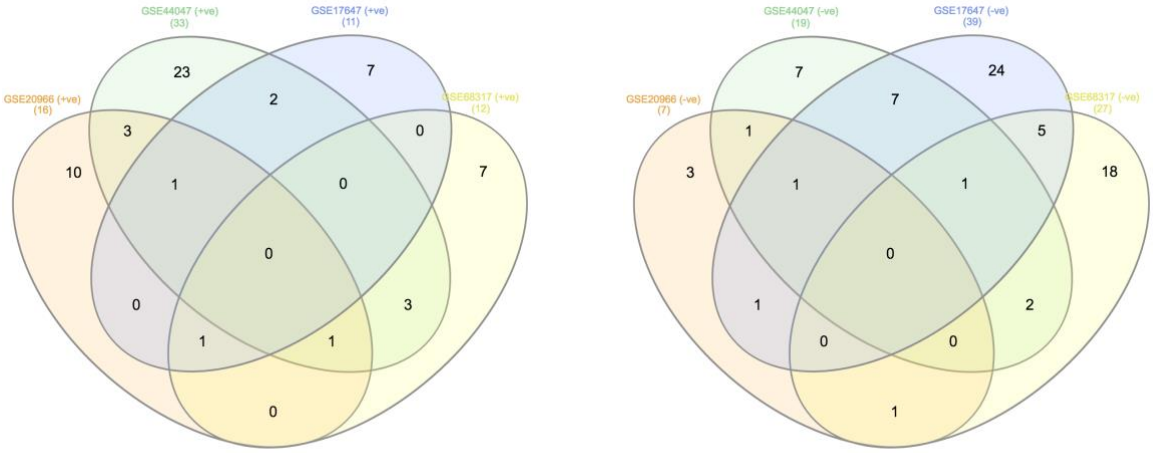

Figure 3.17: TAAR1 correlated genes under pathological conditions

Hierarchical clustering analysis followed by Venn diagram yielded no common gene which consistently changed with TAAR1 gene expression pattern across all the four studies. However, following genes were found to be consistently changed with TAAR1 expression levels in three out of four studies:
A) *Adora1*, *Gnas* and *Ggnt1* were consistently positively correlated to TAAR1 gene expression pattern.
B) *Gng5* and *Mapk1* were consistently negatively correlated to TAAR1 gene expression pattern.

4.0 Discussion

4.1 RO5256390 enhances glucose-dependent insulin secretion

An *in-vitro* study using the highly selective TAAR1 ligand RO5256390 in the rat pancreatic beta cell line INS-1E, which has a higher TAAR1 expression (Raab et al., 2016), would aid in better understanding the role of TAAR1 in modulating GSIS. Previous *in vitro* studies (Michael et al., 2019; Raab et al., 2016; Regard et al., 2007) in pancreatic beta cells with varying TAAR1 ligands have shown they potentiate GSIS. Adding to that, a recent study (Cripps et al., 2020) with INS-1 cells, when subjected to *p*-tyramine and 2-phenylethylamine , has shown a significant increase in glucose-induced insulin secretion. To validate these results, I incubated INS-1E cells with varying concentrations of glucose (2.5 , 5 , 10 , 15 and 20 mM) in the absence or presence of various concentrations of RO5256390 (1, 10 and 100 nM). In the absence of RO5256390, insulin secretion (ng/µg of INS-1E cells) in response to varying concentration of glucose (2.5 , 5 , 10 , 15 and 20 mM) was increased as expected (*P=0.0018)* (Figure 3.1), confirming the responsiveness of INS-1E cells towards glucose.

Having confirmed glucose responsiveness of the INS1E cells the effect of RO5256390 on GSIS was then determined. Significant main effects of glucose concentration (*P<0.0001*) and RO5256390 (*P<0.0001)* were observed with no significant interaction between the two (*P=0.4984*). *Post-hoc* Dunnett's multiple comparisons revealed that RO5256390 selectively enhanced GSIS at higher concentrations (Figure 3.2). This is generally consistent with previous studies (Michael et al., 2019; Raab et al., 2016) and confirms the ability of TAAR1 to enhance GSIS. Given that this primarily is seen at higher and not lower glucose concentrations, this

further supports previous reports (Raab et al., 2016) that TAAR1 agonists would not be expected to cause hypoglycemic adverse effects *in vivo*.

Having confirmed TAAR1-dependent enhancment of GSIS I sought to further clarify the associated downstream signalling pathway involved in this effect. Initially I sought to do this by determining the effect of RO5256390 on potassium-stimulated insulin secretion. As the resting membrane potential of the beta cells sets at nearly -70 mV and is maintained by the flux of potassium ions via the activity of K_{ATP} channel (Ashcroft & Rorsman, 1989) I aimed to by-pass the glucose-stimulated pathway to membrane depolarization step (Figure 1.1) by using varying KCl concentrations.

4.2 RO5256390 does not alter potassium stimulated insulin secretion

A significant (*P=0.0006)* concentration-dependent effect of KCl (3.6 mM – 60 mM) on secreted insulin was observed (Figure 3.3) indicating that the electrical circuitry of the INS-1E cells was also responsive. Having this confirmed, the effect of RO5256390 on potassium-stimulated insulin secretion was determined. A significant main effect of KCl *(P<0.0001*) but no effect of RO5256390 (*P = 0.3358*) or interaction between the two (*P=0.9866*) was found (Figure 3.4). Considering, this study has never been done before potential reasons why the experiment didn't work couldn't be established. However, a significant effect of RO5256390 on glucose- but not on potassium-stimulated insulin secretion indicates that TAAR1 is most likely interacting with a component of the glucose-stimulated pathway upstream of K_{ATP} channel closure and membrane depolarization.

4.3 No glucose or KCl concentration-response effect on membrane potential

I planned to next examine the effect of RO5256390 on plasma membrane depolarization and the activity of the K_{ATP} channel by measuring membrane potential using $DiBAC_4(3)$ and a K-channel selective fluorescent sensor. Although an initial increase in the fluorescence was observed with $DiBAC_4(3)$, indicating membrane depolarization, no concentration-dependent effect of either glucose or K^+ was seen at any cell density (Figures 3.5 – 3.8). As such the effect of RO5256390 on glucose-dependent membrane depolarization could not be studied. A similar lack of glucose concentration-dependent effects on membrane depolarization in INS1E cells has previously been reported (Merglen et al., 2004). These effects have been attributed to mitochondrial electron transport becoming fully saturated at lower glucose or KCl concentrations compared to the concentrations eliciting elevated secretory responses (Antinozzi et al., 2002; Merglen et al., 2004). Attempts to measure the K_{ATP} channel actively directly using the commercial FluxOR Potassium Ion Channel Assay kit were unsuccessful in establishing baseline responses (data not shown) and therefore were not utilized further.

4.4 TAAR1 correlated transcripts involved in the regulation of TAAR1-mediated GSIS were identified

Affymetrix-based microarray data analysis of seven studies associated with pancreatic beta cells, downloaded from NCBI GEO database, generated TAAR1 correlated transcripts which could be the potential downstream targets of the TAAR1-mediated GSIS pathway. These seven studies were subdivided into two groups as mentioned before (section 2.5.1 and 3.4). Identified TAAR1 correlated transcripts pertaining to each group, with their relevance to TAAR1-mediated GSIS pathway are discussed below separately (section 4.4.1 and 4.4.2).

4.4.1 TAAR1 correlated genes from the studies examining physiological processes

Three microarray-based studies (Table 2.2) on pancreatic beta cells under varying physiological conditions were individually analyzed by average linkage hierarchical clustering to yield a positively and negatively correlated clusters to the TAAR1 gene expression pattern (Figure 3.9 – 3.11). Three genes (*Cacna1e, Gng7,* and *Gria2*) were found to be positively correlated with TAAR1 gene expression and consistently changed across all the three studies (Figure 3.12 (A)).

Cacna1e encodes for R-type $Ca_v2.3$ calcium channels. These channels play a crucial role in the second phase of insulin secretion, with very little role in first phase. Functioning of R-type $Ca_v2.3$ calcium channels are critical for insulin granule recruitment, mobilization and priming during the second phase of insulin release (Jing et al., 2005). Inhibition of these channels has been shown to reduce the second phase of insulin secretion by 80% (Jing et al., 2005). In humans, the *Cacna1e* gene is located on chromosome 1q25-31 a region with demonstrated linkage to type 2 diabetes (Hanson et al., 1998) and elevated blood glucose levels (Jun et al., 2014), suggesting a potential role of *Cacna1e* in type-2 diabetes pathophysiology. A recent study (Michael et al., 2019) has also demonstrated a role of TAAR1 activation in stimulating calcium flux, however a putative direct role of TAAR1 on regulation of the calcium channel has not been previously studied. Since calcium channels are downstream of K_{ATP} channels, and TAAR1 does not regulate K-induced insulin secretion, this suggests that the positive correlation between TAAR1 and calcium channels is not due to them being a direct target of TAAR1.

Gng7 encodes for G protein subunit gamma 7. GPCR activation causes the dissociation of the GDP bound inactive heterotrimer $G\alpha\beta\gamma$ into activated GTP bound $G\alpha$ subunit and $G\beta\gamma$ dimers,

both of which can interact with several downstream effector proteins and regulate the level of secondary messengers to regulate physiological responses. Although a specific role for the *Gng7* subunit in GSIS has not previously been suggested, specific Gβγ dimers have been shown to activate several effector proteins such as adenylyl cyclase (Boran, Chen, & Iyengar, 2011), membrane bound phospholipase C β (Park et al., 1993), and ion channels particularly GirK (Wickman et al., 1994) which provides a mechanism by which *Gng7* as a part of βγ dimers might play a role in downstream TAAR1 signaling. However, it is too early to infer anything about *Gng7* and further study is needed to better determine any potential relevance to the putative link to TAAR1 expression identified here.

Gria2 encodes for the glutamate ionotropic receptor AMPA type subunit 2. As stated earlier (section 1.5.4), TAAR1 has been shown to regulate glutamatergic NMDA receptor subunits GluN1 and GluN2B (Espinoza et al., 2015) as well as the AMPAR subunit GluA1 (Alvarsson et al., 2015) in the CNS. TAAR1 activation in CNS has been shown to attenuate the phosphorylation status of the AMPAR in response to L-DOPA (Alvarsson et al., 2015). Similar to NMDA receptors, AMPAR are ionotropic glutamate receptors which function by forming tetrameric complexes of their subunits (Takahashi, Yokoi, & Seino, 2019). AMPAR subunits, particularly *Gria2*, have been shown to be expressed in mouse beta cells (Wu et al., 2012). Activation of AMPAR at higher glucose concentrations in beta cells has been shown to increase the extracellular, as well as intracellular, calcium flux, promoting docking of insulin granules from RRP at the plasma membrane. AMPAR activation has also been shown to promote the closure of the K_{ATP} channels by increasing cytosolic cGMP levels, thereby inducing depolarization of the plasma membrane and promoting GSIS (Wu et al., 2012). Considering

these previous results and our data showing effects of TAAR1 activation on GSIS but not K+-induced insulin secretion, I propose *Gria2* as the most likely downstream target of TAAR1 for the selective regulation of GSIS.

In addition to the genes discussed above, several genes encoding different subunits of GirK and K_{ATP} proteins were consistently found to be positively correlated to TAAR1 expression across the three studies. However, no individual sub-unit was consistently identified in all three studies. Different GirK subunits (Girk1, Girk2 and Girk3) have been shown to be expressed in rat and human islets (Smith, Sellers, & Humphrey, 2001). The pore forming component of K_{ATP} channels are composed of four subunits of either Kir6.1 or Kir6.2. Closure of K^+-channels results in an increased membrane depolarization, calcium influx through the voltage gated calcium ion channel, and subsequently increased insulin secretion. Although studies on TAAR1 effects on GirK and K_{ATP} channel activity in modulating GSIS is lacking, a previous study (Bradaia et al., 2009) has shown TAAR1 activation in VTA dopaminergic neurons in CNS regulates GirK channel activity, making this another good possibility for the downstream target of TAAR1 signalling in beta cells.

Similarly, three genes (*Fam105a*, *Gnb2*, and *Nfatc1*) negatively correlated and consistently changed with TAAR1 across all the three studies were identified (Figure 3.12 (B)). *Fam105a* encodes for the family with sequence similarity 105, member A protein. In a study (Taneera et al., 2014) utilizing microarray-based gene expression data isolated from pancreatic islets of cadaver donors, *Fam105a* gene was found to be positively correlated with insulin secretion and negatively correlated to HbA1C levels. In the same study, *Fam105a* was shown to be down-

regulated in the hyperglycemic state. In contrast, acute exposure of high glucose had no effect on the expression of the gene. In INS-1 cells, silencing of *Fam105a* results in a significant reduction in the insulin secretion (Taneera et al., 2014). This indicates a role of *Fam105a* in the control of insulin secretion and potentially the pathogenesis of diabetes, however, surprisingly no further studies have validated these results or further clarified how *Fam105a* interacts with the insulin secretion machinery. The negative correlation identified here contrasts both with my *in-vitro* study results and the previous studies of *Fam105a* relationship to insulin secretion and suggests it is not a relevant downstream TAAR1 target in the regulation of GSIS. Considering only one such study has been done so far using *Fam105a*, further studies using validated cell culture and animal models are warranted to validate and ascertain effects of *Fam105a* on insulin secretion.

Gnb2 encodes for the G protein subunit beta 2. TAAR1-induced adenylyl cyclase-cAMP signaling pathway to promote GSIS employs activated Gαs protein (Cripps et al., 2020; Michael et al., 2019). As previously indicated, studies pertaining to the role of Gβ subunits or Gβγ dimers in TAAR1 signaling are absent. However, as discussed above in the same section, Gβ subunits in association with Gγ have been shown to activate several effector proteins to mediate different functions relevant to insulin secretion (Milligan & Kostenis, 2006). Indeed a role of G protein subunit beta 2 in the regulation of the insulin secretion pathway has been ascertained by the Reactome biological pathway database (Lennikov et al., 2018) but how it may modulate insulin secretion is not clear. Together the results suggest that TAAR1 may regulate GSIS by promoting particular Gβγ combinations, and thereby inducing a form of signalling bias into the insulin secretome.

Nfatc1 encodes for the nuclear factor of activated T-cells 1 protein. TAAR1 activation in lymphocytes has been shown to activate NFAT signaling to mediate the immune responses of B cells and T cells (Panas et al., 2012). This activation of NFAT signaling has been found to be associated with the release of intracellular calcium stores. *Nfatc1* has also been shown to be expressed in both mouse and human pancreatic islets where it promotes β-cell development and proliferation (Heit et al., 2006; Keller et al., 2016). *Nfatc1* has been shown to promote insulin secretion in response to high glucose and KCl concentrations in mouse islets, but not in human islets, by regulating several genes involved in the insulin secretory cascade such as *Munc13-1* and *Tcf7l2*, and voltage gated ion channels (Keller et al., 2016). A negative correlation of *Nfatc1* with TAAR1 indicates a reduced glucose and potassium stimulated-insulin secretion upon TAAR1 activation. As with Fam105a, this contradicts both with my *in-vitro* data and previous studies, indicating it is likely of limited relevance to the TAAR1 regulation of GSIS.

Apart from the three genes, negatively correlated with TAAR1 gene expression discussed above, several genes encoding different subunits of the protein AMP-activated protein kinase (AMPK) were found to be negatively correlated with TAAR1 across the three studies. However, none of the individual sub-units consistently changed with TAAR1 gene expression pattern in all three studies. AMPK is a heterotrimeric protein complex composed of α, ß and γ subunits. Different isoforms of all these subunits, such as α1, α2, ß1, ß2, γ1, γ2 and γ3, have been identified (Carling, 2004). AMPK is a metabolic master enzyme complex that is involved in maintaining metabolic homeostasis (Viollet et al., 2003). Increases in the cellular AMP/ATP ratio activates AMPK (Gowans et al., 2013) to boost mitochondrial ATP synthesis while limiting the synthesis of glucose, protein and lipid to maintain energy homeostasis (Hardie et al., 2003). In beta cells

pharmacological activation of AMPK has been shown to potentiate insulin secretion (Düfer et al., 2010). However, during physiological conditions when oxidative phosphorylation is curtailed AMPK activation does not enhance insulin secretion (Düfer et al., 2010). In a recent study (Yang, Munhall, & Johnson, 2020) on rat midbrain slices, it was found that AMPK can inhibit TAAR1 activation in dopaminergic neurons by suppressing dopamine intake via an unknown low-affinity, high capacity uptake mechanism. As such, the potential correlation identified here is unlikely to be relevant to downstream TAAR1 signalling, and is more likely to represent an up-stream regulator of TAAR1 functioning.

4.4.2 TAAR1 correlated genes from the studies examining pathological processes

Four microarray-based studies (Table 2.2) on pancreatic beta cells under varying pathological conditions were individually analyzed by average linkage hierarchical clustering algorithm (Figure 3.13 – 3.16). Although Venn diagram analysis revealed no genes which were consistently correlated with TAAR1 across the four studies, a number of genes were correlated in at least three out of four studies.

Adora1, *Gnas* and *Gngt1* were found to be positively correlated with TAAR1 gene expression pattern in three out of four studies. *Gnas* encodes for stimulatory Gα-protein a well-known component of the TAAR1 signal transduction cascade (Borowsky et al., 2001; Bunzow et al., 2001; Cripps et al., 2020) resulting in the subsequent activation of both PKA and Epac (Michael et al., 2019). Consistent with these studies, a positive correlation of TAAR1 with *Gnas* here further validates the Gαs-protein as a downstream TAAR1 target in modulating GSIS.

Adora1 encodes for the adenosine A1 receptor which belongs to the GPCR family, and mediates its actions by coupling with $G_{i/o}$ proteins, inhibiting adenylyl cyclase with subsequent activation of phospholipase-C (Ballesteros-Yáñez et al., 2018). A1 receptor activation has been shown to modulate glucose and insulin homeostasis by inhibiting insulin and promoting glucagon secretion (Burnstock & Novak, 2012; Yang et al., 2015), an effect opposite to that of TAAR1. The putative correlation identified here is therefore unlikely to be relevant to the signal transduction initiated by TAAR1.

Gngt1 encodes for G protein subunit gamma 1. As previously described Gβγ heterodimers do regulate downstream effector proteins and secondary messengers and an ability of TAAR1 signalling to bias the individual G protein isoforms present could be functionally important and relevant to downstream TAAR1 signaling.

In addition to the above three, genes encoding different AMPAR subunits positively correlated to TAAR1 gene expression in all four studies under pathological conditions. However, none of the individual sub-units consistently changed across these studies. This is particularly interesting given that *Gria2* was also identified as a highly likely downstream target of TAAR1 signaling in the studies examining physiological processes. A consistent positive correlation of AMPAR subunits with TAAR1 gene expression pattern across all the physiological and pathological studies strengthens the suggestion that AMPAR are a promising TAAR1 target in modulating GSIS, possibly secondary to changes in cytosolic calcium influx from extracellular as well as intracellular calcium stores as previously reported by (Michael et al., 2019). In such a situation TAAR1 would be predicted to be particularly relevant to the second phase of insulin secretion,

ultimately promoting insulin granule docking at the plasma membrane from the RRP. Further studies are warranted to determine the putative molecular relationships between AMPA and TAAR1 receptors.

Two genes (*Gng5* and *Mapk1*) were negatively correlated with TAAR1 gene expression pattern in three out of four studies. *Gng5* encodes for G protein subunit gamma 5, which has previously been negatively correlated to insulin secretion and positively with HbA1C (Taneera et al., 2014). Further, *Gng5* expression was found to be upregulated in islets isolated from diabetic subjects compared to non-diabetic islets and when pancreatic islets were subjected to higher glucose concentrations (Taneera et al., 2014). As such, the ability of TAAR1 activation to negatively regulate *Gng5* expression should be systematically investigated, and further adds to the possibility of G protein sub-unit bias in TAAR1 signalling.

Mapk1 encodes for mitogen-activated protein kinase 1. MAPK isozymes are serine-threonine protein kinases which upon activation by extracellular stimuli phosphorylate several downstream transcription factors and kinases to induce cellular responses (Sidarala & Kowluru, 2016). In a recent study (Michael et al., 2019), TAAR1 has been shown to activate a different member of the MAPK family (ERK1/2) via PKA and Epac-dependent activation of upstream mediators of ERK1/2, Raf and MEK1/2. This TAAR1-mediated activation of ERK1/2 promoted beta cell proliferation. MAPK activation has been shown to be associated with the beta cell proliferation and not with insulin secretion (Khoo & Cobb, 1997). As such, although the role of *Mapk1* in insulin secretion is unclear, further investigation of whether this is a relevant downstream

effector of TAAR1 signaling in beta-cells *in vivo* where effects on proliferation could be more relevant, is warranted.

Apart from these two genes, genes encoding different subunits of Ca^{+2}/calmodulin-activated protein kinase II (CAMKII) were found to be negatively correlated with TAAR1 across the four studies under pathological condition, although none of the individual subunits were identified in all four studies. CAMKII, is a serine-threonine protein kinase, whose activation is initially dependent on Ca^{+2}/calmodulin binding (Swulius & Waxham, 2008). Four isoforms of CAMKII (α, β, γ and δ) have been identified in mammals (Swulius & Waxham, 2008). CAMKII has been shown to phosphorylate different proteins such as synapsin I, SNAP, and synaptobrevin which are involved in insulin granule exocytosis to promote insulin secretion (Tabuchi et al., 2000). Given this promotes insulin secretion, the negative correlation identified here is not likely to be relevant to TAAR1 signalling of GSIS.

4.5 Conclusions

The goal of this thesis was to determine the downstream molecular targets of TAAR1 in regulating GSIS. I first confirmed that TAAR1 activation selectively elevates GSIS. By short circuiting the glucose-stimulated pathway to membrane depolarization using KCl, it was found that TAAR1 activation does not alter potassium stimulated-insulin secretion. From this it was deduced that TAAR1 interacts with insulin secretion components upstream of membrane depolarization. Analysis of Affymetrix-microarray based studies under physiological and pathological conditions, identified specific genes that are most likely to be involved in the

downstream TAAR1 signalling of GSIS. Based on this I propose the following molecular mechanism for TAAR1 regulation of GSIS (Figure 4.1):

TAAR1 has been confirmed to be linked with Gαs-protein (*Gnas*) and Gβγ dimers (*Gng7* and *Gngt1*). TAAR1-mediated GSIS has been shown to utilize Gαs dependent signaling pathway (Cripps et al., 2020; Michael et al., 2019). Activated G protein subunits can interact downstream to the most likely identified TAAR1 target i.e. AMPA receptor (*Gria2*), shown to be consistently positively correlated with the TAAR1 gene expression levels under both physiological and pathological conditions. AMPAR activation stimulates the closure of the K_{ATP} channels by increasing cytosolic cGMP promoting GSIS. Activation of these receptors also potentiates the influx of Ca^{+2} from both extracellular as well as intracellular calcium stores to promote further GSIS. Another likely TAAR1 target identified was voltage-gated calcium ion channel (*Cacna1e*) which are downstream of K_{ATP} channels supporting K_{ATP} channels as the probable TAAR1 target in the regulation of GSIS. Different pore forming subunits of K_{ATP} channels i.e. Kir6.1 (*Kcnj8*) and Kir6.2 (*Kcnj11*) have also been found to be positively correlated to TAAR1 expression levels. Confirming these proposed links between the identified targets and TAAR1 should be the basis for future work.

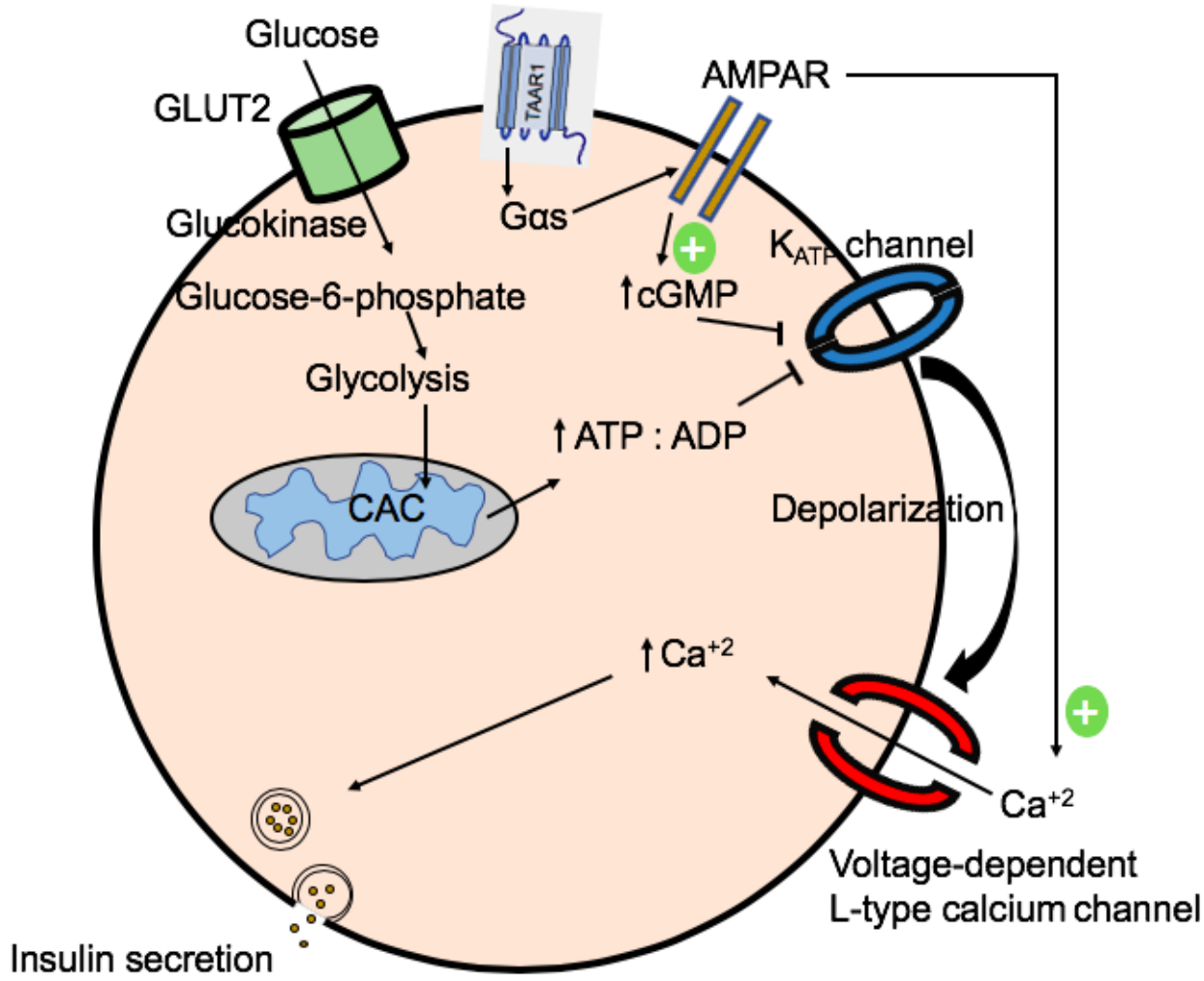

Figure 4.1: Proposed molecular mechanism for TAAR1 regulation of GSIS

TAAR1 activation coupled to Gαs-protein activates AMPAR which elevates cytosolic cGMP levels resulting in the inhibition of K_{ATP} channels. Changes in the membrane depolarization stimulates the opening of calcium channel promoting Ca^{+2} influx for insulin exocytosis.

4.6 Future directions

Based on the above future *in-vitro* studies should specifically examine:

1. The effect of varying glutamate concentrations with or without TAAR1 agonist on insulin secretion.

2. The ability of TAAR1 activation to modify AMPAR function, particularly with respect to its role in GSIS.

3. Assay levels of GTP and ATP in beta cells in response to TAAR1 agonist.

4. Investigating TAAR1-mediated bias in G protein sub-unit composition.

5. Screening of beta-cell inward rectifier potassium channels (GirK and K_{ATP}) for potential modulation by TAAR1.

6. Investigating the effect of TAAR1 activation on calcium flux using a fluorescent dye.

4.7 Limitations

1. TAAR1 effect on insulin secretion was only analyzed in vitro. Studies confirming the in vivo relevance of responses would strengthen the conclusions made.

2. My bioinformatics study provides a series of correlations between TAAR1 gene expression and that of various other genes. Correlation, however, does not necessarily translate to causation and a functional relationship. Further, especially with receptors and enzymes, gene expression is not necessarily reflective of protein levels, and more especially, protein activity. The effects of TAAR1 activation on protein activity needs to be investigated in order to validate the putative relationships identified here.

3. The Affymetrix-microarray data analysis included a relatively small sample size. More robust conclusions could be made with the inclusion of a greater sample size.

5.0 References

Adriaenssens, A., Lam, B. Y. H., Billing, L., Skeffington, K., Sewing, S., Reimann, F., & Gribble, F. (2015). A transcriptome-led exploration of molecular mechanisms regulating somatostatin-producing D-cells in the gastric epithelium. *Endocrinology*, *156*(11), 3924–3936.

Aguayo-Mazzucato, C., van Haaren, M., Mruk, M., Lee, T. B., Jr, Crawford, C., Hollister-Lock, J., Sullivan, B. A., Johnson, J. W., Ebrahimi, A., Dreyfuss, J. M., Van Deursen, J., Weir, G. C., & Bonner-Weir, S. (2017). β Cell Aging Markers Have Heterogeneous Distribution and Are Induced by Insulin Resistance. *Cell metabolism*, *25*(4), 898–910.e5.

Ahrén, B., & Schmitz, O. (2004). GLP-1 receptor agonists and DPP-4 inhibitors in the treatment of type 2 diabetes. *Hormone and Metabolic Research*, *36*(11–12), 867–876.

Aleksandrov, A. A., Dmitrieva, E. S., Volnova, A. B., Knyazeva, V. M., Gerasimov, A. S., & Gainetdinov, R. R. (2018). TAAR5 receptor agonist affects sensory gating in rats. *Neuroscience Letters*, *666*(November 2017), 144–147.

Alvarsson, A., Zhang, X., Stan, T. L., Schintu, N., Kadkhodaei, B., Millan, M. J., Perlmann, T., & Svenningsson, P. (2015). Modulation by Trace Amine-Associated Receptor 1 of Experimental Parkinsonism, L-DOPA Responsivity, and Glutamatergic Neurotransmission. *The Journal of neuroscience : the official journal of the Society for Neuroscience*, *35*(41), 14057–14069.

American Diabetes Association. (2009). Diagnosis and classification of diabetes mellitus. *Diabetes Care*, *32*(SUPPL. 1), S62–S67.

Antinozzi, P. A., Ishihara, H., Newgard, C. B., & Wollheim, C. B. (2002). Mitochondrial metabolism sets the maximal limit of fuel-stimulated insulin secretion in a model pancreatic

beta cell: A survey of four fuel secretagogues. *Journal of Biological Chemistry*, *277*(14), 11746–11755.

Asfari, M., Janjic, D., Meda, P., Li, G., Halban, P. A., & Wollheim, C. B. (1992). Establishment Differentiated. *Endocrinology*, *130*(1), 167–178.

Ashcroft, F. M., & Rorsman, P. (1989). Electrophysiology of the pancreatic β-cell. *Progress in Biophysics and Molecular Biology*, *54*(2), 87–143.

Asif-Malik, A., Hoener, M.C. & Canales, J.J. (2017). Interaction Between the Trace Amine-Associated Receptor 1 and the Dopamine D2 Receptor Controls Cocaine's Neurochemical Actions. *Scientific Reports* 7.

Azuma, T., Witke, W., Stossel, T. P., Hartwig, J. H., & Kwiatkowski, D. J. (1998). Gelsolin is a downstream effector of rac for fibroblast motility. *EMBO Journal*, *17*(5), 1362–1370.

Babusyte, A., Kotthoff, M., Fiedler, J., & Krautwurst, D. (2013). Biogenic amines activate blood leukocytes via trace amine-associated receptors TAAR1 and TAAR2. *Journal of Leukocyte Biology*, *93*(3), 387–394.

Baggio, L. L., & Drucker, D. J. (2007). Biology of Incretins: GLP-1 and GIP. *Gastroenterology*, *132*(6), 2131–2157.

Bailey, C. J. (2015). The current drug treatment landscape for diabetes and perspectives for the future. *Clinical Pharmacology and Therapeutics*, *98*(2), 170–184.

Ballesteros-Yáñez, I., Castillo, C. A., Merighi, S., & Gessi, S. (2018). The role of adenosine receptors in psychostimulant addiction. *Frontiers in Pharmacology*, *8*(JAN), 1–18.

Barak, L. S., Salahpour, A., Zhang, X., Masri, B., Sotnikova, T. D., Ramsey, A. J., Violin, J. D., Lefkowitz, R. J., Caron, M. G., & Gainetdinov, R. R. (2008). Pharmacological characterization of membrane-expressed human trace amine-associated receptor 1 (TAAR1)

by a bioluminescence resonance energy transfer cAMP biosensor. *Molecular pharmacology*, *74*(3), 585–594.

Beagley, J., Guariguata, L., Weil, C., & Motala, A. A. (2014). Global estimates of undiagnosed diabetes in adults. *Diabetes Research and Clinical Practice*, *103*(2), 150–160.

Beaulieu, J.-M., Gainetdinov, R. R., & Caron, M. G. (2009). Akt/GSK3 Signaling in the Action of Psychotropic Drugs. *Annual Review of Pharmacology and Toxicology*, *49*(1), 327–347.

Beitz, J. M. (2014). School of Nursing-Camden, Rutgers University, 311 N. 5. *Frontiers in Bioscience*, *6*(3), 65–74.

Bensellam, M., Van Lommel, L., Overbergh, L., Schuit, F. C., & Jonas, J. C. (2009). Cluster analysis of rat pancreatic islet gene mRNA levels after culture in low-, intermediate- and high-glucose concentrations. *Diabetologia*, *52*(3), 463–476.

Bermudez, V., Finol, F., Parra, N., Perez, A., Penaranda, L., Vilchez, D., Rojas, J., Arraiz, N., & Velasco, M. (2010). PPAR- agonists and their role in type 2 diabetes mellitus management. *American Journal of Therapeutics*, *17*(3), 274–283.

Berry, M. D. (2004). Mammalian central nervous system trace amines. Pharmacologic amphetamines, physiologic neuromodulators. *Journal of Neurochemistry*, *90*(2), 257–271.

Berry, M. D. (2007). The Potential of Trace Amines and Their Receptors for Treating Neurological and Psychiatric Diseases. *Reviews on Recent Clinical Trials*, *2*(1), 3–19.

Berry, M. D., Shitut, M. R., Almousa, A., Alcorn, J., & Tomberli, B. (2013). Membrane permeability of trace amines: Evidence for a regulated, activity-dependent, nonexocytotic, synaptic release. *Synapse*, *67*(10), 656–667.

Berry, M.D., Hart, S., Pryor, A.R., Hunter, S., & Gardiner, D. (2016). Pharmacological characterization of a high-affinity p-tyramine transporter in rat brain synaptosomes. *Sci Rep,*

6, 38006.

Berry, M. D., Gainetdinov, R. R., Hoener, M. C., & Shahid, M. (2017). Pharmacology of human trace amine-associated receptors: Therapeutic opportunities and challenges. *Pharmacology and Therapeutics*, *180*, 161–180.

Berry, M.D., Scarr, E., Zhu, M-Y., Paterson, I.A. & Juorio, A.V. (1994). The effects of administration of monoamine ocidase inhibitors on rat striatal neurone responses to dopamine. *British journal of pharmacology, 113,* 1159-1166.

Berry, M. D., Juorio, A. V., Li, X. M., & Boulton, A. A. (1996). Aromatic l-amino acid decarboxylase: A neglected and misunderstood enzyme. *Neurochemical Research*, *21*(9), 1075–1087.

Bly, M. (2005). Examination of the trace amine-associated receptor 2 (TAAR2). *Schizophrenia Research*, *80*(2–3), 367–368.

Boran, A. D. W., Chen, Y., & Iyengar, R. (2011). Identification of new Gβγ interaction sites in adenylyl cyclase 2. *Cellular Signalling*, *23*(9), 1489–1495.

Borowsky, B., Adham, N., Jones, K. A., Raddatz, R., Artymyshyn, R., Ogozalek, K. L., Durkin, M. M., Lakhlani, P. P., Bonini, J. A., Pathirana, S., Boyle, N., Pu, X., Kouranova, E., Lichtblau, H., Ochoa, F. Y., Branchek, T. A., & Gerald, C. (2001). Trace amines: identification of a family of mammalian G protein-coupled receptors. *Proceedings of the National Academy of Sciences of the United States of America*, *98*(16), 8966–8971.

Boulton, A. A., & Wu, P. H. (1972). Biosynthesis of cerebral phenolic amines. I. In vivo formation of p-tyramine, octopamine, and synephrine. *Canadian Journal of Biochemistry*, *50*(3), 261–267.

Boulton, Alan A. (1982). Some aspects of basic psychopharmacology: The trace amines.

Progress in Neuropsychopharmacology and Biological Psychiatry, *6*(4–6), 563–570.

Boyle, P. J. (2007). Diabetes Mellitus and Macrovascular Disease: Mechanisms and Mediators. *American Journal of Medicine*, *120*(9 SUPPL. 2), 12–17.

Bradaia, A., Trube, G., Stalder, H., Norcross, R. D., Ozmen, L., Wettstein, J. G., Pinard, A., Buchy, D., Gassmann, M., Hoener, M.C. & Bettler, B. (2009). The selective antagonist EPPTB reveals TAAR1-mediated regulatory mechanisms in dopaminergic neurons of the mesolimbic system. *Proceedings of the National Academy of Sciences of the United States of America*, *106*(47), 20081–20086.

Brewer, K. D., Bacaj, T., Cavalli, A., Camilloni, C., Swarbrick, J. D., Liu, J., Zhou, A., Zhou, P., Barlow, N., Xu, J., Seven, A. B., Prinslow, E. A., Voleti, R., Häussinger, D., Bonvin, A. M., Tomchick, D. R., Vendruscolo, M., Graham, B., Südhof, T. C., & Rizo, J. (2015). Dynamic binding mode of a Synaptotagmin-1-SNARE complex in solution. *Nature structural & molecular biology*, *22*(7), 555–564.

Bumgarner, R. (2013). Overview of dna microarrays: Types, applications, and their future. *Current Protocols in Molecular Biology*, (SUPPL.101), 1–11.

Bunzow, J. R., Sonders, M. S., Arttamangkul, S., Harrison, L. M., Zhang, G., Quigley, D. I., Darland, T., Suchland, K. L., Pasumamula, S., Kennedy, J. L., Olson, S. B., Magenis, R. E., Amara, S. G., & Grandy, D. K. (2001). Amphetamine, 3,4-methylenedioxymethamphetamine, lysergic acid diethylamide, and metabolites of the catecholamine neurotransmitters are agonists of a rat trace amine receptor. *Molecular pharmacology*, *60*(6), 1181–1188.

Burnstock, G., & Novak, I. (2012). Purinergic signalling in the pancreas in health and disease. *Journal of Endocrinology*, *213*(2), 123–141.

Carling, D. (2004). The AMP-activated protein kinase cascade - A unifying system for energy control. *Trends in Biochemical Sciences*, *29*(1), 18–24.

Cenci, M. A., Ohlin, K. E., & Rylander, D. (2009). Plastic effects of L-DOPA treatment in the basal ganglia and their relevance to the development of dyskinesia. *Parkinsonism and Related Disorders*, *15*(SUPPL. 3), S59–S63.

Cernea, S., & Dobreanu, M. (2013). Diabetes and beta cell function: from mechanisms to evaluation and clinical implications. *Biochemia Medica*, *23*(3), 266–280.

Chang, H. S., Heo, J. S., Shin, S. W., Bae, D. J., Song, H. J., Jun, J. A., Kim, J. D., Park, J. S., Park, B. L., Shin, H. D., & Park, C. S. (2015). Association between TAAR6 polymorphisms and airway responsiveness to inhaled corticosteroids in asthmatic patients. *Pharmacogenetics and genomics*, *25*(7), 334–342.

Chatterjee, S., Khunti, K., & Davies, M. J. (2017). Type 2 diabetes. *The Lancet*, *389*(10085), 2239–2251.

Chaudhury, A., Duvoor, C., Reddy Dendi, V. S., Kraleti, S., Chada, A., Ravilla, R., Marco, A., Shekhawat, N. S., Montales, M. T., Kuriakose, K., Sasapu, A., Beebe, A., Patil, N., Musham, C. K., Lohani, G. P., & Mirza, W. (2017). Clinical Review of Antidiabetic Drugs: Implications for Type 2 Diabetes Mellitus Management. *Frontiers in endocrinology*, *8*, 6.

Chen, L., Magliano, D. J., & Zimmet, P. Z. (2012). The worldwide epidemiology of type 2 diabetes mellitus - Present and future perspectives. *Nature Reviews Endocrinology*, *8*(4), 228–236.

Chhibber-Goel, J., Gaur, A., Singhal, V., Parakh, N., Bhargava, B., & Sharma, A. (2016). The complex metabolism of trimethylamine in humans: endogenous and exogenous sources. *Expert Reviews in Molecular Medicine*, *18*, 1–11.

Chiellini, G., Erba, P., Carnicelli, V., Manfredi, C., Frascarelli, S., Ghelardoni, S., Mariani, G., & Zucchi, R. (2012). Distribution of exogenous [125I]-3-iodothyronamine in mouse in vivo: relationship with trace amine-associated receptors. *The Journal of endocrinology*, *213*(3), 223–230.

Choi, U. B., Strop, P., Vrljic, M., Chu, S., Brunger, A. T., & Weninger, K. R. (2010). Single-molecule FRET-derived model of the synaptotagmin 1-SNARE fusion complex. *Nature Structural and Molecular Biology*, *17*(3), 318–324.

Churcher, A. M., Hubbard, P. C., Marques, J. P., Canário, A. V. M., & Huertas, M. (2015). Deep sequencing of the olfactory epithelium reveals specific chemosensory receptors are expressed at sexual maturity in the European eel Anguilla anguilla. *Molecular Ecology*, *24*(4), 822–834.

Cisneros, I.E., & Ghorpade, A. (2014). Methamphetamine and HIV-1-induced neurotoxicity: Role of trace amine associated receptor 1 cAMP signaling in astrocytes. *Neuropharmacology, 85C*, 499-507.

Cotter, R., Pei, Y., Mus, L., Harmeier, A., Gainetdinov, R.R., Hoener, M.C. & Canales, J.J. (2015). The trace amine-associated receptor 1 modulates methamphetamine's neurochemical and behavioral effects. *Front Neurosci*, *9*, 39.

Cripps, M. J., Bagnati, M., Jones, T. A., Ogunkolade, B. W., Sayers, S. R., Caton, P. W., Hanna, K., Billacura, M.P., Fair, K., Nelson, C., Lowe, R., Hitman, G.A., Berry, M.D., & Turner, M. D. (2020). Identification of a subset of trace amine-associated receptors and ligands as potential modulators of insulin secretion. *Biochemical Pharmacology*, *171*, 113685.

Davidson, M. A., Mattison, D. R., Azoulay, L., & Krewski, D. (2018). Thiazolidinedione drugs in the treatment of type 2 diabetes mellitus: past, present and future. *Critical Reviews in*

Toxicology, *48*(1), 52–108.

Davis, B. A., & Boulton, A. A. (1994). The trace amines and their acidic metabolites in depression - an overview. *Progress in Neuropsychopharmacology and Biological Psychiatry*, *18*(1), 17–45.

Davis, S. N., Piatti, P. M., Monti, L., Brown, M. D., Branch, W., Hales, C. N., & Alberti, K. G. M. M. (1993). Proinsulin and insulin concentrations following intravenous glucose challenges in normal, obese, and non-insulin-dependent diabetic subjects. *Metabolism*, *42*(1), 30–35.

Dedic, N., Jones, P. G., Hopkins, S. C., Lew, R., Shao, L., Campbell, J. E., Spear, K. L., Large, T. H., Campbell, U. C., Hanania, T., Leahy, E., & Koblan, K. S. (2019). SEP-363856, a Novel Psychotropic Agent with a Unique, Non-D_2 Receptor Mechanism of Action. *The Journal of pharmacology and experimental therapeutics*, *371*(1), 1–14.

Deshpande, A. D., Harris-Hayes, M., & Schootman, M. (2008). Epidemiology of diabetes and diabetes-related complications. *Physical therapy*, *88*(11), 1254–1264.

Dieren, S., Beulens, J. W., van der Schouw, Y. T., Grobbee, D. E., & Neal, B. (2010). The global burden of diabetes and its complications: an emerging pandemic. *European journal of cardiovascular prevention and rehabilitation : official journal of the European Society of Cardiology, Working Groups on Epidemiology & Prevention and Cardiac Rehabilitation and Exercise Physiology*, *17 Suppl 1*, S3–S8.

Dimitriadis, G., Mitrou, P., Lambadiari, V., Maratou, E., & Raptis, S. A. (2011). Insulin effects in muscle and adipose tissue. *Diabetes research and clinical practice*, *93 Suppl 1*, S52–S59.

Ding, S., Wang, X., Zhuge, W., Yang, J. & Zhuge, Q. (2017). Dopamine induces glutamate accumulation in astrocytes to disrupt neuronal function leading to pathogenesis of minimal

hepatic encephalopathy. *Neuroscience*.

Diniz, W. J. S., & Canduri, F. (2017). Bioinformatics: An overview and its applications. *Genetics and Molecular Research*, *16*(1), 1–21.

Dinter, J., Mühlhaus, J., Wienchol, C. L., Yi, C. X., Nürnberg, D., Morin, S., Grüters, A., Köhrle, J., Schöneberg, T., Tschöp, M., Krude, H., Kleinau, G., & Biebermann, H. (2015). Inverse agonistic action of 3-iodothyronamine at the human trace amine-associated receptor 5. *PloS one*, *10*(2), e0117774.

Duan, J., Martinez, M., Sanders, A. R., Hou, C., Saitou, N., Kitano, T., Mowry, B. J., Crowe, R. R., Silverman, J. M., Levinson, D. F., & Gejman, P. V. (2004). Polymorphisms in the trace amine receptor 4 (TRAR4) gene on chromosome 6q23.2 are associated with susceptibility to schizophrenia. *American journal of human genetics*, *75*(4), 624–638.

Düfer, M., Noack, K., Krippeit-Drews, P., & Drews, G. (2010). Activation of the AMP-activated protein kinase enhances glucose-stimulated insulin secretion in mouse β-cells. *Islets*, *2*(3), 156–163.

Dulubova, I., Lou, X., Lu, J., Huryeva, I., Alam, A., Schneggenburger, R., Südhof, T. C., & Rizo, J. (2005). A Munc13/RIM/Rab3 tripartite complex: from priming to plasticity?. *The EMBO journal*, *24*(16), 2839–2850.

Durden, D. A., & Davis, B. A. (1993). Determination of regional distributions of phenylethylamine and meta-and para-tyramine in rat brain regions and presence in human and dog plasma by an ultra-sensitive negative chemical ion gas chromatography-mass spectrometric (NCI-GC-MS) method. *Neurochemical Research*, *18*(9), 995–1002.

Durden, D. A., & Philips, S. R. (1980). Kinetic Measurements of the Turnover Rates of Phenylethylamine and Tryptamine In Vivo in the Rat Brain. *Journal of Neurochemistry*,

34(6), 1725–1732.

Dyck, L. E. (1989). Release of some endogenous trace amines from rat striatal slices in the presence and absence of a monoamine oxidase inhibitor. *Life Sciences*, *44*(17), 1149–1156.

Edgar, R. (2002). Gene Expression Omnibus: NCBI gene expression and hybridization array data repository. *Nucleic Acids Research*, *30*(1), 207–210.

Efrat, S., Tal, M., & Lodish, H. F. (1994). REVIEWS The pancreatic beta cell glucose sensor, *1*(DECEMBER), 535–538.

Elliott, J., Callingham, B. A., & Sharman, D. F. (1989). Semicarbazide-Sensitive Amine Oxidase (SSAO) of the rat aorta. Interactions with some naturally occurring amines and their structural analogues. *Biochemical Pharmacology*, *38*(9), 1507–1515.

Espinoza, S., Ghisi, V., Emanuele, M., Leo, D., Sukhanov, I., Sotnikova, T. D., Chieregatti, E., & Gainetdinov, R. R. (2015). Postsynaptic D2 dopamine receptor supersensitivity in the striatum of mice lacking TAAR1. *Neuropharmacology*, *93*, 308–313.

Espinoza, S., Lignani, G., Caffino, L., Maggi, S., Sukhanov, I., Leo, D., Mus, L., Emanuele, M., Ronzitti, G., Harmeier, A., Medrihan, L., Sotnikova, T. D., Chieregatti, E., Hoener, M. C., Benfenati, F., Tucci, V., Fumagalli, F., & Gainetdinov, R. R. (2015). TAAR1 Modulates Cortical Glutamate NMDA Receptor Function. *Neuropsychopharmacology : official publication of the American College of Neuropsychopharmacology*, *40*(9), 2217–2227.

Espinoza, S., Salahpour, A., Masri, B., Sotnikova, T. D., Messa, M., Barak, L. S., Caron, M. G., & Gainetdinov, R. R. (2011). Functional interaction between trace amine-associated receptor 1 and dopamine D2 receptor. *Molecular pharmacology*, *80*(3), 416–425.

Espinoza, S., Manago, F., Leo, D., Sotnikova, T.D. & Gainetdinov, R.R. (2012). Role of Catechol-OMethyltransferase (COMT)-Dependent Processes in Parkinson's Disease and L-

DOPA Treatment. *Cns Neurol Disord-Dr*, *11*, 251-263.

Espinoza, S., Sukhanov, I., Efimova, E. V., Kozlova, A., Antonova, K. A., Illiano, P., Leo, D., Merkulyeva, N., Kalinina, D., Musienko, P., Rocchi, A., Mus, L., Sotnikova, T. D., & Gainetdinov, R. R. (2020). Trace Amine-Associated Receptor 5 Provides Olfactory Input Into Limbic Brain Areas and Modulates Emotional Behaviors and Serotonin Transmission. *Frontiers in molecular neuroscience*, *13*, 18.

Eyun, S. Il, Moriyama, H., Hoffmann, F. G., & Moriyama, E. N. (2016). Molecular evolution and functional divergence of trace amine-associated receptors. *PLoS ONE*, *11*(3), 1–24.

Fargion, S., Dongiovanni, P., Guzzo, A., Colombo, S., Valenti, L., & Fracanzani, A. L. (2005). Iron and insulin resistance. *Alimentary Pharmacology and Therapeutics, Supplement*, *22*(2), 61–63.

Fennema, D., Phillips, I. R., & Shephard, E. A. (2016). Trimethylamine and trimethylamine N-oxide, a Flavin-Containing Monooxygenase 3 (FMO3)-mediated host-microbiome metabolic axis implicated in health and disease. *Drug Metabolism and Disposition*, *44*(11), 1839–1850.

Ferragud, A., Howell, A.D., Moore, C.F., Ta, T.L., Hoener, M.C., Sabino, V. & Cottone, P. (2017). The Trace Amine-Associated Receptor 1 Agonist RO5256390 Blocks Compulsive, Binge-like Eating in Rats. *Neuropsychopharmacology : official publication of the American College of Neuropsychopharmacology*, *42*, 1458-1470.

Ferrero, D. M., Wacker, D., Roque, M. A., Baldwin, M. W., Stevens, R. C., & Liberles, S. D. (2012). Agonists for 13 trace amine-associated receptors provide insight into the molecular basis of odor selectivity. *ACS Chemical Biology*, *7*(7), 1184–1189.

Filippas-Ntekouan, S., Filippatos, T. D., & Elisaf, M. S. (2018). SGLT2 inhibitors: are they safe?

Postgraduate Medicine, *130*(1), 72–82.

Foretz, M., Guigas, B., Bertrand, L., Pollak, M., & Viollet, B. (2014). Metformin: From mechanisms of action to therapies. *Cell Metabolism*, *20*(6), 953–966.

Fowler, M. J. (2011). Microvascular and Macrovascular Complications of Diabetes. *Clin Diabetes*, *29*(3), 116–122.

Gainetdinov, R. R., Hoener, M. C., & Berry, M. D. (2018). Trace Amines and Their Receptors. *Pharmacological reviews*, *70*(3), 549–620.

Galley, G., Beurier, A., Décoret, G., Goergler, A., Hutter, R., Mohr, S., Pähler, A., Schmid, P., Türck, D., Unger, R., Zbinden, K. G., Hoener, M. C., & Norcross, R. D. (2015). Discovery and Characterization of 2-Aminooxazolines as Highly Potent, Selective, and Orally Active TAAR1 Agonists. *ACS medicinal chemistry letters*, *7*(2), 192–197.

Gandasi, N. R., & Barg, S. (2014). Contact-induced clustering of syntaxin and munc18 docks secretory granules at the exocytosis site. *Nature Communications*, *5*(May), 1–14.

Gao, H., Dong, B., Liu, X., Xuan, H., Huang, Y., & Lin, D. (2008). Metabonomic profiling of renal cell carcinoma: High-resolution proton nuclear magnetic resonance spectroscopy of human serum with multivariate data analysis. *Analytica Chimica Acta*, *624*(2), 269–277.

Gardini, F., Özogul, Y., Suzzi, G., Tabanelli, G., & Özogul, F. (2016). Technological factors affecting biogenic amine content in foods: A review. *Frontiers in Microbiology*, *7*(AUG), 1–18.

Giovannucci, E., Harlan, D. M., Archer, M. C., Bergenstal, R. M., Gapstur, S. M., Habel, L. A., Pollak, M., Regensteiner, J. G., & Yee, D. (2010). Diabetes and cancer: a consensus report. *Diabetes care*, *33*(7), 1674–1685.

Gisladottir, R. S., Ivarsdottir, E. V., Helgason, A., Jonsson, L., Hannesdottir, N. K., Rutsdottir,

G., Arnadottir, G. A., Skuladottir, A., Jonsson, B. A., Norddahl, G. L., Ulfarsson, M. O., Helgason, H., Halldorsson, B. V., Nawaz, M. S., Tragante, V., Sveinbjornsson, G., Thorgeirsson, T., Oddsson, A., Kristjansson, R. P., Bjornsdottir, G., Thorgeirsson, G., Jonsdottir, I., Holm, H., Gudbjartsson, D., Thorsteinsdottir, U., Stefansson, H., Sulem, P., & Stefansson, K. (2020). Sequence Variants in TAAR5 and Other Loci Affect Human Odor Perception and Naming. *Current biology : CB*, *30*(23), 4643–4653.e3.

Gowans, G. J., Hawley, S. A., Ross, F. A., & Hardie, D. G. (2013). AMP is a true physiological regulator of amp-activated protein kinase by both allosteric activation and enhancing net phosphorylation. *Cell Metabolism*, *18*(4), 556–566.

Gozal, E. A., O'Neill, B. E., Sawchuk, M. A., Zhu, H., Halder, M., Chou, C. C., & Hochman, S. (2014). Anatomical and functional evidence for trace amines as unique modulators of locomotor function in the mammalian spinal cord. *Frontiers in Neural Circuits*, *8*(November), 1–20.

Gustavsson, N., Lao, Y., Maximov, A., Chuang, J. C., Kostromina, E., Repa, J. J., Li, C., Radda, G. K., Südhof, T. C., & Han, W. (2008). Impaired insulin secretion and glucose intolerance in synaptotagmin-7 null mutant mice. *Proceedings of the National Academy of Sciences of the United States of America*, *105*(10), 3992–3997.

Hadjiconstantinou, M., Wemlinger, T. A., Sylvia, C. P., Hubble, J. P., & Neff, N. H. (1993). Aromatic L-Amino Acid Decarboxylase Activity of Mouse Striatum Is Modulated via Dopamine Receptors. *Journal of Neurochemistry*, *60*(6), 2175–2180.

Han, H. S., Kang, G., Kim, J. S., Choi, B. H., & Koo, S. H. (2016). Regulation of glucose metabolism from a liver-centric perspective. *Experimental and Molecular Medicine*, *48*(3), 1–10.

Hanson, R. L., Ehm, M. G., Pettitt, D. J., Prochazka, M., Thompson, D. B., Timberlake, D., Foroud, T., Kobes, S., Baier, L., Burns, D. K., Almasy, L., Blangero, J., Garvey, W. T., Bennett, P. H., & Knowler, W. C. (1998). An autosomal genomic scan for loci linked to type II diabetes mellitus and body-mass index in Pima Indians. *American journal of human genetics*, *63*(4), 1130–1138.

Hardie, D. G., Scott, J. W., Pan, D. A., & Hudson, E. R. (2003). Management of cellular energy by the AMP-activated protein kinase system. *FEBS Letters*, *546*(1), 113–120.

Harmeier, A., Obermueller, S., Meyer, C. A., Revel, F. G., Buchy, D., Chaboz, S., Dernick, G., Wettstein, J. G., Iglesias, A., Rolink, A., Bettler, B., & Hoener, M. C. (2015). Trace amine-associated receptor 1 activation silences GSK3β signaling of TAAR1 and D2R heteromers. *European neuropsychopharmacology : the journal of the European College of Neuropsychopharmacology*, *25*(11), 2049–2061.

Hashiguchi, Y., & Nishida, M. (2007). Evolution of trace amine-associated receptor (TAAR) gene family in vertebrates: Lineage-specific expansions and degradations of a second class of vertebrate chemosensory receptors expressed in the olfactory epithelium. *Molecular Biology and Evolution*, *24*(9), 2099–2107.

Heberle, H., Meirelles, V. G., da Silva, F. R., Telles, G. P., & Minghim, R. (2015). InteractiVenn: A web-based tool for the analysis of sets through Venn diagrams. *BMC Bioinformatics*, *16*(1), 1–7.

Heit, J. J., Apelqvist, Å. A., Gu, X., Winslow, M. M., Neilson, J. R., Crabtree, G. R., & Kim, S. K. (2006). Calcineurin/NFAT signalling regulates pancreatic β-cell growth and function. *Nature*, *443*(7109), 345–349.

Henwood, R. W., Boulton, A. A., & Phillis, J. W. (1979). Iontophoretic studies of some trace

amines in the mammalian CNS. *Brain Research*, *164*(1–2), 347–351.

Holman, N., Young, B., & Gadsby, R. (2015). Current prevalence of Type 1 and Type 2 diabetes in adults and children in the UK. *Diabetic Medicine*, *32*(9), 1119–1120.

Horowitz, L.F., Saraiva, L.R., Kuang, D., Yoon, K.H. & Buck, L.B. (2014). Olfactory receptor patterning in a higher primate. *The Journal of neuroscience : the official journal of the Society for Neuroscience, 34,* 12241-12252.

Humbert, J.A., Hammond, K.B. & Hathaway, W.E. (1970). Trimethylaminuria: the fish-odour syndrome. *Lancet, 2,* 770-771.

Hussain, A., Saraiva, L. R., & Korsching, S. I. (2009). Positive Darwinian selection and the birth of an olfactory receptor clade in teleosts. *Proceedings of the National Academy of Sciences of the United States of America*, *106*(11), 4313–4318.

Hutton J. C. (1994). Insulin secretory granule biogenesis and the proinsulin-processing endopeptidases. *Diabetologia, 37 Suppl 2,* S48–S56.

International DiabetesFederation. (2017). IDF Diabetes Atlas 8th Edition, 155.

Inzucchi, S. E., Bergenstal, R. M., Buse, J. B., Diamant, M., Ferrannini, E., Nauck, M., Peters, A. L., Tsapas, A., Wender, R., & Matthews, D. R. (2015). Management of hyperglycemia in type 2 diabetes, 2015: a patient-centered approach: update to a position statement of the American Diabetes Association and the European Association for the Study of Diabetes. *Diabetes care*, *38*(1), 140–149.

Ito, J., Ito, M., Nambu, H., Fujikawa, T., Tanaka, K., Iwaasa, H., & Tokita, S. (2009). Anatomical and histological profiling of orphan G-protein-coupled receptor expression in gastrointestinal tract of C57BL/6J mice. *Cell and Tissue Research*, *338*(2), 257–269.

Janjic, D., Maechler, P., Bartley, C., Annen, A. S., & Wollheim, C. B. (1999). Free radical

modulation of insulin release in INS-1 cells exposed to alloxan. *Biochemical Pharmacology*, *57*(6), 639–648.

Jaskowiak, P. A., Campello, R. J. G. B., & Costa, I. G. (2014). On the selection of appropriate distances for gene expression data clustering. *BMC Bioinformatics*, *15*(Suppl 2), 1–17.

Jing, X., Li, D. Q., Olofsson, C. S., Salehi, A., Surve, V. V., Caballero, J., Ivarsson, R., Lundquist, I., Pereverzev, A., Schneider, T., Rorsman, P., & Renström, E. (2005). CaV2.3 calcium channels control second-phase insulin release. *The Journal of clinical investigation*, *115*(1), 146–154.

Jones, R. S. G. (1981). Specific enhancement of neuronal responses to catecholamine by p-tyramine. *Journal of Neuroscience Research*, *6*(1), 49–61.

Jönsson, C., Batista, A. P. C., Kjølhede, P., & Strålfors, P. (2019). Insulin and β-adrenergic receptors mediate lipolytic and anti-lipolytic signalling that is not altered by type 2 diabetes in human adipocytes. *Biochemical Journal*, *476*(19), 2883–2908.

Jun, G., Song, Y., Stein, C. M., & Iyengar, S. K. (2014). Type 2 diabetes. *Nursing Standard (Royal College of Nursing (Great Britain) : 1987)*, *28*(46), 19.

Juorio, A. V., Greenshaw, A. J., & Wishart, T. B. (1988). Reciprocal changes in striatal dopamine and β-phenylethylamine induced by reserpine in the presence of monoamine oxidase inhibitors. *Naunyn-Schmiedeberg's Archives of Pharmacology*, *338*(6), 644–648.

Kahn, C. R., Chen, L., & Cohen, S. E. (2000). Unraveling the mechanism of action of thiazolidinediones. *Journal of Clinical Investigation*, *106*(11), 1305–1307.

Kalwat, M. A., & Thurmond, D. C. (2013). Signaling mechanisms of glucose-induced F-actin remodeling in pancreatic islet β cells. *Experimental and Molecular Medicine*, *45*(8), e37-12.

Kalwat, M. A., Wiseman, D. A., Luo, W., Wang, Z., & Thurmond, D. C. (2012). Gelsolin

associates with the N terminus of syntaxin 4 to regulate insulin granule exocytosis. *Molecular Endocrinology*, *26*(1), 128–141.

Katzenschlager, R., & Lees, A. J. (2002). Treatment of Parkinson's disease: Levodopa as the first choice. *Journal of Neurology, Supplement*, *249*(2), 19–24.

Keller, M. P., Paul, P. K., Rabaglia, M. E., Stapleton, D. S., Schueler, K. L., Broman, A. T., Ye, S. I., Leng, N., Brandon, C. J., Neto, E. C., Plaisier, C. L., Simonett, S. P., Kebede, M. A., Sheynkman, G. M., Klein, M. A., Baliga, N. S., Smith, L. M., Broman, K. W., Yandell, B. S., Kendziorski, C., … Attie, A. D. (2016). The Transcription Factor Nfatc2 Regulates β-Cell Proliferation and Genes Associated with Type 2 Diabetes in Mouse and Human Islets. *PLoS genetics*, *12*(12), e1006466.

Khoo, S., & Cobb, M. H. (1997). Activation of mitogen-activating protein kinase by glucose is not required for insulin secretion. *Proceedings of the National Academy of Sciences of the United States of America*, *94*(11), 5599–5604.

Kim, H., & Ahn, Y. (2004). in the Glucose-Sensing Apparatus of Liver and ␣ -Cells. *Biochemistry*, *53*(February), 1–6.

Kleinridders, A., Ferris, H. A., Cai, W., & Kahn, C. R. (2014). Insulin action in brain regulates systemic metabolism and brain function. *Diabetes*, *63*(7), 2232–2243.

Knowler, W. C., Barrett-Connor, E., Fowler, S. E., Hamman, R. F., Lachin, J. M., Walker, E. A., Nathan, D. M., & Diabetes Prevention Program Research Group (2002). Reduction in the incidence of type 2 diabetes with lifestyle intervention or metformin. *The New England journal of medicine*, *346*(6), 393–403.

Kolic, J., & MacDonald, P. E. (2015). cAMP-independent effects of GLP-1 on β cells. *The Journal of clinical investigation*, *125*(12), 4327–4330.

Kong, A. P. S., Xu, G., Brown, N., So, W. Y., Ma, R. C. W., & Chan, J. C. N. (2013). Diabetes and its comorbidities - Where East meets West. *Nature Reviews Endocrinology*, *9*(9), 537–547.

Leahy, J. L. (2005). Pathogenesis of type 2 diabetes mellitus. *Archives of Medical Research*, *36*(3), 197–209.

Lee, S. H., Zabolotny, J. M., Huang, H., Lee, H., & Kim, Y. B. (2016). Insulin in the nervous system and the mind: Functions in metabolism, memory, and mood. *Molecular metabolism*, *5*(8), 589–601.

Leite, R. S., Marlow, N. M., & Fernandes, J. K. (2013). Oral health and type 2 diabetes. *The American Journal of the Medical Sciences*, *345*(4), 271–273.

Lennikov, M. S., Lennikov, A., Tang, S., & Huang, H. (2018). Proteomics reveals ablation of placental growth factor inhibits the insulin resistance pathways in diabetic mouse retina. *bioRxiv*, 338368.

Leo, D., Sukhanov, I., Zoratto, F., Illiano, P., Caffino, L., Sanna, F., Messa, G., Emanuele, M., Esposito, A., Dorofeikova, M., Budygin, E. A., Mus, L., Efimova, E. V., Niello, M., Espinoza, S., Sotnikova, T. D., Hoener, M. C., Laviola, G., Fumagalli, F., Adriani, W., & Gainetdinov, R. R. (2018). Pronounced Hyperactivity, Cognitive Dysfunctions, and BDNF Dysregulation in Dopamine Transporter Knock-out Rats. *The Journal of neuroscience : the official journal of the Society for Neuroscience*, *38*(8), 1959–1972.

Li, Q., Korzan, W.J., Ferrero, D.M., Chang, R.B., Roy, D.S., Buchi, M., Lemon, J.K., Kaur, A.W., Stowers, L., Fendt, M. & Liberles, S.D. (2013). Synchronous evolution of an odor biosynthesis pathway and behavioral response. *Current Biology*, *23*(1), 11–20.

Li, Q., Tachie-Baffour, Y., Liu, Z., Baldwin, M.W., Kruse, A.C. & Liberles, S.D. (2015). Non-

classical amine recognition evolved in a large clade of olfactory receptors. *Elife*, *4*, e10441.

Liberles, S. D., & Buck, L. B. (2006). A second class of chemosensory receptors in the olfactory epithelium. *Nature*, *442*(7103), 645–650.

Liberles, S.D. (2015). Trace amine-associated receptors: ligands, neural circuits, and behaviors. *Current opinion in neurobiology*, *34*, 1-7.

Lindemann, L., Ebeling, M., Kratochwil, N. A., Bunzow, J. R., Grandy, D. K., & Hoener, M. C. (2005). Trace amine-associated receptors form structurally and functionally distinct subfamilies of novel G protein-coupled receptors. *Genomics*, *85*(3), 372–385.

Lindemann, L., & Hoener, M. C. (2005). A renaissance in trace amines inspired by a novel GPCR family. *Trends in Pharmacological Sciences*, *26*(5), 274–281.

Lindemann, L., Meyer, C. A., Jeanneau, K., Bradaia, A., Ozmen, L., Bluethmann, H., Bettler, B., Wettstein, J. G., Borroni, E., Moreau, J. L., & Hoener, M. C. (2008). Trace amine-associated receptor 1 modulates dopaminergic activity. *The Journal of pharmacology and experimental therapeutics*, *324*(3), 948–956.

Lipscombe, L., Eurich Bsp, D. T., Goldenberg, R., Khan, N., Maccallum Bscphm, L., Shah, B. R., & Simpson Bsp, S. (2018). Diabetes Canada Clinical Practice Guidelines Expert Commitee - 2018 Clinical Practice Guidelines, Pharmacologic Glycemic Management of Type 2 Diabetes in Adults. *Canadian Journal of Diabetes*, *42*, S88–S103.

Liu, J. F., Seaman, R., Jr, Siemian, J. N., Bhimani, R., Johnson, B., Zhang, Y., Zhu, Q., Hoener, M. C., Park, J., Dietz, D. M., & Li, J. X. (2018). Role of trace amine-associated receptor 1 in nicotine's behavioral and neurochemical effects. *Neuropsychopharmacology : official publication of the American College of Neuropsychopharmacology*, *43*(12), 2435–2444.

Lundberg, P. Å., Oreland, L., & Engberg, G. (1985). Inhibition of locus coeruleus neuronal

activity by beta-phenylethylamine. *Life Sciences*, *36*(19), 1889–1896.

Luscombe, N. M., Greenbaum, D., & Gerstein, M. (2001). What is bioinformatics? A proposed definition and overview of the field. *Methods of Information in Medicine*, *40*(4), 346–358.

Lynch, L.J., Sullivan, K.A., Vallender, E.J., Rowlett, J.K., Platt, D.M. & Miller, G.M. (2013). Trace amine associated receptor 1 modulates behavioral effects of ethanol. *Substance abuse : research and treatment, 7*, 117-126.

Ma, C., Li, W., Xu, Y., & Rizo, J. (2011). Munc13 mediates the transition from the closed syntaxin-Munc18 complex to the SNARE complex. *Nature Structural and Molecular Biology*, *18*(5), 542–549.

Malle, E. K., Zammit, N. W., Walters, S. N., Koay, Y. C., Wu, J., Tan, B. M., Villanueva, J. E., Brink, R., Loudovaris, T., Cantley, J., McAlpine, S. R., Hesselson, D., & Grey, S. T. (2015). Nuclear factor κB-inducing kinase activation as a mechanism of pancreatic β cell failure in obesity. *The Journal of experimental medicine*, *212*(8), 1239–1254.

Manning, S., & Batterham, R. L. (2014). The Role of Gut Hormone Peptide YY in Energy and Glucose Homeostasis: Twelve Years On. *Annual Review of Physiology*, *76*(1), 585–608.

Marselli, L., Thorne, J., Dahiya, S., Sgroi, D. C., Sharma, A., Bonner-Weir, S., Marchetti, P., & Weir, G. C. (2010). Gene expression profiles of Beta-cell enriched tissue obtained by laser capture microdissection from subjects with type 2 diabetes. *PloS one*, *5*(7), e11499.

Martens, G. A., Motté, E., Kramer, G., Stangé, G., Gaarn, L. W., Hellemans, K., Nielsen, J. H., Aerts, J. M., Ling, Z., & Pipeleers, D. (2013). Functional characteristics of neonatal rat β cells with distinct markers. *Journal of molecular endocrinology*, *52*(1), 11–28.

Maruthur, N. M., Tseng, E., Hutfless, S., Wilson, L. M., Suarez-Cuervo, C., Berger, Z., Chu, Y., Iyoha, E., Segal, J. B., & Bolen, S. (2016). Diabetes Medications as Monotherapy or

Metformin-Based Combination Therapy for Type 2 Diabetes: A Systematic Review and Meta-analysis. *Annals of internal medicine*, *164*(11), 740–751.

McCulloch, L. J., van de Bunt, M., Braun, M., Frayn, K. N., Clark, A., & Gloyn, A. L. (2011). GLUT2 (SLC2A2) is not the principal glucose transporter in human pancreatic beta cells: Implications for understanding genetic association signals at this locus. *Molecular Genetics and Metabolism*, *104*(4), 648–653.

Menza, M. A., Sage, J., Marshall, E., Cody, R., & Duvoisin, R. (1990). Mood changes and "on-off" phenomena in Parkinson's disease. *Movement Disorders*, *5*(2), 148–151.

Merglen, A., Theander, S., Rubi, B., Chaffard, G., Wollheim, C. B., & Maechler, P. (2004). Glucose Sensitivity and Metabolism-Secretion Coupling Studied during Two-Year Continuous Culture in INS-1E Insulinoma Cells. *Endocrinology*, *145*(2), 667–678.

Michael, E. S., Covic, L., & Kuliopulos, A. (2019). Trace amine–associated receptor 1 (TAAR1) promotes anti-diabetic signaling in insulin-secreting cells. *Journal of Biological Chemistry*, *294*(12), 4401–4411.

Milligan, G., & Kostenis, E. (2006). Heterotrimeric G-proteins: a short history. *British journal of pharmacology*, *147 Suppl 1*(Suppl 1), S46–S55.

Misura, K. M. S., Scheller, R. H., & Weis, W. I. (2000). Three-dimensional structure of the neuronal-Sec1-syntaxin 1a complex. *Nature*, *404*(6776), 355–362.

Mühlhaus, J., Dinter, J., Nürnberg, D., Rehders, M., Depke, M., Golchert, J., Homuth, G., Yi, C. X., Morin, S., Köhrle, J., Brix, K., Tschöp, M., Kleinau, G., & Biebermann, H. (2014). Analysis of human TAAR8 and murine Taar8b mediated signaling pathways and expression profile. *International journal of molecular sciences*, *15*(11), 20638–20655.

Natali, A., & Ferrannini, E. (2006). Effects of metformin and thiazolidinediones on suppression

of hepatic glucose production and stimulation of glucose uptake in type 2 diabetes: A systematic review. *Diabetologia*, *49*(3), 434–441.

Neff, N. H., Wemlinger, T. A., Duchemin, A. M., & Hadjiconstantinou, M. (2006). Clozapine modulates aromatic L-amino acid decarboxylase activity in mouse striatum. *Journal of Pharmacology and Experimental Therapeutics*, *317*(2), 480–487.

Nelson, D. A., Tolbert, M. D., Singh, S. J., & Bost, K. L. (2007). Expression of Neuronal Trace Amine-associated Receptor (Taar) mRNAs in Leukocytes. *Journal of Neuroimmunology*, *192*(1–2), 21–30.

Nilsson, N. O., Strålfors, P., Fredrikson, G., & Belfrage, P. (1980). Regulation of adipose tissue lipolysis: effects of noradrenaline and insulin on phosphorylation of hormone-sensitive lipase and on lipolysis in intact rat adipocytes. *FEBS letters*, *111*(1), 125–130.

Niwa, T., Murayama, N., Umeyama, H., Shimizu, M. & Yamazaki, H. (2011). Human liver enzymes responsible for metabolic elimination of tyramine; a vasopressor agent from daily food. *Drug Metab Lett*, *5*, 216-219.

Obici, S., Zhang, B. B., Karkanias, G., & Rossetti, L. (2002). Hypothalamic insulin signaling is required for inhibition of glucose production. *Nature medicine*, *8*(12), 1376–1382.

Olokoba, A. B., Obateru, O. A., & Olokoba, L. B. (2012). Type 2 diabetes mellitus: A review of current trends. *Oman Medical Journal*, *27*(4), 269–273.

Oyelade, J., Isewon, I., Oladipupo, F., Aromolaran, O., Uwoghiren, E., Ameh, F., Achas, M., & Adebiyi, E. (2016). Clustering Algorithms: Their Application to Gene Expression Data. *Bioinformatics and biology insights*, *10*, 237–253.

Pae, C. U., Drago, A., Kim, J. J., Patkar, A. A., Jun, T. Y., De Ronchi, D., & Serretti, A. (2010). TAAR6 variations possibly associated with antidepressant response and suicidal behavior.

Psychiatry Research, *180*(1), 20–24.

Pae, C. U., Drago, A., Kim, J. J., Patkar, A. A., Jun, T. Y., Lee, C., Mandelli, L., De Ronchi, D., Paik, I. H., & Serretti, A. (2008). TAAR6 variation effect on clinic presentation and outcome in a sample of schizophrenic in-patients: an open label study. *European psychiatry : the journal of the Association of European Psychiatrists*, *23*(6), 390–395.

Panas, M. W., Xie, Z., Panas, H. N., Hoener, M. C., Vallender, E. J., & Miller, G. M. (2012). Trace amine associated receptor 1 signaling in activated lymphocytes. *Journal of Neuroimmune Pharmacology*, *7*(4), 866–876.

Park, D., Jhon, D. Y., Lee, C. W., Lee, K. H., & Sue Goo Rhee. (1993). Activation of phospholipase C isozymes by G protein βγ subunits. *Journal of Biological Chemistry*, *268*(7), 4573–4576.

Paterson, I. A. (1993). The potentiation of cortical neuron responses to noradrenaline by 2-phenylethylamine is independent of endogenous noradrenaline. *Neurochemical Research*, *18*(12), 1329–1336.

Patzelt, C., Labrecque, A. D., Duguid, J. R., Carroll, R. J., Keim, P. S., Heinrikson, R. L., & Steiner, D. F. (1978). Detection and kinetic behavior of preproinsulin in pancreatic islets. *Proceedings of the National Academy of Sciences of the United States of America*, *75*(3), 1260–1264.

Pei, Y., Lee, J., Leo, D., Gainetdinov, R. R., Hoener, M. C., & Canales, J. J. (2014). Activation of the trace amine-associated receptor 1 prevents relapse to cocaine seeking. *Neuropsychopharmacology : official publication of the American College of Neuropsychopharmacology*, *39*(10), 2299–2308.

Pétremand, J., Bulat, N., Butty, A. C., Poussin, C., Rütti, S., Au, K., Ghosh, S., Mooser, V.,

Thorens, B., Yang, J. Y., Widmann, C., & Waeber, G. (2009). Involvement of 4E-BP1 in the protection induced by HDLs on pancreatic beta-cells. *Molecular endocrinology (Baltimore, Md.)*, *23*(10), 1572–1586.

Philips, S. R., & Boulton, A. A. (1979). the Effect of Monoamine Oxidase Inhibitors on Some Arylalkylamines in Rat Striatum. *Journal of Neurochemistry*, *33*(1), 159–167.

Phung, O. J., Sobieraj, D. M., Engel, S. S., & Rajpathak, S. N. (2014). Early combination therapy for the treatment of type 2 diabetes mellitus: systematic review and meta-analysis. *Diabetes, Obesity and Metabolism*, *16*(5), 410–417.

Pitts, M. S., McShane, J. N., Hoener, M. C., Christian, S. L., & Berry, M. D. (2019). TAAR1 levels and sub-cellular distribution are cell line but not breast cancer subtype specific. *Histochemistry and Cell Biology*, *152*(2), 155–166.

Pratley, R. E., & Salsali, A. (2007). Inhibition of DPP-4: a new therapeutic approach for the treatment of type 2 diabetes. *Current Medical Research and Opinion*, *23*(4), 919–931.

Proks, P., Reimann, F., Green, N., Gribble, F., & Frances, A. (2002). Sulfonylurea_stimulation_of_in.PDF. *American Diabetes Association*, *51*(3), 368–377.

Punthakee, Z., Goldenberg, R., & Katz, P. (2018). Definition, Classification and Diagnosis of Diabetes, Prediabetes and Metabolic Syndrome. *Canadian Journal of Diabetes*, *42*, S10–S15.

Raab, S., Wang, H., Uhles, S., Cole, N., Alvarez-Sanchez, R., Künnecke, B., Ullmer, C., Matile, H., Bedoucha, M., Norcross, R. D., Ottaway-Parker, N., Perez-Tilve, D., Conde Knape, K., Tschöp, M. H., Hoener, M. C., & Sewing, S. (2015). Incretin-like effects of small molecule trace amine-associated receptor 1 agonists. *Molecular metabolism*, *5*(1), 47–56.

Raghavachari, N., & Garcia-Reyero, N. (2018). Overview of gene expression analysis:

Transcriptomics. *Methods in Molecular Biology*, *1783*, 1–6.

Rebuffat, S. A., Oliveira, J. M., Altirriba, J., Palau, N., Garcia, A., Esteban, Y., Nadal, B., & Gomis, R. (2013). Downregulation of Sfrp5 promotes beta cell proliferation during obesity in the rat. *Diabetologia*, *56*(11), 2446–2455.

Regard, J. B., Kataoka, H., Cano, D. A., Camerer, E., Yin, L., Zheng, Y. W., Scanlan, T. S., Hebrok, M., & Coughlin, S. R. (2007). Probing cell type-specific functions of Gi in vivo identifies GPCR regulators of insulin secretion. *The Journal of clinical investigation*, *117*(12), 4034–4043.

Revel, F. G., Moreau, J. L., Pouzet, B., Mory, R., Bradaia, A., Buchy, D., Metzler, V., Chaboz, S., Groebke Zbinden, K., Galley, G., Norcross, R. D., Tuerck, D., Bruns, A., Morairty, S. R., Kilduff, T. S., Wallace, T. L., Risterucci, C., Wettstein, J. G., & Hoener, M. C. (2013). A new perspective for schizophrenia: TAAR1 agonists reveal antipsychotic- and antidepressant-like activity, improve cognition and control body weight. *Molecular psychiatry*, *18*(5), 543–556.

Revel, F. G., Moreau, J. L., Gainetdinov, R. R., Bradaia, A., Sotnikova, T. D., Mory, R., Durkin, S., Zbinden, K. G., Norcross, R., Meyer, C. A., Metzler, V., Chaboz, S., Ozmen, L., Trube, G., Pouzet, B., Bettler, B., Caron, M. G., Wettstein, J. G., & Hoener, M. C. (2011). TAAR1 activation modulates monoaminergic neurotransmission, preventing hyperdopaminergic and hypoglutamatergic activity. *Proceedings of the National Academy of Sciences of the United States of America*, *108*(20), 8485–8490.

Revel, F. G., Moreau, J. L., Gainetdinov, R. R., Ferragud, A., Velázquez-Sánchez, C., Sotnikova, T. D., Morairty, S. R., Harmeier, A., Groebke Zbinden, K., Norcross, R. D., Bradaia, A., Kilduff, T. S., Biemans, B., Pouzet, B., Caron, M. G., Canales, J. J., Wallace, T. L.,

Wettstein, J. G., & Hoener, M. C. (2012). Trace amine-associated receptor 1 partial agonism reveals novel paradigm for neuropsychiatric therapeutics. *Biological psychiatry*, *72*(11), 934–942.

Riccardi, G., Capaldo, B., & Vaccaro, O. (2005). Functional foods in the management of obesity and type 2 diabetes. *Current Opinion in Clinical Nutrition and Metabolic Care*, *8*(6), 630–635.

Riccardi, G., & Rivellese, A. A. (1991). Effects of dietary fiber and carbohydrate on glucose and lipoprotein metabolism in diabetic patients. *Diabetes care*, *14*(12), 1115–1125.

Röder, P. V., Wong, X., Hong, W., & Han, W. (2016). Molecular regulation of insulin granule biogenesis and exocytosis. *Biochemical Journal*, *473*(18), 2737–2756.

Rorsman, P., Braun, M., & Zhang, Q. (2012). Regulation of calcium in pancreatic α- and β-cells in health and disease. *Cell Calcium*, *51*(3–4), 300–308.

Rossetti, Z. L., Silvia, C. P., Krajnc, D., Neff, N. H., & Hadjiconstantinou, M. (1990). Aromatic L-Amino Acid Decarboxylase Is Modulated by D1 Dopamine Receptors in Rat Retina. *Journal of Neurochemistry*, *54*(3), 787–791.

Sandler, M., Ruthven, C. R., Goodwin, B. L., Reynolds, G. P., Rao, V. A., & Coppen, A. (1980). Trace amine deficit in depressive illness: the phenylalanine connexion. *Acta psychiatrica Scandinavica. Supplementum*, *280*, 29–39.

Santos, P.S., Courtiol, A., Heidel, A.J., Honer, O.P., Heckmann, I., Nagy, M., Mayer, F., Platzer, M., Voigt, C.C. & Sommer, S. (2016). MHC-dependent mate choice is linked to a trace-amineassociated receptor gene in a mammal. *Sci Rep*, *6*, 38490.

Sarwar, N., Gao, P., Seshasai, S. R., Gobin, R., Kaptoge, S., Di Angelantonio, E., Ingelsson, E., Lawlor, D. A., Selvin, E., Stampfer, M., Stehouwer, C. D., Lewington, S., Pennells, L.,

Thompson, A., Sattar, N., White, I. R., Ray, K. K., & Danesh, J. (2010). Diabetes mellitus, fasting blood glucose concentration, and risk of vascular disease: a collaborative meta-analysis of 102 prospective studies. *Lancet (London, England)*, *375*(9733), 2215–2222.

Scanlan, T. S., Suchland, K. L., Hart, M. E., Chiellini, G., Huang, Y., Kruzich, P. J., Frascarelli, S., Crossley, D. A., Bunzow, J. R., Ronca-Testoni, S., Lin, E. T., Hatton, D., Zucchi, R., & Grandy, D. K. (2004). 3-Iodothyronamine is an endogenous and rapid-acting derivative of thyroid hormone. *Nature medicine*, *10*(6), 638–642.

Sebokova, E., Christ, A. D., Wang, H., Sewing, S., Dong, J. Z., Taylor, J., Cawthorne, M. A., & Culler, M. D. (2010). Taspoglutide, an analog of human glucagon-like Peptide-1 with enhanced stability and in vivo potency. *Endocrinology*, *151*(6), 2474–2482.

Serretti, A., Pae, C.U., Chiesa, A., Mandelli, L. & De Ronchi, D. (2009). Influence of TAAR6 polymorphisms on response to aripiprazole. *Prog Neuropsychopharmacol Biol Psychiatry*, *33*, 822-826.

Shih, J. C., & Chen, K. (2004). Regulation of MAO-A and MAO-B Gene Expression. *Current Medicinal Chemistry*, 1995–2005.

Sidarala, V., & Kowluru, A. (2016). The Regulatory Roles of Mitogen-Activated Protein Kinase (MAPK) Pathways in Health and Diabetes: Lessons Learned from the Pancreatic β-Cell. *Recent Patents on Endocrine, Metabolic & Immune Drug Discovery*, *10*(2), 76–84.

Simmler, L. D., Buchy, D., Chaboz, S., Hoener, M. C., & Liechti, M. E. (2016). In vitro characterization of psychoactive substances at rat, mouse, and human trace amine-associated receptor 1s. *Journal of Pharmacology and Experimental Therapeutics*, *357*(1), 134–144.

Smith, P. A., Sellers, L. A., & Humphrey, P. P. A. (2001). Somatostatin activates two types of

inwardly rectifying K+ channels in MIN-6 cells. *Journal of Physiology*, *532*(1), 127–142.

Sotnikova, T.D., Beaulieu, J.M., Espinoza, S., Masri, B., Zhang, X., Salahpour, A., Barak, L.S., Caron, M.G. & Gainetdinov, R.R. (2010). The dopamine metabolite 3-methoxytyramine is a neuromodulator. *PloS one*, *5*, e13452.

Sotnikova, T.D., Zorina, O.I., Ghisi, V., Caron, M.G. & Gainetdinov, R.R. (2008). Trace amine associated receptor 1 and movement control. *Parkinsonism Relat Disord*, *14 Suppl 2*, S99-102.

Srinivasa, S., Fitch, K. V., Lo, J., Kadar, H., Knight, R., Wong, K., Abbara, S., Gauguier, D., Capeau, J., Boccara, F., & Grinspoon, S. K. (2015). Plaque burden in HIV-infected patients is associated with serum intestinal microbiota-generated trimethylamine. *AIDS (London, England)*, *29*(4), 443–452.

Stehouwer, C. D. A. (2018). Microvascular Dysfunction and Hyperglycemia: A Vicious Cycle With Widespread Consequences. *Diabetes*, *67*(January), 1729–1741.

Steiner, D. F., Smeekens, S. P., Ohagi, S., & Chan, S. J. (1992). The new enzymology of precursor processing endoproteases. *The Journal of biological chemistry*, *267*(33), 23435–23438.

Stratton, I. M. (2000). Association of glycaemia with macrovascular and microvascular complications of type 2 diabetes (UKPDS 35): prospective observational study. *Bmj*, *321*(7258), 405–412.

Strodl, E., & Kenardy, J. (2006). Psychosocial and non-psychosocial risk factors for the new diagnosis of diabetes in elderly women. *Diabetes Research and Clinical Practice*, *74*(1), 57–65.

Sturn, A., & Quackenbush, J. (2002). Genesis: cluster analysis of microarray data.

Bioinformatics, *18*(1), 207–208.

Sukhanov, I., Caffino, L., Efimova, E. V., Espinoza, S., Sotnikova, T. D., Cervo, L., Fumagalli, F., & Gainetdinov, R. R. (2016). Increased context-dependent conditioning to amphetamine in mice lacking TAAR1. *Pharmacological research*, *103*, 206–214.

Sutton, R. B., Davletov, B. A., Berghuis, A. M., Sudhof, T. C., & Sprang, S. R. (1995). Structure of the first C2 domain of synaptotagmin I: A novel Ca2+/phospholipid-binding fold. *Cell*, *80*(6), 929–938.

Swulius, M. T., & Waxham, M. N. (2008). Ca2+/calmodulin-dependent protein kinases. *Cellular and Molecular Life Sciences*, *65*(17), 2637–2657.

Tabuchi, H., Yamamoto, H., Matsumoto, K., Ebihara, K., Takeuchi, Y., Fukunaga, K., Hiraoka, H., Sasaki, Y., Shichiri, M., & Miyamoto, E. (2000). Regulation of insulin secretion by overexpression of Ca2+/calmodulin-dependent protein kinase II in insulinoma MIN6 cells. *Endocrinology*, *141*(7), 2350–2360.

Takahashi, H., Yokoi, N., & Seino, S. (2019). Glutamate as intracellular and extracellular signals in pancreatic islet functions. *Proceedings of the Japan Academy Series B: Physical and Biological Sciences*, *95*(6), 246–260.

Taneera, J., Fadista, J., Ahlqvist, E., Atac, D., Ottosson-Laakso, E., Wollheim, C. B., & Groop, L. (2014). Identification of novel genes for glucose metabolism based upon expression pattern in human islets and effect on insulin secretion and glycemia. *Human Molecular Genetics*, *24*(7), 1945–1955.

Taylor, S. R., & Harris, K. B. (2013). The clinical efficacy and safety of sodium glucose cotransporter-2 inhibitors in adults with type 2 diabetes mellitus. *Pharmacotherapy*, *33*(9), 984–999.

Tengholm, A. (2012). Cyclic AMP dynamics in the pancreatic β-cell. *Upsala Journal of Medical Sciences*, *117*(4), 355–369.

Thangavel, N., Al Bratty, M., Akhtar Javed, S., Ahsan, W., & Alhazmi, H. A. (2017). Targeting Peroxisome Proliferator-Activated Receptors Using Thiazolidinediones: Strategy for Design of Novel Antidiabetic Drugs. *International Journal of Medicinal Chemistry*, *2017*, 1–20.

Thorn, D. A., Jing, L., Qiu, Y., Gancarz-Kausch, A. M., Galuska, C. M., Dietz, D. M., Zhang, Y., & Li, J. X. (2014). Effects of the trace amine-associated receptor 1 agonist RO5263397 on abuse-related effects of cocaine in rats. *Neuropsychopharmacology : official publication of the American College of Neuropsychopharmacology*, *39*(10), 2309–2316.

Timofeeva, A. (2019). Evaluating the robustness of goodness-of-fit measures for hierarchical clustering. *Journal of Physics: Conference Series*, *1145*(1).

Tokarz, V. L., MacDonald, P. E., & Klip, A. (2018). The cell biology of systemic insulin function. *Journal of Cell Biology*, *217*(7), 1–17.

Toro-Funes, N., Bosch-Fuste, J., Latorre-Moratalla, M. L., Veciana-Nogués, M. T., & Vidal-Carou, M. C. (2015). Biologically active amines in fermented and non-fermented commercial soybean products from the Spanish market. *Food Chemistry*, *173*, 1119–1124.

Tsuboi, T., & Fukuda, M. (2006). Rab3A and Rab27A cooperatively regulate the docking step of dense-core vesicle exocytosis in PC12 cells. *Journal of Cell Science*, *119*(11), 2196–2203.

Tuomilehto J., Indstrom J., Eriksson J., Valle T., H. E. & U. M. (2001). Numb Er 18 Prevention of Type 2 Diabetes Mellitus By Changes in Lifestyle Among Subjects With Impaired Glucose Tolerance. *The New England Journal of Medicine*, *344*(18), 1343–1350.

Underhill, S. M., Hullihen, P. D., Chen, J., Fenollar-Ferrer, C., Rizzo, M. A., Ingram, S. L., & Amara, S. G. (2019). Amphetamines signal through intracellular TAAR1 receptors coupled

to Gα13 and GαS in discrete subcellular domains. *Molecular Psychiatry*.

Vallender, E. J., Xie, Z., Westmoreland, S. V., & Miller, G. M. (2010). Functional evolution of the trace amine associated receptors in mammals and the loss of TAAR1 in dogs. *BMC Evolutionary Biology*, *10*(1), 0–8.

Vanti, W. B., Muglia, P., Nguyen, T., Cheng, R., Kennedy, J. L., George, S. R., & O'Dowd, B. F. (2003). Discovery of a null mutation in a human trace amine receptor gene. *Genomics*, *82*(5), 531–536.

Viollet, B., Andreelli, F., Jørgensen, S. B., Perrin, C., Flamez, D., Mu, J., Wojtaszewski, J. F., Schuit, F. C., Birnbaum, M., Richter, E., Burcelin, R., & Vaulont, S. (2003). Physiological role of AMP-activated protein kinase (AMPK): insights from knockout mouse models. *Biochemical Society transactions*, *31*(Pt 1), 216–219.

Wallrabenstein, I., Kuklan, J., Weber, L., Zborala, S., Werner, M., Altmüller, J., Becker, C., Schmidt, A., Hatt, H., Hummel, T., & Gisselmann, G. (2013). Human trace amine-associated receptor TAAR5 can be activated by trimethylamine. *PloS one*, *8*(2), e54950.

Wang, Z., & Thurmond, D. C. (2009). Mechanisms of biphasic insulin-granule exocytosis - Roles of the cytoskeleton, small GTPases and SNARE proteins. *Journal of Cell Science*, *122*(7), 893–903.

Wickman, K. D., Iñiguez-Lluhl, J. A., Davenport, P. A., Taussig, R., Krapivinsky, G. B., Linder, M. E., Gilman, A. G., & Clapham, D. E. (1994). Recombinant G-protein beta gamma-subunits activate the muscarinic-gated atrial potassium channel. *Nature*, *368*(6468), 255–257.

Wilson, J. R., Ludowyke, R. I., & Biden, T. J. (2001). A redistribution of actin and myosin IIA accompanies Ca2+-dependent insulin secretion. *FEBS Letters*, *492*(1–2), 101–106.

Wolfe R. R. (2000). Effects of insulin on muscle tissue. *Current opinion in clinical nutrition and metabolic care*, *3*(1), 67–71.

Wu, Z. Y., Zhu, L. J., Zou, N., Bombek, L. K., Shao, C. Y., Wang, N., Wang, X. X., Liang, L., Xia, J., Rupnik, M., & Shen, Y. (2012). AMPA receptors regulate exocytosis and insulin release in pancreatic β cells. *Traffic (Copenhagen, Denmark)*, *13*(8), 1124–1139.

Xie, Z., & Miller, G. M. (2008). β-phenylethylamine alters monoamine transporter function via trace amine-associated receptor 1: Implication for modulatory roles of trace amines in brain. *Journal of Pharmacology and Experimental Therapeutics*, *325*(2), 617–628.

Xie, Z., & Miller, G. M. (2009). Trace amine-associated receptor 1 as a monoaminergic modulator in brain. *Biochemical Pharmacology*, *78*(9), 1095–1104.

Xie, Z., Westmoreland, S. V., Bahn, M. E., Chen, G. L., Yang, H., Vallender, E. J., Yao, W. D., Madras, B. K., & Miller, G. M. (2007). Rhesus monkey trace amine-associated receptor 1 signaling: enhancement by monoamine transporters and attenuation by the D2 autoreceptor in vitro. *The Journal of pharmacology and experimental therapeutics*, *321*(1), 116–127.

Xie, Z., Vallender, E.J., Yu, N., Kirstein, S.L., Yang, H., Bahn, M.E., Westmoreland, S.V. & Miller, G.M. (2008). Cloning, expression, and functional analysis of rhesus monkey trace amineassociated receptor 6: evidence for lack of monoaminergic association. *J Neurosci Res*, *86*, 3435-3446.

Xie, Z., Westmoreland, S. V., & Miller, G. M. (2008). Modulation of monoamine transporters by common biogenic amines via trace amine-associated receptor 1 and monoamine autoreceptors in human embryonic kidney 293 cells and brain synaptosomes. *Journal of Pharmacology and Experimental Therapeutics*, *325*(2), 629–640.

Yang, H. Y., & Neff, N. H. (1973). Beta-phenylethylamine: a specific substrate for type B

monoamine oxidase of brain. *The Journal of pharmacology and experimental therapeutics*, *187*(2), 365–371.

Yang, T., Gao, X., Sandberg, M., Zollbrecht, C., Zhang, X. M., Hezel, M., Liu, M., Peleli, M., Lai, E. Y., Harris, R. A., Persson, A. E., Fredholm, B. B., Jansson, L., & Carlström, M. (2015). Abrogation of adenosine A1 receptor signalling improves metabolic regulation in mice by modulating oxidative stress and inflammatory responses. *Diabetologia*, *58*(7), 1610–1620.

Yang, W., Munhall, A. C., & Johnson, S. W. (2020). Dopamine Evokes a Trace Amine Receptor-dependent Inward Current that is Regulated by AMP Kinase in Substantia Nigra Dopamine Neurons. *Neuroscience*, *427*, 77–91.

Yang, Y. X., Mu, C. L., Luo, Z., & Zhu, W. Y. (2016). Bromochloromethane, a methane analogue, affects the microbiota and metabolic profiles of the rat gastrointestinal tract. *Applied and environmental microbiology*, *82*(3), 778-787.

Yasuda, T., Shibasaki, T., Minami, K., Takahashi, H., Mizoguchi, A., Uriu, Y., Numata, T., Mori, Y., Miyazaki, J., Miki, T., & Seino, S. (2010). Rim2alpha determines docking and priming states in insulin granule exocytosis. *Cell metabolism*, *12*(2), 117–129.

Yim, O., & Ramdeen, K. T. (2015). Hierarchical Cluster Analysis: Comparison of Three Linkage Measures and Application to Psychological Data. *The Quantitative Methods for Psychology*, *11*(1), 8–21.

Zhang, J., Pacifico, R., Cawley, D., Feinstein, P., & Bozza, T. (2013). Ultrasensitive detection of amines by a trace amine-associated receptor. *Journal of Neuroscience*, *33*(7), 3228–3239.

Zhang, L. S., & Davies, S. S. (2016). Microbial metabolism of dietary components to bioactive metabolites: Opportunities for new therapeutic interventions. *Genome Medicine*, *8*(1), 1–18.

Zheng, Y., Ley, S. H., & Hu, F. B. (2018). Global aetiology and epidemiology of type 2 diabetes mellitus and its complications. *Nature Reviews Endocrinology*, *14*(2), 88–98.

Zhu, D., Xie, L., Karimian, N., Liang, T., Kang, Y., Huang, Y. C., & Gaisano, H. Y. (2015). Munc18c mediates exocytosis of pre-docked and newcomer insulin granules underlying biphasic glucose stimulated insulin secretion in human pancreatic beta-cells. *Molecular Metabolism*, *4*(5), 418–426.

Zhu, M. Y., Juorio, A. V., Paterson, I. A., & Boulton, A. A. (1992). Regulation of Aromatic l-Amino Acid Decarboxylase by Dopamine Receptors in the Rat Brain. *Journal of Neurochemistry*, *58*(2), 636–641.

Zhu, Meng Yang, Juorio, A. V., Alick Paterson, I., & Boulton, A. A. (1993). Regulation of striatal aromatic L-amino acid decarboxylase: Effects of blockade or activation of dopamine receptors. *European Journal of Pharmacology*, *238*(2–3), 157–164.

6.0 Appendix

Supplemental R source code for the generation of RMA normalized data (oligo package) and list of differentially expressed genes (Limma package):

>setwd("C:/Datasets") # Sets folder from which R will retrieve .CEL files pertaining to an Affymetrix-microarray study.

>source("http://bioconductor.org/biocLite.R")

>biocLite() # Install Bioconductor packages like Affy, affydata, affyPLM, affyQCReport, annaffy, annotate, Biobase, biomaRt, Biostrings, DynDoc, gcrma, genefilter, geneplotter, GenomicRanges, hgu95av2.db, limma, marray, multtest, vsn, and xtable.

>biocLite("oligo") # Install oligo package

>library(oligo) # Load oligo package in the workspace

>biocLite("Annotation file") # Install array package/annotation file like pd.hugene.1.0.st.v1, mouse4302cdf, rat2302.db etc. It can also be installed from: www.bioconductor.org/packages/release/data/annotation/.

>library(Annotation file) # Load array package in the workspace.

>celfiles <- list.celfiles() # Lists all CEL files in folder.

>celfiles

>data<-read.celfiles(celfiles) # Automatically selects the installed array package/annotation file, and generates gene feature set.

>data

>hist(data) # Analyze raw data prior to rma normalization.

>boxplot(data)

#Normalization and background correction

>genes <- rma(data) # Generates expression set, target=core analyzes at the whole gene level for gene chips.

>genes

>hist(genes) # Analyze data post rma normalization

>boxplot(genes)

>write.exprs(genes.file="rma_normalized_data.txt") # Write rma normalized genes expression values to a text file.

#Limma

>biocLite("limma") # Install Limma package.

>library(limma) # Load Limma package in the workspace.

>getwd() # Check if working directory is set to the right folder.

>design<-model.matrix(~0+factor(c(1,1,1,1,2,2,2,2,3,3,3,3,4,4,4,4))) # Example of four treatments, three replicates for each treatment.

>colnames(design)<-c("two","five","ten","thirty")

>design

>contrast.matrix <- makeContrasts(five-two, ten-two, thirty-two, levels=design) # Indicates the comparison between the treatments.

>contrast.matrix # Check the comparison. Order is important for read-out.

>fit<-lmFit(genes,design)

>fit2 <- contrasts.fit(fit, contrast.matrix)

>fit3 <- eBayes(fit2)

>results <- decideTests(fit3, p.value=0.01)

>vennDiagram(results, include="up")

>vennDiagram(results, include="down")

>vennDiagram(results, include="both")

>write.csv(fit3, file="control") # Get data from all contrasts for all the genes across the gene chip.

#To get list of differentially expressed genes

>tt <- topTable(fit3, coef=1, n=10000, adjust="fdr", sort.by="logFC", p.value=0.01)

>tt

>write.csv(tt, file="Top table probe IDs.csv") # Write differentially expressed genes expression values to a text file.